UNDERSTANDING THE METABOLIC AND GENETIC REGULATION OF BREAST CANCER RECURRENCE USING MAGNETIC RESONANCE-BASED INTEGRATIVE METABOLOMICS

Dania Daye

A DISSERTATION

in

Bioengineering

Presented to the Faculties of the University of Pennsylvania

in

Partial Fulfillment of the Requirements for the

Degree of Doctor of Philosophy

2013

Supervisor of Dissertation

_____

Lewis A. Chodosh, M.D., Ph.D.

Professor of Cancer Biology

Co-Supervisor of Dissertation

_____

Mitchell D. Schnall, M.D., Ph.D.

Professor of Radiology

Graduate Group Chairperson

_____

Daniel A. Hammmer, Ph.D.

Professor of Bioengineering

Dissertation Committee:

Peter F. Davies, Ph.D., Professor of Pathology and Laboratory Medicine (Chair)

M. Celeste Simon, Ph.D., Professor of Cell and Developmental Biology

Jim Delikatny, Ph.D., Research Associate Professor of Radiology

UNDERSTANDING THE METABOLIC AND GENETIC REGULATION OF BREAST CANCER RECURRENCE USING MAGNETIC RESONANCE-BASED INTEGRATIVE METABOLOMICS

COPYRIGHT

2013

Dania Daye

This work is licensed under the
Creative Commons Attribution-
NonCommercial-ShareAlike 3.0
License

To view a copy of this license, visit

http://creativecommons.org/licenses/by-nc-sa/3.0/

To my grandmother who remains my greatest inspiration in my academic pursuits

ACKNOWLEDGMENTS

This work would not have been possible without the assistance and support of several people. I could not have wished for better advisors than Dr. Lewis A. Chodosh and Dr. Mitchell D. Schnall. Your scientific foresight, dedication, teaching and mentorship have enriched my PhD and made me the scientist that I am. I am also deeply indebted to Dr. Anthony Mancuso, Dr. Suzanne Wehrli, Dr. Stephen Pickup, Dr. Itzhak Nissim, Samantha L. Dwyer and Dr. Liz Yeh for the countless hours that they have spent teaching me, answering my questions and discussing ideas. I would also like to convey my warmest thanks for my committee members, Dr. Peter Davies, Dr. Celeste Simon and Dr. Jim Delikatny, for their invaluable input on this work, as well as Dr. Kathryn Wellen for many helpful scientific discussions.

My sincere thanks to all members of the Chodosh lab for making the last three years an experience that I will always fondly look back on. Particularly, I would like to thank Ania Payne, Lauren Smith, Jason Ruth, Daniel Abravanel, Tien-Chi Pan, Dhruv Pant, James Alvarez, Yi Feng, Chien-Chung Chen, Yan Chen, Chris Sterner, George Belka, Judy Farrell, Carrie Kitzmiller, Katelyn Wichert and Judith Smith for all of their help through various stages of my project.

I was also very fortunate to receive tremendous encouragement and support from many mentors and role models who believed in me and continuously provided me with the inspiration to persist on this path during both the rewarding and challenging phases of this process. I would like to extend my deepest gratitude to Dr. Emily Conant, Dr. Despina Kontos, Dr. Becky Wells, Dr. Susan Margulies, Dr. Vivian Cheung, Dr. Skip Brass, Dr. Ann Tiao, Dr. Brad Keller and Maggie Krall. Thank you for your support and for your unwavering confidence and belief in me.

I would like to acknowledge the funding sources of my graduate training: the Howard Hughes Medical Institute Gilliam Fellowship and the Paul and Daisy Soros Fellowship. Lastly, I would like to thank Dr. Rebecca Richards-Kortum, my undergraduate research advisor, for serving for many years as an exceptional role model and for inspiring me to pursue a career in science.

ABSTRACT

UNDERSTANDING THE METABOLIC AND GENETIC REGULATION OF BREAST CANCER RECURRENCE USING MAGNETIC RESONANCE-BASED INTEGRATIVE METABOLOMICS

Dania Daye

Lewis A. Chodosh, M.D., Ph.D.

Mitchell D. Schnall, M.D., Ph.D.

Breast cancer is the most commonly diagnosed malignancy in women and is the leading cause of cancer-related death in the female population worldwide. In these women, breast cancer recurrence—local, regional, or distant—represents the principal cause of death from this disease. The mechanisms underlying tumor recurrence remain largely unknown. To dissect those mechanisms, our laboratory has developed inducible transgenic mouse models that accurately recapitulate key features of the natural history of human breast cancer progression: primary tumor development, tumor dormancy and recurrence. Dysregulated metabolism has long been known to be a key feature in tumorigenesis. Yet, very little is known about the connection, if any, between cellular metabolic changes and breast cancer recurrence. In this work, I design and implement a systems engineering-based approach, magnetic resonance-based integrative metabolomics, to better understand the metabolic and genetic regulation of breast cancer recurrence. Through a combination of ^{1}H and ^{13}C magnetic resonance spectroscopy (MRS), mass spectrometry (MS) as well as gene expression profiling and functional metabolic and genetic studies, I aim to identify the metabolic profile of mammary tumors during breast cancer progression, identify the molecular basis and role of differential glutamine uptake and metabolism in breast cancer recurrence and finally,

investigate the molecular basis and role of differential lactate production in breast cancer recurrence. Our findings suggest an evolving metabolic phenotype of tumors during breast cancer progression as well as metabolic dysregulation in some of the key regulatory nodes that control that evolution. Identifying the metabolic changes associated with tumor recurrence can pave the way for identifying novel diagnostic strategies and therapeutic targets that can contribute to improved clinical management and outcome for breast cancer patients.

TABLE OF CONTENTS

ACKNOWLEDGMENTS ..... **IV**

ABSTRACT ..... **V**

LIST OF TABLES ..... **VIII**

LIST OF ILLUSTRATIONS ..... **IX**

CHAPTER 1: Breast Cancer Recurrence and Metabolism **1**

CHAPTER 2: Magnetic Resonance-Based Integrative Metabolomics: Design and Implementation of a Systems Engineering-Based Approach **22**

CHAPTER 3: Metabolic and Genetic Profiling of Mammary Tumor Recurrence Using ^{1}H Magnetic Resonance Spectroscopy **36**

CHAPTER 4: Metabolic Reprogramming in Cancer: Unraveling the Role of Glutamine in Tumorigenesis **67**

CHAPTER 5: Glutamine Addiction: a Targetable Hallmark of Breast Cancer Recurrence **91**

CHAPTER 6: Ldhb Downregulation by Sirt3 Contributes to the Warburg Effect and Promotes Breast Cancer Recurrence **126**

CHAPTER 7: Conclusions and Future Directions **160**

BIBLIOGRAPHY **190**

LIST OF TABLES

Table 3.1. ^{1}H Metabolites assessed in by NMR in primary and recurrent tumors

Table 3.2. Metabolite level quantification in primary and recurrent mammary tumors

Table 7.1. Correlation between AKT pathway activity and *SLC1A5* expression in human breast cancer datasets

Table 7.2. Representative reaction rate constants computed from hyperpolarized MRS data using a 5-parameter fit solution to modified Bloch equation model for 2-site chemical exchange

Table 7.3. Logistic regression analysis to assess independent contribution of metabolic gene expression signature in predicting recurrence risk after adjusting for a number of clinicoprognostic variables in breast cancer patients

LIST OF ILLUSTRATIONS

Figure 2.1. Magnetic resonance-based integrative metabolomics: functional architecture of the proposed process-based system to better understand the metabolic and genetic regulation of breast cancer recurrence

Figure 3.1. Primary and recurrent mammary tumors exhibit different metabolic phenotypes

Figure 3.2. Lactate metabolism is upregulated in mammary tumor recurrence

Figure 3.3. Glycine metabolism is upregulated in mammary tumor recurrence

Figure 3.4. Glutamine, choline and succinate metabolism exhibit marked changes during mammary tumor recurrence

Figure 3.5. High metabolic gene expression score is associated with decreased relapse-free survival in HER2-positive human breast cancer

Figure 4.1. Glutamine metabolism in cancer cells

Figure 4.2. Coordination of glutamine and glucose utilization during proliferation

Figure 5.1. Recurrent tumors exhibit increased glutamine metabolism

Figure 5.2. Recurrent tumors exhibit higher glutaminolytic flux and increased reductive carboxylation

Figure 5.3. Recurrent tumor cells are glutamine-addicted

Figure 5.4. Slc1a5 is upregulated in recurrence and is required for tumor growth

Figure 5.5. Gls1 is upregulated in recurrence and is required for tumor growth

Figure 5.6. *SLC1A5*, but not *GLS1* expression is associated with recurrence risk in human breast cancer

Figure 5.7. Myc is upregulated in recurrence and causes *Slc1a5* and *Gls1* upregulation

Figure 6.1.Recurrent tumors exhibit higher lactate levels than primary tumors

Figure 6.2. Recurrent tumors exhibit lower Ldhb expression levels

Figure 6.3. *Ldhb* downregulation results in higher lactate levels

Figure 6.4. Lower *Ldhb* levels promote tumor recurrence in mice and are correlated with decreased recurrence-free survival in human breast cancer

Figure 6.5. Sirt3 downregulation reduces *Ldhb* levels in recurrence

Figure 6.6. Sirt3 downregulation of *Ldhb* is mediated through Hif1

Figure 7.1. Model of increased lactate promoting breast cancer recurrence

Figure 7.2. Recurrent tumors exhibit increased serine biosynthesis pathway activity

Figure 7.3. Model of metabolic reprogramming in breast cancer recurrence

Figure 7.4. Akt might be another regulator of glutamine metabolism

Figure 7.5. Glud1 as an additional glutaminolytic target in breast cancer recurrence

Figure 7.6. Hyperpolarized magnetic resonance spectroscopy in primary and recurrent tumor-bearing mice

Figure 7.7. Performance of metabolic gene expression signature in predicting tumor recurrence in breast cancer patients

CHAPTER 1

Breast Cancer Recurrence and Metabolism

1.1 Breast Cancer Recurrence

Epidemiology

Breast cancer is the most commonly diagnosed malignancy in women and the leading cause of cancer-related death in the female population worldwide[1]. In the United States, breast cancer is the second leading cause of death in women and the leading cause of death in females aged 40 to 59[2]. This year, approximately 230,000 women are projected to be diagnosed with invasive breast cancer and approximately 40,000 will die from this disease[3]. Since 1975, breast cancer mortality rates have declined with the wide adoption of screening mammography and improvements in available treatment options. However, this trend is largely due to improvements in the diagnosis and treatment of primary breast cancer, as recurrent breast cancer remains a fatal disease[4].

A number of risk factors are associated with the development of breast cancer. These include older age and female gender, which are among the strongest risk factors. Women are 100 times more likely to develop breast cancer than men, with 207,000 breast cancers diagnosed among women, as compared to 2,000 diagnosed in men in 2010[5]. Breast cancer incidence rates also increase with age[2]. Other risk factors include race/ethnicity, reproductive and hormonal factors, environmental factors and exposure to ionizing radiation.

In the US, breast cancer is the most commonly diagnosed malignancy in women of all major ethnic groups[4]. However, the highest incidence rates are reported in Caucasians (124 per 100,000) and the lowest in Asian Americans (82 per 100,000) with African Americans, Hispanics and Native Americans having intermediate incidence rates (113 per 100,000, 90 per 100,000 and 92 per 100,000 respectively)[6]. Reproductive and endocrine factors have also been reported to strongly contribute to breast cancer risk. For instance, younger age at menarche and later age at menopause are associated with increased risk for breast cancer[7]. Furthermore, nulliparity and older age at first birth are associated with increased risk of breast cancer[7, 8]. Other risk factors for breast cancer include exposure to ionizing radiation at a young age, especially in patients who have undergone treatment for Hodgkin's lymphoma[9].

A number of studies have reported an association between breast cancer risk and lifestyle and dietary factors. Substantial evidence suggests an association between high body mass index (BMI), low physical activity, smoking, high alcohol intake and high fat intake and an increased risk of breast cancer[10-13]. Finally, a positive family history of breast cancer in a first-degree relative is also an important risk factor. Although family history is reported in only about 15 to 20% of women with breast cancer, familial inheritance of certain gene mutations (such as in *BRCA1*, *BRCA2*, *p53*, *ATM* and *PTEN*) is an established risk factor that predisposes to a high susceptibility of developing this disease[14]. In addition, having a personal history of invasive breast cancer also increases the risk of developing cancer in the contralateral breast by approximately 1 percent per year[15].

With declining mortality rates resulting from widespread adoption of screening mammography and improvements in adjuvant therapy, more women are surviving their

primary breast cancers with earlier detection and better treatment regimens[16]. In this regard, breast cancer patients are at risk for developing a recurrent tumor in the ipsilateral breast. Breast cancer recurrence describes the return of breast cancer after primary treatment. There are three types of recurrent breast cancer: local, regional and distant. In local recurrence, breast cancer appears at the original tumor site. In regional recurrence, cancer occurs in the chest wall or regional lymph nodes. In distant recurrence, breast cancer can reappear in other sites including the lungs, liver, bone, brain and other organs. Most breast cancer recurrences appear in the first decade following primary treatment, with the majority occurring in years 2 to 5[17]. Recurrences can also occur much later, especially for ER-positive tumors with up to one half of those recurrences happening more than five years after diagnosis[18].

Recurrence rates of primary breast cancers are associated with the mode of therapy used to treat the primary tumors, as well as a number of important prognostic markers that include lymph node involvement at diagnosis and primary tumor size[19]. In patients treated with surgery but not adjuvant therapy, recurrence rates can approach 50% in lymph node-positive patients and 32% in node-negative patients in the 10-year period following diagnosis[20]. Current treatment guidelines recommend adjuvant therapy for qualifying patients, combined with either surgical breast conservation therapy with radiation therapy (BCT + RT) or mastectomy for most breast cancer patients. Recurrence rates post-mastectomy generally range between 8 and 10%[21, 22]. Recurrence rates in the treated breast following BCT with radiation therapy have been reported to range between 10 and 15%[23]. However, women who only receive BCT, without radiation therapy, have rates of local recurrence as high as 34%[21, 24].

With breast conservation therapy, recurrences tend to appear later compared to patients treated with mastectomy, with a median time of three to four years with the former versus two to three years with the latter[25]. For patients treated for invasive breast cancer, more than 80% of locoregional recurrences following BCT are also invasive and 75% are isolated to the ipsilateral breast[26, 27]. Following mastectomy, recurrences tend to occur in the chest wall (50 to 70%) or regional nodes (40%) with the latter being associated with poorer survival[28]. Five-year survival rates for women with breast cancer recurrences range from 7 to 50% with combined chest wall and supraclavicular node recurrences carrying the worst prognosis[28].

According to the American Cancer Society, the current 5-year survival rate of women afflicted with primary breast cancer ranges between 67-93% for women diagnosed with stages 0-III disease[29]. However, this mortality rate is disproportionately being observed in the cohort of breast cancer patients diagnosed with primary tumors. Recurrent disease is almost uniformly fatal. Our understanding of breast cancer recurrence remains relatively limited. More research is needed in this area in an effort to achieve better survival and improved quality-of-life in patients afflicted with recurrent disease.

Recurrence Risk Assessment

In breast cancer management, it is important to have access to prognostic markers capable of providing information on the clinical outcome of patients. To date, pathologic evaluation of tumor tissue remains the gold standard for this purpose. In particular, clinicians often rely on lymph node status, tumor size, histologic grade, histologic tumor

type and the presence or absence of lymphatic and vascular invasion as the key factors for predicting clinical outcome in breast cancer patients[30, 31]. Each of these factors has been associated with increased likelihood of cancer recurrence. Lymph node involvement remains one of the strongest factors associated with increased recurrence: the higher the number of involved lymph nodes, the worse the patient's prognosis. Conversely, negative lymph node status has been consistently associated with a favorable outcome[31]. Histologically, positive excision margin, larger tumor size, higher histological grade, vascular invasion and higher proliferation rate predict increased likelihood of recurrence[31, 32]. High proliferation rate is associated with shorter disease-free and overall survival[33]. Hormone receptor status is also an important predictor of prognosis, whereby ER and PR receptor positivity are each associated with favorable outcomes[23]. In contrast, the presence of HER2/*neu* amplification and overexpression is associated with high rates of relapse and poor overall prognosis[34].

In 2005, the St. Gallen expert consensus meeting defined three risk categories of breast cancer recurrence in patients with operable breast cancer based on the above prognostic factors[35]. According to their classification criteria, patients can be divided into those with low, intermediate or high recurrence risks. Their report concluded that patients had a low risk for recurrence if they had node-negative breast cancer of size less than 2 cm, histologic grade of 1, negative HER2/*neu* receptor status, no peritumoral vascular invasion and the patient is older than 35 at the time of diagnosis. Patients are at intermediate risk of recurrence if their disease is node-negative and at least one of the following is present: tumor size greater than 2 cm, histologic grade of 2 or 3, presence of peritumoral vascular invasion, HER2/*neu* overexpression or amplification, or the patient is younger than 35. Patients can also have an intermediate risk of recurrence if they

have node-positive disease, but no HER2/*neu* overexpression. Finally, patients have a high risk for breast cancer recurrence if they have node-positive disease with HER2/*neu* amplification or overexpression. Based on these risk categories, treatment recommendations were established that highlight the importance of personalizing treatment options based on patient prognosis.

More recently, commercial genetic assays have been introduced to aid in assessing patient prognosis and predicting recurrence risk. One of these is Oncotype DX, a 21-gene assay that is used to generate a prognostic score predicting recurrence risk in patients with newly diagnosed node-negative ER-positive disease[36]. The use of this multigene assay to aid in patient prognostication and treatment decisions is now recommended in treatment guidelines promulgated by the American Society of Clinical Oncology (ASCO). The wide implementation of this test highlights the importance of prognostic molecular profiling research in breast cancer management.

Diagnosis of Tumor Recurrence

With more women surviving their primary breast cancers as a result of advances in detection and treatment options, post-treatment surveillance strategies to detect recurrent disease are taking center stage. The primary goal of these strategies is the early detection and treatment of potentially curable recurrent disease. With the majority of breast cancer recurrences reported in the first 5 years following diagnosis, the greatest emphasis of surveillance is during that time period. However, lifelong follow-up remains warranted as recurrent tumors may arise as late as 20 years following primary tumor development[18]. According to published guidelines by ASCO and the National

Comprehensive Cancer Network (NCCN), routine history and physical exam as well as regularly scheduled mammograms are the standard of care for the surveillance of breast cancer survivors[37].

According to the published guidelines, breast cancer survivors should be seen every three to six months during the first three years post primary therapy, every six to twelve months for the next two years, and then annually[18]. Mammograms are recommended starting six months after definitive treatment, then obtained every 6 to 12 months thereafter. Local recurrences are detected by mammography alone in 40 to 75% of cases, by physical exam alone in 10 to 30% of the cases, and by combination of the two in 10 to 15% of the cases[38, 39]. With a large number of recurrences diagnosed by routine screening mammography, most published guidelines recommend long-term follow-up with screening mammography even in older patients. Potentially curable local recurrences have been reported up to 10-years post treatment[38]. Notably, however, breast conservation therapy can lead to marked architectural distortion of the breast, which thereby limits the sensitivity of both clinical exam and mammography. These facts warrant the exploration of other imaging modalities for the early detection of recurrent disease.

The detection of clinically or radiographically suspicious lesions triggers further work-up, including biopsy. Core needle biopsy or excisional biopsy are typically performed to confirm or rule out the diagnosis of local recurrence. If confirmed, the biopsied tissue is assayed for receptor status and HER2/*neu* overexpression for prognostic information and to aid in treatment decisions.

Role of Imaging in Breast Cancer Recurrence

Mammography is currently considered the gold standard for post-treatment surveillance of breast cancer survivors. However, with both radiation therapy and surgery being the mainstay of treatment, the breast frequently undergoes architectural distortion and local mass-like fibrosis that renders the detection of local recurrence more challenging. In those patients, up to one half of local recurrences are mammographically occult. With reduced mammographic sensitivity in this context, MRI is being explored as a potential technique to complement mammographic surveillance. Accumulating evidence suggests that MRI is able to detect mammographically occult lesions in architecturally distorted breasts[40, 41]. However, while MRI provides increased sensitivity, this technique is far less specific and has a high rate of false-positives. As a result, the widespread clinical implementation for surveillance remains controversial. Current clinical guidelines recommend that MRI be used in women at high risk for recurrence with the decision being made based on the complexity of the clinical scenario.

Additional evidence exists suggesting a benefit of adding ultrasound to screening mammography to complement the surveillance of breast cancer survivors. A large randomized clinical trial conducted to address this question revealed an increased diagnostic yield with 4.2 additional recurrences detected due to the addition of ultrasound for every 1,000 women screened[42]. However, similar to MRI, the addition of ultrasound to mammography also resulted in a substantial increase in false-positives, making its widespread clinical implementation also controversial.

At present, PET imaging is primarily used for the staging of women in whom breast cancer has been detected. However, its role in surveillance remains less clear.

To our knowledge, no trials are currently available that have considered this question. Some retrospective cohort studies have reported a high sensitivity of PET for the early detection of recurrent lesions[43, 44]. It is not clear, however, whether PET will have specificity drawbacks similar to MRI and ultrasound. It is possible that the use of PET for surveillance might be a promising approach. Further studies are needed to assess its role.

At present, mammography remains the mainstay for the surveillance of breast cancer patients as indicated by the guidelines of the American Society of Clinical Oncology (ASCO). Other imaging modalities might hold additional promise for improved sensitivity. However, larger clinical trials are needed to validate their potential role in the surveillance of breast cancer survivors.

Treatment of Breast Cancer Recurrence

Treatment decisions for breast cancer recurrence are made following biopsying the detected lesion as part of the staging process. During that process, hormone receptor status as well as HER2/*neu* overexpression is determined. This information aids the clinician to better tailor treatment choices to complement standard therapeutic approaches. Treatment decisions are also primarily dictated by the initial therapy that was employed to eradicate the primary tumor, typically consisting of either breast conservation therapy (BCT) with radiation therapy or mastectomy. Of note, some recurrent lesions are not amenable to biopsy such as in the case of bone metastasis. In these instances and although not an ideal approach, treatment decisions are based on the features of the original primary tumor.

For patients who originally underwent BCT for their primary cancers, the most established predictor of prognosis following surgical excision has been reported to be the duration of time between BCT and recurrence detection. Recurrences occurring less than 2 years from diagnosis tend to have worse prognosis than those that are detected more than 2 years after diagnosis[23]. Mastectomy is the principal treatment for local recurrence following BCT. After mastectomy, the risk of a subsequent recurrence has been reported to be less than 10%[45]. Addition of radiation therapy to the treatment regimen is often not possible, as most patients undergo whole breast irradiation during initial treatment of their primary tumor, making it less likely to improve survival rates.

For patients who underwent mastectomy as part of the treatment for their primary breast cancer, recommended treatment options for locoregional recurrence consist of wide local excision of all gross disease combined with radiation therapy[28, 46]. However, with a post-mastectomy recurrence, the likelihood of a subsequent recurrence following treatment can be as high as 70%[47]. Similar to BCT, the likelihood of local control of disease is greatest when recurrence happens more than 2 years following initial therapy and when recurrent disease is focal rather than multifocal[48, 49].

For locoregional recurrences occurring after BCT or mastectomy, established treatment guidelines recommend the addition of systemic therapy to surgery and radiation therapy. Chemotherapy is recommended for women with hormone receptor-negative disease, as is hormonal therapy for those with hormone receptor-positive disease. Addition of trastuzumab is indicated in women with HER2/*neu*-positive disease. Although recommended, the clear benefit of systemic therapy following local disease control (i.e. surgery and radiation therapy) has not been fully established.

Randomized clinical trials are warranted to further validate the effect of this treatment approach.

HER2/*neu* Amplification and Breast Cancer Recurrence

HER2/*neu* is amplified and overexpressed in 18 to 20% of human breast cancers[50, 51]. The HER2/*neu* oncogene encodes a 185 KD transmembrane glycoprotein with an intrinsic intracellular tyrosine kinase activity[52]. It activation is critical for the activation of intracellular signaling pathways responsible for epithelial cell growth and differentiation[53]. Assessing HER2/*neu* status in diagnosed breast cancers is an essential part of standard clinical management, as HER2/*neu* overexpression carries both predictive and prognostic value. HER2/*neu* positivity identifies women likely to benefit from treatments targeted against HER2/*neu* such as trastuzumab and lapatinib. In addition, HER2/*neu* status may identify women who are more likely to be sensitive or resistant to certain systemic treatment regimens. Women with HER2/*neu*-positive breast cancers tend to be more sensitive to anthracyclines, but display relative resistance to endocrine therapies, mainly selective estrogen modulator therapy (SERM)[54, 55].

In addition to its predictive value in the clinical management of breast cancer patients, HER2/*neu* status also provides prognostic information. In particular, HER2/*neu* overexpression is associated with high rates of disease recurrence and acquired resistance to therapy. HER2/*neu* overexpression is also correlated with other pathologic factors previously shown to predict poor prognosis such as tumor grade, tumor size and lymph node status[51, 55, 56]. HER2/*neu* amplification and overexpression is an

independent predictor of decreased 10-year relapse free survival in both node-positive and node-negative breast cancer patients[57].

In 2005, assessing HER2/*neu* overexpression took center stage when the St. Gallen International expert consensus added HER2/*neu* status as a feature defining recurrence risk category. According to their published report published, "HER2/*neu* status should be regarded as useful for patient care, with overexpression indicating worse prognosis."[35] Today, HER2/*neu*-status is also part of a 21-gene recurrence score assay that is widely used clinically, Oncotype DX. This test is recommended by ASCO for the assessment of recurrence risk in women with ER-positive, node-negative disease to guide treatment decisions[36].

Although trastuzumab is the mainstay therapy for women with HER2/*neu*-positive disease, resistance to therapy develops commonly, especially in the context of recurrent disease. Studies suggest that a number of recurrent cancers downregulate HER2/*neu*, upregulate other genes or activate alternative pathways to escape therapy, particularly PI3K, IGF-1 and MYC[58-60]. A subset of tumors also express p95HER2 , a truncated form of HER2 that has intrinsic kinase activity but lacks the extracellular trastuzumab binding domain[61]. These cancers tend to have worse prognosis. Acquiring a better understanding of the mechanisms contributing to the resistance to therapy and worse prognosis typically associated with HER2/*neu* overexpression is vital to achieve better survival rates in patients diagnosed with HER2/*neu*-positive disease.

Mouse Model of HER2/neu Breast Cancer Recurrence

As was summarized above, despite significant improvements in five-year survival rates in recent years, breast cancer recurrence still constitutes the principal cause of morbidity and mortality in this disease. At present, the mechanisms underlying tumor recurrence remain largely unknown. As such, identifying critical drivers of breast cancer recurrence is essential for improving the long-term survival of breast cancer patients. To dissect the mechanisms responsible for breast cancer recurrence, our laboratory has developed a number of inducible transgenic mouse models that accurately recapitulate key features of the natural history of human breast cancers, including primary tumor development, minimal residual disease, tumor dormancy and tumor recurrence[62-66]. One of those models, the MMTV-rtTa;TetO-HER2/*neu* model, is a mammary-specific inducible transgenic model designed to investigate the molecular underpinnings of HER2/*neu*-induced tumorigenesis as well as the treatment and recurrence of mammary tumors induced by this oncogene[66].

The MMTV-rtTa;TetO-HER2/*neu* model is a doxycycline-inducible bitransgenic mouse model, in which the reverse tetracycline-inducible transactivator (rtTA) is specifically expressed in the epithelial compartment of the mammary gland under the control of the mouse mammary tumor virus (MMTV) promoter. Following the administration of doxycycline, rtTA binds to the TetO operator and induces the expression of the *neu* oncogene, leading to the eventual development of a primary mammary tumor. Upon doxycycline withdrawal, HER2/*neu* expression is acutely downregulated and tumors regress to a non-palpable state. Here, genetic downregulation of HER2/*neu* mimics the effect of targeted phamacologic inhibition against this receptor. However, as observed in patients, the tumors subsequently recur

in a stochastic manner following a latent period that reflects tumor dormancy. Accordingly, we believe that assessing the molecular and phenotypic differences between primary and recurrent mammary tumors in this model will shed light on mechanisms of tumor recurrence that may contribute to the reported association between HER2/*neu*-positive breast cancers and poor prognosis. Moreover, understanding the molecular pathways responsible for recurrence will be essential for enabling improvements in the detection and treatment of recurrent disease.

1.2 HER2/*neu* Overexpression and Cancer Metabolism

HER2/*neu* over-expression in breast cancer results in activation of the (PI3K)-AKT signaling pathway[67, 68]. Persistent activation of the (PI3K)-AKT pathway, independent of HER2/*neu* activation, is associated with poorer response and resistance to trastuzumab in humans[59, 69] as well as an increased risk of local tumor recurrence[70]. The (PI3K)-AKT pathway plays a central role in the regulation of cellular metabolism and is thought to underlie the increased dependence of cancer cells on glycolysis[71, 72]. Accordingly, understanding the metabolic dependencies of cancer cells during breast cancer progression might further our understanding of recurrence and permit the identification of novel prognostic markers and therapeutic targets.

Dysregulated cellular metabolism is a key feature of tumorigenesis[73-75]. Among the numerous metabolic pathways altered in cancer cells, aerobic glycolysis (the Warburg effect), glutamine metabolism and fatty acid/lipid synthesis are among the most established of these and have been found to be required for tumor growth within

different contexts[73]. In what follows, we briefly summarize the key features of each of these three pathways.

Role of Aerobic Glycolysis (Warburg Effect) in Tumorigenesis

The Warburg effect, which consists of high glucose utilization and increased lactate production in tumors despite the presence of oxygen, is among the most fundamental alterations observed in tumor metabolism[76]. AKT induction can increase glycolysis and lactate production and is sufficient to induce the Warburg effect in nontransformed cells as well as cancer cells[77-79]. Given the established association of the (PI3K)-AKT pathway with breast cancer recurrence[70] and the role of AKT in inducing the Warburg effect, studying alterations in glycolysis and lactate production during breast cancer progression could help elucidate key metabolic control points that might contribute to carcinogenesis.

Increased lactate production has been directly implicated in established hallmarks of cancer. For example, high lactate levels have been correlated with avoidance of immunosurveillance within the tumor microenvironment[80]. Patients with high lactate levels in their sera tend to exhibit higher tumor burden and worse overall prognosis[81]. Similarly, high lactate levels have also been associated with increased tumor invasion and metastasis[82]. At the molecular level, a number of enzymes directly implicated in modulating lactate levels have been shown to be required for tumor growth. Particularly, inhibition of the expression of the A subunit of lactate dehydrogenase (Ldha) as well as the expression of the M2 isoform of pyruvate kinase (Pkm2) have been shown to reduce the growth rate of primary tumors in vivo[83, 84]. Ldha is the enzyme directly

responsible for lactate production. Pkm2 is the embryonic isoform of pyruvate kinase, the isoform that is preferentially expressed in cancer cells and that has been shown to be associated with increased lactate levels.

In the glycolytic pathway, lactate dehydrogenase catalyzes the interconversion of pyruvate and lactate with concomitant interconversion of NADH and NAD+. Functional lactate dehydrogenases, considered to be key mediators of glycolysis, are homo- and hetero-tetramers of M and H proteins encoded by the *Ldha* and *Ldhb* genes respectively[85]. Five iso-enzymes, with different activity levels, have been described in the literature: LDH-1 (4H), LDH-2 (3H1M), LDH-3 (2H2M), LDH-4 (1H3M) and LDH-5 (4M)[85]. High LDH-5 levels have been associated with worse prognosis and have been shown to play a direct functional role in promoting cancer growth[84, 86]. On the other hand, while some reports suggest a possible contribution of Ldhb in cancer progression[87], its role remains less well understood.

Glutamine Metabolism in Cancer

Another metabolic pathway required for the growth of certain tumor types is mitochondrial glutamine metabolism. Since the 1950s, glutamine has been recognized as an important tumor nutrient that contributes to key metabolic processes in proliferating cancer cells[88, 89]. Glutamine participates in bioenergetics, supports cell defenses against oxidative stress, complements glucose metabolism and is an obligate nitrogen donor for nucleotide and amino acid synthesis[73, 75, 90-93].

The metabolism of glutamine can be divided into reactions that use its α-nitrogen, γ-nitrogen or carbon skeleton. The γ-nitrogen from glutamine's amide group is a

required nitrogen source for *de novo* nucleotide synthesis. This nitrogen is needed in three independent enzymatic steps in purine synthesis, as well as in two independent steps in pyrimidine synthesis[92]. The γ-nitrogen is also required for hexosamine biosynthesis, a precursor for glycosylation reactions. The rate-limiting step of hexosamine production is catalyzed by glutamine:fructose-6-phosphate amido-transferase. This reaction uses glutamine's amido nitrogen to produce glucoasamine-6-phosphate, a precursor for O-linked and N-linked glycosylation in cells[90].

Glutamine's γ-nitrogen is released following glutamine's conversion into glutamate by glutaminase (Gls). The glutaminase-catalyzed reaction leads to the formation of glutamate and ammonia. The latter is a potentially toxic metabolite, mostly secreted from the cell and shown to play a role in inducing autophagy[94, 95]. Glutamate carries glutamine's remaining nitrogen and is a major nitrogen source for nonessential amino acid production in cells. Alanine transaminase and aspartate aminotransferase catalyze the transfer of glutamate's amino group directly into alanine and aspartate, respectively. Furthermore, transfer of the amino group from glutamate to alpha-ketoacids is also used to generate serine, glycine, cysteine, arginine, asparagine and proline. In addition to its role in nonessential amino acid synthesis, glutamate is also an important component of the synthesis of glutathione, an endogenous antioxidant that protects cells against various forms of oxidative stress.

The final major fate of glutamine is the oxidation of its carbon backbone in mitochondria. Entry of glutamine's carbon into the TCA cycle requires conversion of glutamine into glutamate by glutaminase, followed by conversion of glutamate into alpha-ketoglutarate by glutamate dehydrogenase, alanine transaminase or aspartate transaminase. The complete oxidation of glutamine's carbon backbone in the TCA

cycle, through a process termed glutaminolysis, contributes to lipid synthesis and results in the production of lactate through the malic enzyme, conversion to pyruvate and, finally, re-introduction into the TCA cycle as acetyl-coA. This process allows glutamine to participate in lipid synthesis and to support anaplerosis, the replenishment of TCA cycle intermediates. It also leads to the production of ATP and NADPH. The latter is an important reducing equivalent required for lipid and nucleotide synthesis as well as for maintaining GSH in the reduced state.

Glutamine itself also influences a number of signaling pathways that contribute to tumor growth, in part through maintaining activation of the mTOR kinase, a major component of the (PI3K)-AKT pathway. Myc activation has also recently been found to induce glutamine addiction in certain cancer cell lines[96, 97]. Specifically, Myc can render tumor cells dependent on glutamine uptake to sustain their viability by directly regulating the levels of the glutamine transporter *slc1a5* and indirectly regulating *gls1* (glutaminase) expression through miR-23a/b[92, 96, 98, 99]. Glutaminase is a key glutaminolytic enzyme that converts glutamine to glutamate and whose expression is required for tumor growth[100, 101]. While MYC amplification is linked to aggressive tumor behavior and poor prognosis[102-111], to date no association has been established between increased glutamine metabolism and breast cancer recurrence. Establishing such a connection could suggest new avenues for diagnostic and targeted therapeutic strategies in breast cancer recurrence.

Lipid Biosynthesis is Tumorigenesis

Another characteristic feature of cancer cells is increased lipogenesis, the process by which acetyl-coA is converted to lipids. Increased lipid biosynthesis is of particular importance with its key contribution to membrane synthesis in rapidly proliferating cancer cells, as well as its role in forming the backbone for lipid-based signaling molecules[112]. In lipogenesis, glucose-derived pyruvate enters the TCA cycle through it conversion to acetyl-coA, a reaction catalyzed by pyruvate dehydrogenase (PDH). This, in turn, is condensed with oxaloacetate to produce citrate by citrate synthase. Citrate is then exported into the cytoplasm where it is converted back to acetyl-coA by ATP citrate lyase (ACL), the entry point to lipogenesis.

Emerging evidence also suggests a contribution of glutamine-derived carbon to citrate production under hypoxic conditions[113]. This occurs through a process termed reductive carboxylation where glutamine carbon is consumed while proceeding in the "reverse" direction in the TCA cycle to act as a major contributor to citrate production and lipid synthesis in glutamine-dependent cancer cells subjected to hypoxic conditions.

A number of oncogenic signaling pathways are involved in regulating lipid metabolism. In Particular, the PI3K-(AKT) pathway as well as the MAPK pathway have each been found to play a role in lipid biosynthesis, through regulation of SREBP-dependent transcription of several key lipogenic enzymes, primarily ATP citrate lyase (ACL) and fatty acid synthase (FAS)[114, 115]. Due to its importance in the synthesis of cholesterol and fatty acid synthesis, ACL is an especially promising therapeutic target in cancer cells. FAS catalyzes the reaction in lipogenesis that leads to the production of fatty acids. Both ACL and FAS have been shown to be required for cancer growth within

the context of AKT-driven tumors. ACL knockdown reduces the rate of tumor growth in vivo[116, 117]. Similarly, FAS inhibition results in the reduced proliferation of tumor cells both in vitro and in vivo[118].

While modulation of lipid metabolism is increasingly seen as a promising approach to cancer treatment, the role of lipogenesis in cancer progression remains less understood. Further research in this area is warranted to explore changes in the lipogenic phenotype, if any, that accompany cancer progression. Identifying such changes could help elucidate novel therapeutic targets in cancer progression and recurrence.

1.3 Thesis Objectives

The goal of this work was to identify the metabolic changes that occur during breast cancer progression. Specifically, we proposed to use ^{1}H Magnetic Resonance Spectroscopy (MRS) and ^{13}C MRS for the in vivo study of alterations in cellular metabolism that occur during breast cancer progression. Magnetic resonance-based results were subsequently used to guide the implementation of an integrative metabolomics approach, where we further characterized the observed metabolic phenotypes using mass spectrometry, gene expression profiling, biochemical assays and functional genetic experiments to better understand the metabolic and genetic regulation of breast cancer recurrence. These studies were pursued through three aims:

SA1: Identify the evolving metabolic profile of mammary tumors during breast cancer progression using ^{1}H MRS.

SA2: Identify the molecular basis and role of differential glutamine uptake and metabolism during breast cancer recurrence.

SA3: Investigate the molecular basis and role of differential lactate production during breast cancer recurrence.

Understanding the metabolic dependencies of cancer cells during breast cancer recurrence will further our understanding of cancer progression. This has the potential to pave the way for the identification of early diagnostic markers of recurrence as well as prognostic markers and therapeutic targets that could be used to improve the care and outcome of women with breast cancer.

CHAPTER 2

Magnetic Resonance-based Integrative Metabolomics: Design and Implementation of a Systems Engineering-based Approach

2.1 Introduction

In this chapter, we aim to design and implement a process-based system to establish a structured and optimizable framework that allows for better understanding of the metabolic and genetic regulation of breast cancer recurrence. In an effort to achieve this end, we use a systems engineering-based approach as a guiding strategy. Systems engineering is an interdisciplinary engineering field that focuses on solving complex technical problems. It often involves working on projects residing at the intersection of different technical fields and typically necessitates the coordination of teams with diverse scientific backgrounds. In systems engineering, the basic principles of addressing a given problem consist of a 3-step approach: 1) define the problem and its components; 2) develop and deploy a system aimed to solve the problem at hand; and 3) assess, validate and optimize the performance of the proposed system. Among those, the development of a system is the most crucial step of this process. A system consists of a group of components that work together to achieve a specific purpose. Proposed systems can be process-oriented, product-oriented or service-oriented. Here, we attempt to design a process-oriented system to define a structured framework for understanding the metabolic and genetic regulation of breast cancer recurrence.

The first step in a systems engineering development approach involves decomposing the problem at hand into smaller measurable components. For our purposes, those can consist of:

1. Identifying the metabolic differences between primary and recurrent tumors in a mouse model of breast cancer recurrence
2. Investigating the precise dysregulated steps in the identified metabolic pathways
3. Identifying the underlying molecular/genetic determinants of the observed metabolic changes
4. Assessing the functional effect of the identified changes on tumorigenesis
5. Investigating the translational potential and relevance of our findings to human breast cancer

The second step of the systems engineering approach consists of analyzing and proposing individual solutions to each of the identified components. Here, we propose the following solutions to each of the steps identified above:

1. Unsupervised metabolic profiling using ^{1}H Magnetic Resonance Spectroscopy to identify metabolic differences between primary and recurrent tumors
2. Pathway-focused characterization of key dysregulated steps and fluxes using ^{13}C-labeling experiments followed by Mass Spectrometry and/or ^{13}C-Magnetic Resonance Spectroscopy
3. Genetic expression profiling at the mRNA and protein level and enzyme activity assessment of potential underlying molecular/genetic determinants of observed changes

4. Genetic engineering of cells to modulate expression levels of identified genetic changes in order to assess their role in tumor growth and progression
5. Computational biology and statistical modeling using microarray and outcome data in human cancers to assess the clinical translational potential of a given metabolic observation

In this approach, we rely on established metabolic engineering strategies to derive insights about breast cancer progression. By detecting dysregulated metabolites using ^{1}H-MRS, we first identify, on a macroscopic level, metabolic alterations that accompany tumor recurrence across multiple pathways. Subsequently, pathway-specific characterization is performed using isotopic tracers. Metabolism of these tracers generates a pool of labeled metabolites with various levels of enrichment that reflect the metabolic state of the pathway catabolizing the labeled substrate. Analysis of the enrichment distribution enables identification of kinetic limiting steps in a given pathway and sheds light on genetic modifications that might underlie the observed metabolic changes. The identified genetic underpinning is further interrogated using biochemical and molecular biology techniques to assess its functional role in tumor growth and progression as well as its translational potential.

Combined, the above two steps enable development of the functional architecture of the proposed process-based system. Lastly, the final step of the systems engineering approach involves aggregation of the proposed solutions to ensure that the combined product of the system provides an adequate and measurable solution to the problem at hand. Using the system proposed above, the final outcome for a metabolic observation that successfully fulfills each of the components of this process-based system, will result in a well-characterized metabolic dysregulation that exerts a functional effect on

tumorigenesis, as well as evidence for potential clinical relevance. In aggregate, this should result in a better understanding of the metabolic and genetic regulation of breast cancer recurrence.

The interdisciplinary approach articulated above, which we will term **magnetic resonance-based integrative metabolomics**, will combine molecular biology, biochemistry, computational biology, imaging, statistical modeling, clinical science and engineering principles and is envisioned to allow for rigorous assessment of the diagnostic, prognostic and predictive potential of a given metabolic observation. Ultimately, a measurable outcome of this system could include the clinical translation of a metabolic finding identified and characterized using this approach.

In this chapter, we expand on the individual steps of this approach and present a technical overview of some of the underlying technical concepts necessary for the adoption of this system. A schematic of the proposed system is shown is Figure 1 and each step is discussed in further detail in what follows.

2.2 Proposed Approach

I. Unsupervised Magnetic Resonance-based Metabolic Profiling

Magnetic resonance spectroscopy (MRS) is a widely used technique to monitor total metabolite concentrations in vivo and in tissue samples[119, 120]. MRS exploits the magnetic properties of NMR active nuclei. For instance, nuclei with spin quantum number ½ (such as ^{1}H and ^{13}C) can orient themselves either parallel (‘‘spin up’’) or anti-parallel (‘‘spin down’’) to an externally-applied magnetic field. The net magnetization and the available NMR signal are proportional to the population difference between the

two states. By convention, an external magnetic field is assigned to act along the z-axis of a 3-dimensional frame of reference. Thus, at thermal equilibrium, the spins of NMR-active nuclei exhibit a net magnetization along the z-direction. In magnetic resonance spectroscopy, a 90-degree radio frequency (RF) pulse is typically applied to a sample placed in a magnetic field. This rotates the net magnetization from the z-direction to the y-direction. The spins subsequently precess about the z-axis while simultaneously relaxing to align back along the original direction of the externally-applied magnetic field. The behavior of spins placed in a magnetic field and subjected to RF excitation can be described using the Bloch equations:

$$\frac{dM_x}{dt} = \gamma M_y B_o - \frac{M_x}{T_2}$$
$$\frac{dM_y}{dt} = -\gamma M_x B_o - \frac{M_y}{T_2}$$
$$\frac{dM_z}{dt} = -\frac{(M_z - M_O)}{T_1}$$

where gamma corresponds to the gyromagnetic ratio; Mx, My and Mz correspond to the magnetization along the x,y and z directions, respectively; Bo is the externally-applied magnetic field; T_1 is the spin-lattice relaxation and T_2 is the spin-spin relaxation.

Following RF excitations, as the spins relax to align along the externally-applied magnetic field, they generate RF pulses that are collectively detected by the NMR system as a free induction decay (FID) signal. This signal, which represents the behavior of spins as a function of time, is a convolution of the RF pulses being emitted by the decaying spins. Applying a Fourier transform operation to the resulting FID leads to the generation of the 1D NMR spectrum that represents each of the component resonance frequencies of the molecules present in a sample. Each peak (or collection

of peaks) in a spectrum represents the resonance frequency of one specific nucleus in a particular species of molecule.

When ^{1}H MRS is applied to study the metabolism of a tissue sample, the spectrum typically consists of multiple frequency components due to the many detectable molecular constituents of the tissue. Of note, different components can possess molecular groups with similar chemical shifts allowing their peaks to overlap, which can limit the utility of these spectra for the detection and quantification of certain compounds within tissues.

^{1}H MRS permits the identification and quantification of a relatively large number of metabolites that are present in tumor samples. The area under each peak is proportional to the molar concentration of the molecule identified at a specific chemical shift on the spectrum. This approach provides an unsupervised metabolic profiling technique, where we are able to broadly screen and identify metabolic differences between primary and recurrent tumors in a mouse model of breast cancer recurrence. Those differences can then be further assessed using pathway-specific characterization.

Other unsupervised metabolic profiling techniques are also available, such as mass spectrometry. These can also be alternatively pursued for this step of the process for yet broader metabolic screening.

II. Pathway-focused Metabolic Characterization Using ^{13}C-Labeling Experiments

In order to better characterize pathway-specific metabolic dysregulation in primary and recurrent tumors, we propose the implementation of ^{13}C-labeling experiments. In these experiments, a ^{13}C-labeled tracer is infused into mice bearing primary or recurrent tumors. Tumors can then be dissected and ^{13}C isotopic enrichment as well as positional labeling assessed. This technique allows for the construction of a metabolic flux map for

a specific compound and provides information about the amount and distribution of each labeled metabolite in a given pathway. The two most-widely used techniques for this purpose are mass spectrometry and ^{13}C-MRS. MRS is the preferred technique when determination of positional labeling in a compound is desired. Mass spectrometry (MS), on the other hand, provides information about the amount of ^{13}C-enrichment of individual metabolite isotopomers with no information on which carbon is labeled within a molecule. The information provided by MS and ^{13}C-MRS studies can be highly complementary in metabolic studies.

The basis of ^{13}C-MRS is similar to that described above. In mass spectrometry, samples are typically first derivatized and fractionated by liquid or gas chromatography. Following fractionation, samples are ionized by electron impact. The resulting ions are subsequently characterized based on their mass to charge ratio (m/z). With ions typically carrying a single charge, the fragments are separated based on their molecular weight. The typical MS spectrum contains a number of peaks corresponding to different fragments of a given compound. Mass isotopomers are molecules that have incorporated the same number of labeled atoms. They are usually denoted by M0 (no label incorporation beyond natural abundance), M+1 (molecule has incorporated 1 labeled carbon), M+2 (molecule has incorporated 2 labeled carbons) etc... ^{13}C-enrichment is typically reported in molar percent enrichment (MPE), reflecting the mol fraction (%) of analytes containing ^{13}C atoms in excess of natural abundance, where:

$$\text{MPE } (M+i) = \% \, A_{M+i}/[A_M + \Sigma \, A_{M+i}]$$

A_M and A_{M+I} represent the peak area from MS ions corrected for natural abundance and corresponding to the unlabeled (M0) and ^{13}C-labeled (M+i) mass isotopomers, respectively. The number of labeled carbons in a molecule can sometimes provide

information about the direction in which a pathway is proceeding, such as in the case of reductive carboxylation in the TCA cycle. The extent of labeling can provide information about the flux in a specific pathway as well as help identify any potential dysregulated enzymatic steps.

In this work, we use ^{13}C-MRS when looking for compounds with relatively high concentration in tumors, allowing for their easy detection by MRS. In these cases, compounds labeled at only one or two carbons are used and positional labeling and concentration are assessed by following the label on the NMR spectrum through some of the successive steps of the given pathway.

On the other hand, when attempting to investigate metabolic flux and trying to characterize individual enzymatic steps known to yield low-concentration products, MS is used. In those cases, we use uniformly labeled compounds to assess the amount of labeling and the isotopomers present for each metabolic step in a given pathway. The combination of ^{13}C-MRS and MS following tracer infusion allows for a focused approach to identify key steps within a pathway where metabolism might be dysregulated in primary and recurrent tumors.

Another emerging technique that could further aid in this step of our approach is hyperpolarized magnetic resonance spectroscopy. This technique allows the characterization of single enzyme-characterized reactions in real-time following the injection of a hyperpolarized ^{13}C-tracer. Future studies will seek to incorporate this technique to further refine our proposed approach.

III. Genetic Profiling of Potential Underlying Determinants of Observed Metabolic Changes

Once a key dysregulated metabolic step is identified in a metabolic pathway, assessing its underlying molecular determinants constitutes the next step in our proposed approach. To achieve this end, we perform expression profiling of the genes expressing the key enzymes known to catalyze the identified dysregulated metabolic reactions. Expression profiling is done at both the mRNA as well as the protein level to account for any post-translational modifications that might underly the observed metabolic changes. mRNA levels are assessed by qRT-PCR and protein levels are assessed by immunoblotting.

Changes in metabolite levels can also result solely from changes in enzymatic activity, rather than gene expression. To address this possibility, we also perform enzymatic activity assays and zymography experiments. Enzymatic activity assays allows the user to measure the rate of conversion of a given metabolite into a product while measuring a surrogate of the reaction rate constant. Zymography, on the other hand, provides for a mean to isolate different isozymes of a given enzyme and to assess their individual activity. These techniques can be complementary depending on the enzyme being investigated.

Finally, in order to establish a direct association between a given metabolic change and an identified change in gene expression, we genetically engineer primary and recurrent tumor cells to downregulate or overexpress the gene in question. This is followed by assessment of the levels of the associated metabolite relative to its levels in control cells. A change in the metabolite levels in the expected direction in the context of gene expression level modulation establishes the identified genetic change as the most likely molecular determinant of the changing metabolite level.

IV. Assessment of the Functional Effect of the Identified Metabolic and *Genetic Change*

Once a genetic change is identified and characterized, the next step consists of assessing the functional role of this change in tumorigenesis. This can be achieved through orthotopic tumor experiments where genetically-engineered cells, in which the expression level of the metabolic gene of interest has been modulated, are injected into the mammary fat pads of immunocompromised mice. The effect of gene modulation on tumor growth can then be followed and assessed. Differences in the growth rates of tumors with gene downregulation (or overexpression) relative to controls indicates a functional role for the identified metabolic and genetic alteration in tumorigenesis. Furthermore, we also perform a tumor recurrence assay to assess the effect of metabolic gene modulation on the complex phenotype of tumor regression and recurrence. The details of this assay are detailed in Chapter 6.

If a functional effect is demonstrated, we proceed to identify the mechanism that might underlie the observed metabolic and genetic change as well as to characterize the molecular pathway by which the observed metabolic and genetic changes might contribute to tumorigenesis and/or recurrence. This can enable the identification of upstream metabolic regulators that could serve as useful therapeutic targets.

V. Assessment of the Translational Potential of a Functional Metabolic and Genetic Finding

In an effort to assess the translational potential of an identified functional metabolic and genetic finding, we conduct human association analysis where we assess the effect of the expression of the identified metabolic gene on prognosis in human breast cancer datasets. In this work, we investigate the correlation between metabolic gene

expression from microarray data and recurrence-free survival in breast cancer patients. This is done following the stratification of patients into cancer subtype-specific subsets to reduce the contribution of confounding variables. Most of this analysis is conducted in node-negative patients and patients not treated with chemotherapy in order to evaluate the effect of each gene on outcome data, independent of those variables. In the context of this analysis, identifying a correlation between metabolic gene expression level and outcome using Cox proportional hazards modeling indicates a potential prognostic role for a metabolic change in breast cancer patients. Eventual clinical translational, however, will require proving that a newly-identified marker can add to existing clinicopathological prognostic markers. In this work, we show a proof-of-concept of such an approach at the end of chapter 7.

Further clinical translational can also be assessed by investigating whether the identified metabolic gene can act as a predictive marker for response to therapy. Such an analysis will necessitate access to datasets of treated patients with available outcome data of partial versus complete pathologic response post-treatment. Finally, one can also assess the translational potential of a metabolic finding where imaging techniques can be developed and assessed for a potential role either in the early detection of tumors upregulating a specific metabolic pathway or monitoring response to therapies targeted against that pathway.

2.3 System Impact and Validation

In summary, our proposed systems-based approach, magnetic resonance-based integrative metabolomics, involves combining multi-disciplinary techniques to address the problem of understanding the metabolic and genetic regulation of breast cancer recurrence. By combining molecular biology, biochemistry, computational biology,

imaging, statistical modeling, clinical science and engineering principles, our system provides a top-down framework for the assessment of the clinical and functional relevance of specific pre-clinical metabolic observations. It is our hope that this approach will lead to better avenues for clinical translation of newly identified functional metabolic and genetic findings and better aid in the management and treatment of cancer patients.

In what follows, we attempt to validate and optimize our proposed system. In chapter 3, we present results of the unsupervised metabolic profiling of primary and recurrent tumors conducted in our mouse model using ^{1}H-MRS. In chapters 5 and 6, we validate the remaining steps of our approach by studying the roles of glutaminolysis and lactate metabolism in breast cancer recurrence. This is followed by an assessment of the translational potential of findings from those studies.

2.4 Figure Legend

Figure 1. Magnetic resonance-based integrative metabolomics: functional architecture of the proposed process-based system to better understand the metabolic and genetic regulation of breast cancer recurrence. Presented is the proposed multi-step algorithm aimed to address the problem at hand. Following systems engineering conceptual frameworks, the algorithm consists of 3 key steps: 1) problem formulation; 2) the proposed multi-step process-based system; and 3) system assessment, optimization and validation.

2.5 Figures

Figure 1

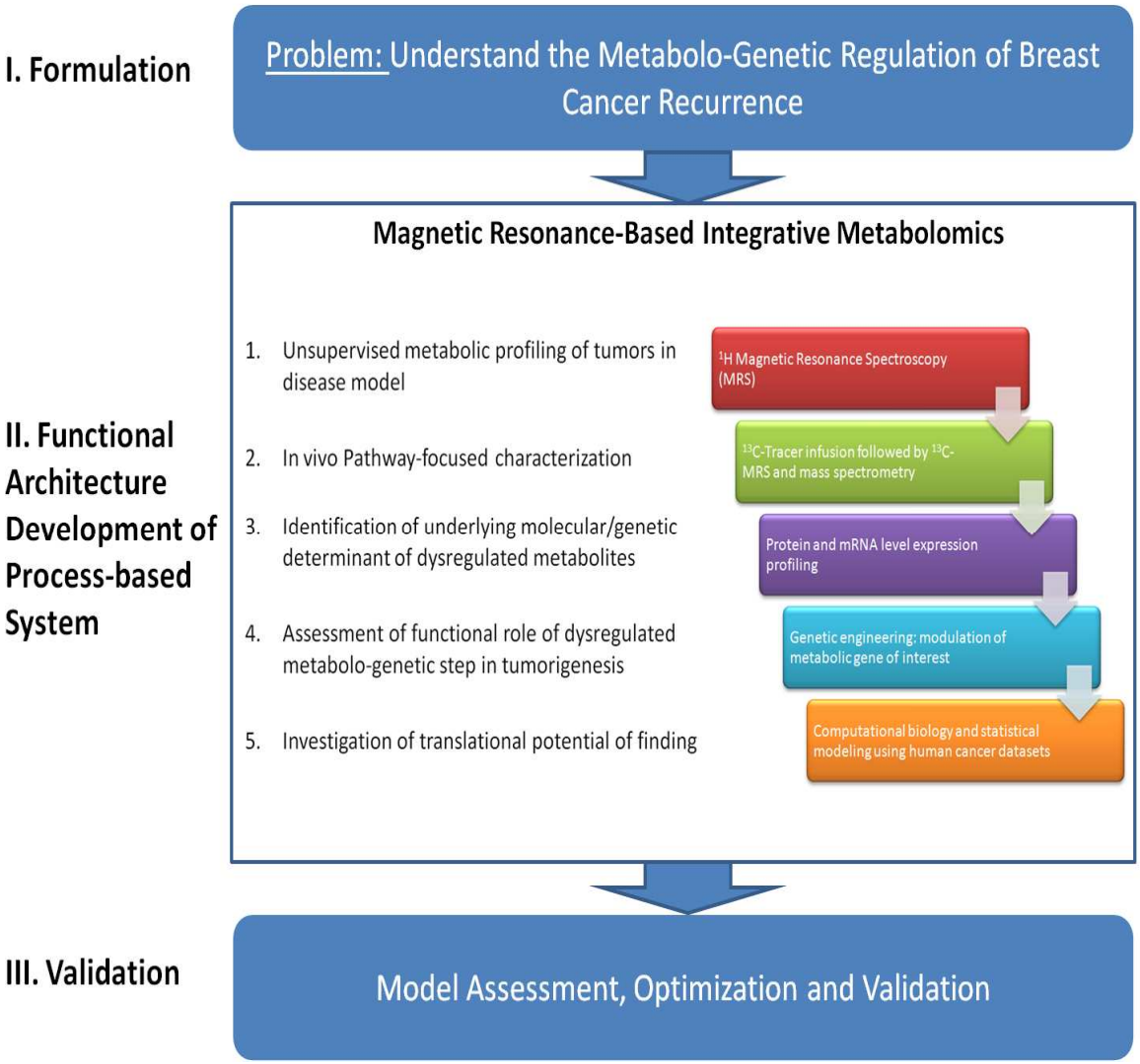

CHAPTER 3

Metabolic and Genetic Profiling of Mammary Tumor Recurrence using ^{1}H Magnetic Resonance Spectroscopy

ABSTRACT

Tumor recurrence represents the principal cause of mortality in human breast cancer, yet little is known about its underlying molecular mechanisms. In particular, while alterations in cellular metabolism have long been recognized as a key feature of the development of primary cancers, the metabolic changes that accompany cancer recurrence are poorly understood, if at all. To address this gap, we have used ^{1}H magnetic resonance spectroscopy (MRS) in combination with expression analysis of key metabolic enzymes to identify changes in metabolism that occur during mammary tumor recurrence in genetically engineered mice. The resulting metabolic and genetic profile revealed highly reproducible alterations in recurrent mammary tumors, which displayed higher levels of lactate and glycine, lower levels of succinate and phosphocholine (PC), and a higher glutamate to glutamine ratio (glu/gln) compared to primary tumors. These characteristic changes in metabolites were accompanied by concordant changes in expression of the corresponding enzymes that control their production and consumption. Accordingly, observed changes in the levels of succinate, glu/gln, phosophocholine, glycine and lactate, were significantly correlated with higher expression levels of *Sdhb* and *Gls,* as well as lower levels of *Chka*, *Gldc* and *Ldhb*, respectively. A composite metabolic gene expression activity score based upon observed metabolic and genetic changes in recurrent mouse mammary tumors was associated with decreased relapse-

free survival in women with HER2/*neu*-positive breast cancer. In aggregate, our findings demonstrate that tumor recurrence is accompanied by pronounced and reproducible alterations in tumor metabolism. This, in turn, suggests that increased understanding of the molecular determinants underlying these metabolic alterations will provide insights into the molecular pathways that drive breast cancer recurrence, as well as aid in the identification of novel biological markers and therapeutic targets that could improve clinical outcomes in breast cancer patients.

3.1 Introduction

Breast cancer is the most commonly diagnosed malignancy as well as the leading cause of cancer mortality among women worldwide[1, 121]. While improvements in detection and treatment in recent decades have led to increases in overall survival, breast cancer recurrence remains the principal cause of death from this disease[66]. In fact, up to 20% of women with breast cancer will be diagnosed with recurrent breast cancer within 10 years of completing adjuvant treatment[122]. Nevertheless, despite the unrivaled clinical importance of breast cancer recurrence, little is known about the molecular mechanisms underlying it development.

The HER2/*neu* proto-oncogene is amplified and overexpressed in up to 25% of primary human breast cancers and its amplification is associated with aggressive tumor behavior and poor prognosis, in part due to high rates of relapse[51, 123]. Notably, HER2/*neu* amplification results in downstream activation of the PI3K-AKT signaling pathway, which plays a central role in the regulation of cellular metabolism[67, 68, 71, 72]. However, while the role of dysregulated cellular metabolism in primary cancer

development has been a focus of intense investigation, the metabolic changes that accompany breast cancer recurrence are poorly understood[73-75, 124]. While some studies have examined the association between metabolism and histopathologically-based prognostic features of primary breast cancers[125-127], or have explored predictive models for the early detection of recurrent breast cancer based on metabolic profiles in patient sera[128-131], to date no direct comparisons of the metabolic features of primary and recurrent human breast cancers have been reported.

To address this question, we have employed a mammary-specific, doxycycline-inducible bitransgenic mouse model for HER2/*neu*-induced breast cancer that accurately recapitulates key features of human breast cancer progression, including primary tumor development, tumor dormancy and tumor recurrence [63, 66, 132]. In this study, we have used ^{1}H Magnetic resonance spectroscopy (MRS) to identify metabolic changes that accompany mammary tumor recurrence in mice bearing HER2/*neu*-induced mammary tumors, elucidated some of the molecular determinants that might underlie those changes, and examined the association between the observed metabolic changes and relapse-free survival in women with HER2/*neu*-positive breast cancer. These studies provide new insights into the metabolic alterations that accompany breast cancer progression.

3.2 Methods

Mouse model

Primary and recurrent mouse mammary tumors were generated in MMTV-rtTA;TetO-HER2/*neu* (MTB/TAN) doxycycline-inducible bitransgenic mice as previously

described[63, 66, 132]. HER2/*neu* expression was induced in MTB/TAN mice by the addition of 2 mg/mL doxycycline. Tumors that reached a size of approximately 1 cm x 1cm were dissected and immediately clamp-frozen in liquid nitrogen. Nine primary mammary tumors and nine recurrent mammary tumors were harvested from a cohort of 18 MTB/TAN mice, along with normal mammary tissue from three un-induced MTB/TAN mice. All animal experiments were performed in accordance with protocols approved by the University of Pennsylvania institutional animal care and use committee (IACUC).

Sample preparation

Frozen tissue samples weighing 200±50 mg were homogenized in ice-cold 12% perchloric acid. Care was taken to avoid including visibly necrotic areas of tumors. After homogenization, samples were centrifuged at 15,000 g for 10 min. The supernatant was collected and neutralized with KOH. Samples were then centrifuged at 15,000 g for 10 min and supernatants were collected and lyophilized. Lyophilized samples were dissolved in 0.6 ml D_2O before introduction into a 5-mm NMR tube for spectroscopic analysis.

^{1}H NMR spectroscopy

NMR spectroscopy was performed at 400MHz on a Bruker Avance DMX 400 wide-bore spectrometer. Fully relaxed proton spectra were acquired with a 5 mm inverse probe using the following conditions: PW 45º, TR 8s, water saturation during the relaxation delay, 6775 Hz SW, TD 64k and 64 scans. An external standard made of trimethylsilylpropionic acid (TSP) was introduced into the NMR tube and used as a

chemical shift reference and as a quantification standard. Metabolite resonance assignments were estimated based on previously published spectra in breast cancer tissue[133]. The resonance assignments used in this study are listed in Table 1. Analysis of collected NMR spectra was performed using NUTS (Acorn NMR Inc). Peak integrals were computed for each metabolite and normalized to the number of contributing protons per molecule, to tissue weight, and to the known concentration of the TSP external standard to allow for inter-sample comparison. Metabolite concentrations are provided as µmol/gram of wet weight of tissue.

RNA isolation and qRT-PCR

Snap-frozen primary and recurrent mammary tumor tissue samples were homogenized to prepare for RNA extraction. RNA isolation was performed using the RNeasy RNA isolation kit (Qiagen) according to the manufacturer's protocol. The cDNA High Capacity Reverse Transcriptase Kit (Applied Biosystems) was used for reverse transcription according to the manufacturer's protocol starting from 2 µg of RNA. qRT-PCR was performed using the resulting cDNA. qRT-PCR analysis was carried out on the Applied Biosystems 7900 HT Fast Real-Time PCR system using 6-carboxyfluorescein–labeled Taqman probes (Applied Biosystems). qRT-PCR analysis was performed on the 9 recurrent tumors profiled in this study and 8 primary tumors. Sufficient tissue was not available for one of the primary tumors.

Principal component analysis

Principal component analysis was performed using Matlab (Mathworks Inc.). Briefly, the loadings and scores were computed from a matrix that included metabolite levels for the 14 metabolites analyzed for each of the 21 samples included in this study. The outputted scores represent the principal components. For the analyzed dataset, a scree plot revealed that the first 3 components explained 94% of the observed variance. Accordingly, a plot of the first three principal components is presented.

Statistical analysis

Statistical significance was determined using a two-tailed Student's t-test. Univariate linear regression to assess the correlation between gene expression levels and metabolite levels was performed using Matlab (Mathworks Inc.). Pearson analysis was used to assess the extent of correlation. The significance of the t-test and of the Pearson correlation analysis was determined at $p<0.05$.

Metabolic gene expresion signature generation and human association analysis

A tumor metabolism gene expression signature was generated from the qRT-PCR data of the six profiled metabolic enzymes whose mRNA expression levels exhibited differences between primary and recurrent breast tumors in the MTB/TAN mouse model. The six metabolic enzymes whose expression was included in the signature were Ldhb, Gldc, Phgdh, Gls1, Sdhb, Chka. The metabolic gene expression signature was used to assess the combined activities of these enzymes in microarray data of mouse and human breast tumors using a previously described scoring system[134]. The signature

was validated using a set of 10 primary and recurrent MTB/TAN mammary tumors from another study. Prognostic value of this six-gene signature was subsequently assessed in 943 lymph node-negative patients who did not receive any systemic adjuvant treatment.

In the human association analysis, five human breast cancer microarray data sets[135-139] profiled using the Affymetrix HG-U133A platform were downloaded from Gene Expression Omnibus and RMA-normalized individually. 943 lymph node-negative patients who did not receive any systemic adjuvant therapy were identified from these five data sets according to available clinical information. Microarray data for these patients were mean-centered by gene within each data set and combined into one data set. HER2-positive status was approximated by visual inspection of the rank plot of HER2 mRNA level, and defined as samples having mean-centered log2 expression greater than 1. Patients were assigned to either a high scoring or a low scoring class based on their metabolism signature scores. The cutoff between high- and low-scoring classes was determined by an outcome-oriented approach[140]. Differences in 5-year relapse-free survival between the two classes was assessed by p-value from the log-rank test and hazard ratio from Cox proportional hazards regression. To guard against a high false-positive rate resulting from multiple testing, a corrected p-value was also calculated as part of the cut-point determination step[140]. These analyses were performed specifically for the HER2-positive subset of patients. All data analyses were performed in the R environment[141].

3.3 Results

To identify metabolic differences between primary and recurrent mammary tumors in a genetically defined model system, we made use of a previously described doxycycline-dependent genetically engineered mouse model for HER2/*neu*-induced mammary tumorigenesis[63, 66]. In this model, the reverse tetracycline-dependent transcriptional activator, rtTA, is specifically expressed in the mammary epithelial compartment of MMTV-rtTA (MTB) transgenic mice under the control of the mouse mammary tumor virus promoter/enhancer[132]. When interbred with TetO-HER2/*neu* (TAN) transgenic mice, in which expression of an activated allele of the rat HER2/*neu* proto-oncogene is controlled by the tet operator, administration of doxycycline to MTB/TAN bitransgenic mice results in binding of activated rtTA to the tet operator, and expression of the HER2/*neu* transgene in mammary epithelial cells[63].

Activation of HER2/*neu* in MTB/TAN mice results in mammary epithelial hyperplasia and the eventual development of primary mammary tumors that are addicted to HER2/*neu* expression[63]. Consequently, when doxycycline is withdrawn, the resulting acute downregulation of HER2/*neu* pathway activity results in the regression of mammary tumors to a non-palpable state, akin to the treatment of women with HER2/*neu*-amplified breast cancers with a targeted agent that blocks HER2/*neu* activity[63]. Also akin to human breast cancer patients, primary mammary tumors that regress to a non-palpable state following doxycycline withdrawal subsequently recur with stochastic kinetics following a variable latent period that mimics human tumor dormancy (Figure 1A)[66]. Recurrent mammary tumors in this system do not re-activate the HER2/*neu* transgene, but rather escape their dependence on HER2/*neu* signaling by activating alternate growth and survival pathways[66].

Primary and recurrent mammary tumors exhibit different metabolic profiles

We compared the metabolic profiles of primary mammary tumors arising in doxycycline-induced MTB/TAN mice with recurrent mammary tumors that had arisen in MTB/TAN mice harboring primary tumors that had regressed to a clinically undetectable state following doxycycline withdrawal, and had then recurred in the absence of doxycycline.

Tumors that reached a size of approximately 1 cm were dissected, clamp-frozen and homogenized in ice-cold perchloric acid. Following centrifugation and neutralization of supernatants with KOH, lyophilized samples were dissolved in D_2O. ^1H NMR spectroscopy was performed at 400MHz on a Bruker Avance DMX 400 wide-bore spectrometer and fully relaxed proton spectra were acquired with a 5 mm inverse probe. Trimethylsilylpropionic acid (TSP) was introduced as an external standard and used as a chemical shift reference and quantification standard.

Metabolite resonance assignments were estimated based on published spectra in breast cancer tissue[133] and are listed in Table 1. Analysis of collected NMR spectra was performed using NUTS (Acorn NMR Inc). Peak integrals were computed for each metabolite and normalized to the number of contributing protons per molecule and to tissue weight, as well as to the known concentration of the TSP external standard to enable inter-sample comparison. Metabolite concentrations were calculated as µmol/gram of wet weight of tissue.

^1H MRS metabolic profiling of 9 primary and 9 recurrent mammary tumors from a cohort of 18 MTB/TAN mice revealed clear differences in spectroscopic features between primary and recurrent mammary tumors (Figure 1B). The spectroscopic profiles of tumors were also distinct from those of un-induced mammary glands in which the HER2/*neu* oncogene had not been activated. Quantification of fourteen metabolites

in the ^{1}H spectra of each tumor yielded eight metabolites that exhibited statistically different levels ($p<0.05$) between primary and recurrent tumors (Table 2). Specifically, when compared to primary mammary tumors, recurrent tumors displayed higher levels of lactate, glutamate, taurine and glycine, and lower levels of succinate, glutamine, phosphocholine and myo-Inositol. Alanine, acetate, creatine, choline, glycerophosphocholine and formate levels were unchanged. Further analysis also revealed a higher glutamate to glutamine ratio (glu/gln) and a higher glycine to creatine ratio (Gly/Cr) in recurrent tumors compared to primary tumors. No changes were observed in the ratio of alanine to creatine (Ala/Cr) or the ratio of total choline (the sum of the choline, phosphocholine (PC) and glycerophosphocholine (GPC) integrals) to creatine (tCho/Cr).

Principal component analysis performed on the fourteen quantified metabolites in each spectrum revealed distinct metabolic signatures of primary tumors, recurrent tumors and un-induced mammary glands (Figure 1C). Unsupervised dimensionality reduction of the metabolic data into three orthogonal components led to consistent clustering of the twenty-one analyzed tissue samples by tumor/gland type in principal component space.

Lactate levels increase during mammary tumor recurrence

Recurrent mammary tumors exhibited higher lactate levels than primary tumors. Therefore, we sought to determine the potential underlying molecular determinant of these observed changes. A number of steps in the glycolytic pathways have been previously implicated in dictating cellular lactate levels. These include reactions catalyzed by pyruvate kinase isoform M2 (Pkm2), lactate dehydrogenase A subunit (Ldha) and lactate dehydrogenase B subunit (Ldhb). Pkm2 expression is associated

with increased lactate production. Ldha catalyzes the conversion of pyruvate to lactate and Ldhb is thought to be responsible for catalyzing the reverse reaction of lactate to pyruvate conversion. Quantification of the expression levels of each of the above genes by qRT-PCR revealed similar expression levels of *Ldha* and *Pkm2* in primary and recurrent tumors ($p>0.05$). *Ldhb* expression, however, was downregulated in recurrent tumors compared to primary tumors ($p<0.05$) (Figure 2B).

Univariate linear regression to examine the correlation between lactate levels and the expression of each of the above genes in the analyzed tissue samples revealed a statistically significant correlation between lactate levels and *Ldhb* expression ($r=0.556$, $p=0.017$) as well as between lactate levels and *Pkm2* expression levels ($r=0.496$, $p=0.036$) (Figure 2C). However, whereas *Pkm2* expression was unchanged during the process of recurrence, *Ldhb* expression was downregulated approximately 10-fold in recurrent tumors. As expected from the fact that Ldhb catalyzes the conversion of lactate to pyruvate, the correlation between lactate levels and *Ldhb* expression was negative (Figure 2C). Taken together, these data suggest that recurrent tumors may have higher lactate levels as a consequence of *Ldhb* downregulation.

Glycine levels increase during mammary tumor recurrence

Recurrent mammary tumors exhibit higher levels of glycine. To investigate the underlying molecular determinants of the change in glycine levels during mammary tumor progression, we examined the expression levels of *phosphoglycerate dehydrogenase* (*Phgdh*) and *glycine decarboxylase* (*Gldc*) in primary and recurrent tumors. Each of these genes has been previously implicated in regulating glycine levels during tumorigenesis. Phgdh catalyzes the conversion of the 3-phosophoglycerate glycolytic intermediate into 3-phophohydroxypuruvate contributing glycolytic carbon to

the serine biosynthesis pathway where glycine is produced (Figure 3A). Gldc is a component of the glycine cleavage system and catalyzes the breakdown of glycine into carbon dioxide and ammonia (Figure 3A). qRT-PCR revealed higher levels of *Phgdh* and lower levels of *Gldc* in recurrent tumors compared to primary tumors ($p<0.05$) (Figure 3B). Specifically, recurrent tumors exhibited an approximately 10-fold downregulation in *Gldc* expression and an approximately two-fold increase in *Phgdh* levels compared to primary tumors.

To assess the correlation between glycine levels and the expression of each of these genes, univariate linear regression was performed. Regression analysis revealed a statistically significant correlation between glycine levels and *Gldc* levels when considering all analyzed tumors ($r=0.546$ and $p=0.028$) (Figure 3C). As predicted based on the fact that Gldc catalyzes the breakdown of glycine, the correlation between *Gldc* expression and glycine levels was negative. In contrast, *Phgdh* levels were not significantly correlated with glycine levels in the analyzed tumors. Together, these data indicate that the observed upregulation in glycine levels in recurrent tumors may be due to Gldc downregulation.

Glutamine, choline and succinate metabolism exhibit marked changes during mammary tumor recurrence

Spectroscopic results revealed higher glutamate levels and lower glutamine levels in recurrent tumors compared to primary tumors. Since the inter-conversion of glutamine and glutamate is catalyzed by glutaminase (*Gls*), we sought to identify changes in glutaminase expression levels that might occur during the process of recurrence. qRT-PCR quantification of glutaminase expression revealed a modest increase in *Gls1* (referred to as *Gls* in this study) expression levels in recurrent tumors compared to

primary tumors ($p<0.05$) (Figure 4B). Univariate linear regression analysis revealed a statistically significant correlation between the ratio of glutamate to glutamine (Glu/Gln) and *Gls1* expression levels across all the tumors analyzed ($r=0.53$, $p=0.024$). Since Gls1 catalyzes the conversion of glutamine to glutamate, higher Gls1 levels are thought to be associated with: a) decreased glutamine levels reflecting increased consumption; b) increased glutamate levels reflecting increased production; and, by extension, c) increased glutamate to glutamine ratio. Indeed, the correlation between *Gls1* expression and the glutamate to glutamine ratio was positive. Combined, these data indicate that increased ratio of glutamate to glutamine observed in recurrent tumors might reflect increased glutamine to glutamate conversion due to upregulation of Gls1 expression.

In addition to changes in glutamate to glutamine ratio, recurrent tumors also exhibited lower phosphocholine levels compared to primary tumors. To investigate the molecular determinants of this change, we assessed the expression of *choline kinase α* (*Chka*) in primary and recurrent tumors. Choline kinase catalyzes the conversion of choline to phosphocholine (Figure 4A). qRT-PCR analysis revealed nearly 3-fold lower *Chka* expression in recurrent tumors compared to primary tumors ($p<0.05$) (Figure 4B). Univariate linear regression demonstrates a statistically significant correlation between phosphocholine metabolite levels and *Chka* expression ($r=0.503$, $p=0.034$) (Figure 4C). As anticipated based on the fact that Chka catalyzes the conversion of choline into phosphocholine, the correlation between phosphocholine levels and *Chka* expression was positive. Overall, our data suggest that decrease in phosphocholine level observed in recurrent tumors may be due to Chka downregulation.

Spectroscopic profiling also revealed lower succinate levels in recurrent tumors compared to primary tumors. The conversion of succinate to fumarate in the TCA cycle is catalyzed by succinate dehydrogenase. To investigate whether changes in the

expression of this enzyme might underlie observed changes in succinate levels in recurrent tumors, qRT-PCR quantification of *succinate dehydrogenase B* (*Sdhb*) levels was performed. Recurrent tumors exhibited 2-fold higher *Sdhb* levels compared to primary tumors ($p<0.05$) (Figure 4B). Univariate linear regression also showed a significant correlation between succinate levels and *Sdhb* expression levels among the tumors analyzed ($r=0.486$, $p=0.041$) (Figure 4C). As expected based on the fact that Sdhb catalyzes the conversion of succinate to fumarate, the correlation between succinate levels and *Sdhb* expression was negative. Together, the data suggest that the decreased succinate levels observed in recurrent tumors might be a consequence of increased succinate consumption due to Sdhb upregulation.

Changes in metabolism during mammary tumor recurrence in mice are associated with decreased relapse-free survival in women with HER2-positive human breast cancer

We generate a metabolic gene expression signature based on changes in expression levels of the six profiled metabolic genes whose expression differed between primary and recurrent MTB/TAN tumors examined in this study (Figure 5A). This signature was used to assign a score to individual tumors based on the expression levels of those six genes. As expected, the scores generated using this signature were higher in recurrent MTB/TAN mouse tumors compared to primary tumors, in an independent cohort of mice (Figure 5B). We then assessed the potential prognostic value of this metabolic gene expression signature assessing scores in a group of 947 human breast cancer patients with node-negative breast cancer. Since the signature had been generated and validated in a HER2/*neu*-positive breast cancer mouse model, we preformed a human association analysis in patients whose breast cancers were HER2-positive. This analysis revealed that patients whose breast cancers expressed levels of these

metabolic enzymes that most closely resembled those found in recurrent mouse mammary tumors were more likely to relapse over a 5-year period (HR=2.42, p=0.004 and $p_{corrected}$=0.007) (Figure 5C).

3.4 Discussion

In this study, we show that primary and recurrent mammary tumors display different ^{1}H MRS metabolic profiles and we correlate these metabolic changes with corresponding changes in expression levels of enzymes associated with the production or consumption of those metabolites. Specifically, recurrent tumors exhibit higher levels of lactate, glutamate, taurine and glycine, and lower levels of succinate, glutamine, phosphocholine and myo-inositol. Tumor expression levels of *Ldhb, Gldc, Gls, Sdhb* and *Chka* were significantly correlated with the levels of lactate, glycine, glutamate/glutamine, succinate and phosphocholine, respectively. Furthermore, a metabolic gene expression signature generated based on alterations in gene expression that occur during tumor recurrence in mice was associated with decreased relapse-free survival in HER2-positive breast cancer patients. Combined, these results suggest that tumor metabolism evolves during breast cancer progression and raise the possibility that changes in the expression of certain key metabolic genes may be useful for predicting clinical outcomes in breast cancer patients.

While a role for MRS in evaluating metabolism in breast cancers has previously been established through spectroscopic studies[133, 142-144], few studies have examined differences in metabolism between primary and recurrent tumors. In a study evaluating the role of ^{1}H MRS and GC-MS metabolic profiling in the early detection of breast cancer recurrence, eleven serum metabolites were identified that were able to predict breast cancer recurrence in a cohort of 56 patients[130]. Similarly, studies of human brain tumors

using ^{1}H MRS and ^{31}P MRS identified a number of metabolic changes, including those in glycine, alanine, glutamate and total choline in recurrent astrocytomas and glioblastomas[128, 129]. In agreement with those studies, our results further confirm a changing metabolic landscape during cancer progression.

In this study, we report increased lactate levels in recurrent mammary tumors in mice. Increased lactate concentrations have been correlated with metastatic spread and recurrence in cervical cancer[145] and have been shown to predict prognosis in several cancers, including brain and breast cancers[146, 147]. Spectroscopic studies examining tumor recurrence in breast cancer and brain cancer patients also reported increased lactate levels in recurrent tumors[128-130]. Our results suggest that *Ldhb* dowregulation may be one underlying molecular determinant of the observed increase in lactate levels during tumor progression. Previous studies have implicated Ldha and Pkm2 as key players in modulating lactate concentrations in tumors[83, 148]. The role of Ldhb in tumorigenesis, however, has received relatively little attention. Some have reported Ldhb downregulation and increased lactate levels in highly metastatic prostate cancer cell lines[87] and metastatic hepatocellular carcinoma[149]. We speculate that Ldhb downregulation might play a role in breast cancer recurrence. However, further studies will be needed to investigate this possibility.

Similar to our observation showing increased glycine levels in recurrent tumors in mice, higher glycine levels have been reported in recurrent astrocytomas and recurrent glioblastomas compared to their corresponding primary tumors[128]. Increased glycine production occurs when higher amounts of carbon from glycolysis are diverted into serine biosynthesis, the pathway implicated in glycine and serine production. Genetic profiling of enzymes involved in this pathway in mice revealed increased *Phgdh* levels and lower *Gldc* levels in recurrent tumors. Recent studies have identified Phgdh as a

central player in tumorigenesis and have implicated it in modulating glycine levels in a number of human cancers[150, 151]. In our study however, *Gldc*, but not *Phgdh*, was significantly correlated with glycine levels in tumor samples. Gldc is a key component of the glycine cleavage system. We speculate that lower Gldc levels might result in glycine accumulation due to reduced glycine breakdown. Recent studies suggest a role for glycine decarboxylase in tumor initiatiting cells in non-small cell lung cancer[152]. Further studies will be needed to evaluate the role of Gldc in cancer progression.

Recurrent mouse mammary tumors also exhibited increased levels of glutamate and decreased levels of glutamine, reflected in an increased glutamate to glutamine ratio (glu/gln). An increased glu/gln rato has also been reported in recurrent astroctyomas in humans[128]. Interestingly, examination of sera from patients with recurrent breast cancer showed decreased, rather than increased, glutamate levels compared to patients without recurrence[130]. We speculate that the differences in our findings might stem from the fact that our measurements were made in tumor tissue whereas decreased glutamate levels were reported in patients' sera. While tumor tissue might exhibit increased glutamate production, glutamate might not be readily secreted into the blood.

The observed increase in glu/gln ratio observed in this study could be explained by the increase in *Gls1* levels that are found in recurrent tumors. The production of glutamate from glutamine is catalyzed by glutaminase (Gls1). Here, we report increased *Gls1* levels in recurrent tumor recurrence that correlated with increases in the ratio of glu/gln. Gls1 has been identified as a key component in Myc-driven tumorigenesis[97, 98] and its expression is required for tumor growth in xerograft models[100, 153, 154]. Gls1 has not been previously implicated in the process of tumor recurrence. Indeed, to our knowledge, few studies have examined the association between changes in

glutaminolytic activity and tumor progression. Our data suggest that increased glutamine metabolism may play a role in breast cancer progression.

Another metabolic feature of tumor recurrence observed in our model was decreased phosphocholine production. Choline metabolism in tumorigenesis has been subject of intense study since the 1980s[155]. In particular, phosphocholine has been shown to be a second messenger essential for mitogenic acitivity[156]. Multiple studies have reported an association between increased choline uptake and phosphocholine production and malignant transformation[157-160], as well as progressive increases in total choline during tumor progression[125, 127]. Fewer studies, however, have reported decreased total choline or phosphocholine levels in tumors. Examination of tissue samples from recurrent brain tumors found increased total choline levels in recurrent astrocytoma, but decreased total choline in recurrent glioblastomas, compared to corresponding primary tumors[128]. Similarly, decreases in phosphocholine/glyceryl-phosphocholine ratio have been reported during mammary tumors progression from estrogen-dependent growth to estrogen-independent growth[161].

We speculate that the decrease in phosphocholine levels that we observe in recurrent mouse mammary tumors could be due to the HER2/*neu*-independent growth of recurrent tumors. Activation of the PI3K pathway has been demonstrated to upregulate Chka levels in tumors[162, 163]. In this regard, the PI3K pathway is active in primary HER2/*neu*-driven tumors, but not in recurrent tumors in our model. As predicted from this, we found decreased levels of *Chka* in recurrent mammary tumors. Chka catalyzes the conversion of choline into phosphocholine and expression levels of *Chka* correlated with the observed phosphocholine levels in the samples analyzed. While increased Chka levels and increased choline metabolism have been previously correlated with worse prognosis in human cancer[127, 164], our results suggest that decreased Chka levels

and decreased phosphocholine levels might be a feature of tumor progression in certain cancers.

Recurrent tumors exhibited lower succinate levels compared to primary tumors. Dysregulated succinate metabolism has been linked to tumorigenesis. Specifically, several studies have identified mutations in succinate dehydrogenase that result in succinate accumulation, a phenomenon that promotes tumorignenesis through the stabilization of hypoxia inducible factor (Hif)[165]. The conversion of succinate to fumarate is catalyzed by succinate dehydrogenase (Sdh). In this study, we report increased levels of *Sdhb* expression in recurrent tumors that were correlated with succinate levels. In theory, higher Sdhb levels will be expected to induce higher consumption of succinate, resulting in lower levels of succinate in recurrent tumors. Sdhb dysregulation has been previously reported in familial phaeochromocytomas and paragangliomas[166]. While we have not yet determined whether succinate dehydrogenase is mutated in recurrent tumors, we speculate that increased *Sdhb* expression may contribute to breast cancer progression.

Spectroscopic profiling of recurrent tumors also revealed decreased myo-Inositol and increased taurine levels compared to primary tumors. Previous studies have reported both increases and decreases in myo-inositol and taurine levels with malignant transformation in breast and brain tumors[128, 143, 167] as well as a decrease in myo-inositol levels as astrocytomas progress to higher grades[126]. Both taurine and myo-inositol play a role in cellullar osmoregulation[168]. Myo-inositol has also been shown to contribute to the cellullar messenger inositol polyphosphates pool[169]. However, the precise contribution of myo-inositol and taurine levels to tumorigenesis remains undefined. Based on our findings in this study, we speculate that changes in myo-inositol and

taurine metabolism might be involved in tumor recurrence either through their effect on osmoregulation and/or through the role of myo-inositol in cellullar signaling.

To begin to assess the potential clinical applicability of our findings, we generated a gene expression signature based on the expression of key metabolic enzymes identified in our study and assessed its prognostic potential in a cohort of breast cancer patients. Expression of metabolic enzymes associated with tumor recurrence in mice was associated with decreased recurrence-free survival in patients with HER2-positive breast cancers. Previous studies have suggested a role for metabolic profiling of sera samples in the prognosis assessment of patients with breast cancer[130] as well as colorectal cancer[131]. Our study further confirms that evaluation of the expression of specific metabolic enzymes could potentially aid in predicting risk of relapse in patients diagnosed with HER2-positive breast cancer.

While our study identifies a number of metabolic differences between primary and recurrent mammary tumors, our analysis was limited to fourteen metabolites detectable by ^{1}H MRS. A more comprehensive metabolic profiling study remains to be conducted using mass spectrometry for a broader view of the metabolic changes that occur during tumor progression. Furthermore, the genetic profiling component of this study was limited to assessing gene expression levels by qRT-PCR. Clearly, changes in the expression levels of metabolic enzymes are only one contributing factor to the level of enzymatic activity that can alter metabolite levels. More comprehensive future studies will be needed to directly assess changes in enzyme activity at the protein level. An additional limitation of this study is that the human association analysis focused on patients with HER2-positive breast cancers without stratification by tumor subtype or classical prognostic characteristics. Stratification of larger human datasets by tumor grade and subtype, while accounting for known clinical prognostic factors, could unveil

additional associations between changes in metabolites and breast cancer progression. Finally, this study was limited to examining steady-state metabolite levels in tumor extracts. Given that metabolism is a dynamic process, future studies using isotopic labeling experiments in vivo will be needed to gain a better understanding of the changes in metabolic pathway fluxes that might accompany tumor recurrence.

Taken together, our results suggest that tumor metabolism evolves during breast cancer progression. Specifically, recurrent tumors exhibit increased lactate levels as well as increased glutamate to glutamine ratio that may be indicative of a more active glutaminolytic phenotype. We also found increases in glycine levels that may reflect the diversion of glycolytic intermediates into serine biosynthesis. Finally, recurrent tumors also exhibited decreased phosphocholine and Chka levels. Overall, our results indicate that metabolic profiling could improve our understanding of the molecular pathways involved in breast cancer recurrence. Further assessment of these pathways might enable the identification of novel therapeutic targets as well as diagnostic or prognostic markers useful in the management of breast cancer patients.

3.5 Tables

Table 1. ^{1}H Metabolites assessed in this study. Chemical shifts are measured in reference to 3-trimethylsilylpropionate (TSP) at 0 ppm. (m:multiplet; db:doublet; GPC: glycerophosphocholine; PC: phosphocholine).

Metabolite	**Abbreviation**	**Chemical Shift (ppm)**	**Spin-Spin**	**Proton(s)**
Lactate	Lac	1.33	Doublet	CH_3
Alanine	Ala	1.47	Doublet	CH_3
Acetate	Acet	1.91	Singlet	CH_3
Glutamate	Glu	2.06	Multiplet	CH_2
Succinate	Succ	2.40	Singlet	CH_2
Glutamine	Gln	2.46	db of triplet	CH_2
Creatine	Cr	3.03	Singlet	CH_3
Choline	Cho	3.20	Singlet	$(CH_3)_3$-N^+
PC	PC	3.59	Singlet	$(CH_3)_3$-N^+
GPC	GPC	3.67	Singlet	$(CH_3)_3$-N^+
Taurine	Tau	3.25,3.41	Triplet, triplet	CH_2-N, CH_2-S
Glycine	Gly	3.97	Singlet	CH_2
myo-Inositol	Ino	3.29,3.55,4.07	Triplet, m, triplet	H5;H1,H3;H2
Formate	For	8.46	Singlet	CH-O

Table 2. Metabolite quantification in primary and recurrent mammary tumors. Results are normalized to grams of wet weight of the extracted tumor. g ww: grams of wet weight; gly: glycine; gln: glutamine; glu: glutamate; tCho: total choline; ala: alanine; cr: creatine, pc: phosphocholine, gpc: glycerophophocholine .

Metabolite	**Primary Tumor** (µmol/g ww)	**Recurrent Tumor** (µmol/g ww)	**p-value**
Lactate	7.85 ± 1.66	11.38 ± 1.40	<0.001
Alanine	2.14 ± 0.41	2.08 ± 0.34	0.372
Acetate	1.26 ± 0.92	0.83 ± 0.44	0.122
Glutamate	3.48 ± 0.37	4.45 ± 1.43	0.042
Succinate	0.61 ± 0.10	0.44 ± 0.05	<0.001
Glutamine	0.59 ± 0.19	0.32 ± 0.07	0.002
Creatine	1.82 ± 0.59	1.90 ± 0.70	0.397
Choline	0.35 ± 0.11	0.31 ± 0.06	0.172
PC	1.03 ± 0.39	0.52 ± 0.16	0.002
GPC	1.40 ± 0.40	1.26 ± 0.29	0.216
Taurine	5.20 ± 0.87	7.31 ± 2.14	0.016
Glycine	1.18 ± 0.09	2.18 ± 0.56	<0.001
myo-Inositol	4.42 ± 2.1	2.65 ± 0.66	0.020
Formate	0.99 ± 0.79	0.71 ± 0.31	0.178
Gly/Cr	0.69 ± 0.18	1.22 ± 0.45	0.002
tCho/Cr	1.61 ± 0.46	1.98 ± 2.59	0.342
Ala/Cr	1.27 ± 0.42	1.21 ± 0.47	0.385
Glu/Gln	6.74 ± 2.38	12.67 ± 1.53	<0.001

3.6 Figure Legends

Figure 1. Primary and recurrent mammary tumors exhibit different metabolic phenotypes. (A) The HER2/*neu* doxycycline-inducible bitransgenic mouse model (MTB/TAN) used in this study reproduces key features of human breast cancer progression: primary tumor development, tumor dormancy and tumor recurrence. (B) Sample spectra from an un-induced mammary gland, a primary tumor and a recurrent tumor displaying different metabolic profiles. TSP is used as an external. Spectra are shown for tissue of similar weights. TSP: 3-trimethylsilylpropionate; Lac: Lactate CH_3; Ala: Alanine CH_3; Acet: Acetate CH_3; Glu: Glutamate CH_2-4; Succ: Succinate CH_2; Gln: Glutamine CH_2-4; Cr: Creatine CH_3; Cho: Choline; Phosphocholine (PC) and Glycerophosphocholine (GPC); Ino: Inositol; Tau: Taurine CH_2-N-; Gly: Glycine; For: Formate; tCho is total choline and is the combination of choline, PC and GPC. (C) Principal component analysis conducted on the metabolites analyzed in this study confirms distinct metabolic signatures for primary and recurrent tumors. Un-induced display metabolic profiles distinct from tumors.

Figure 2. Lactate metabolism is upregulated in mammary tumor recurrence. (A) Reactions leading to lactate production in glycolysis. Only enzymes previously shown to affect lactate levels are shown. (B) Expression levels of enzymes implicated in lactate production in primary and recurrent tumors in the MTB/TAN model. (C) Correlation between lactate levels measured by proton MRS and expression levels of associated metabolic enzymes assessed by qRT-PCR. Pkm2: pyruvate kinase isoform M2; Ldha: lactate dehydrogenase A; Ldhb: lactate dehydrogenase B.

Figure 3. Glycine metabolism is upregulated in mammary tumor recurrence. (A) Reactions leading to glycine production. 3-PG is a metabolic intermediate in the glycolytic pathway. (B) Expression levels of enzymes in the pathways implicated in glycine production in primary and recurrent tumors in the MTB/TAN model. (C) Correlation between glycine levels measured by proton MRS and expression levels of associated metabolic enzymes assessed by qRT-PCR. 3-PG: 3-Phophoglycerate; 3-PHP: 3-Phosphohyroxypyruvate; Phgdh: phosphoglycerate dehydrogenase; Gldc: glycine decarboxylase.

Figure 4. Glutamine, choline and succinate metabolism exhibit marked changes during mammary tumor recurrence. (A) Reactions leading to consumption of glutamine, choline and succinate respectively. (B) Expression levels of enzymes implicated in each of the metabolic pathways in primary and recurrent tumors in the MTB/TAN model. (C) Correlation between metabolite levels or ratio measured by proton MRS and expression levels of associated metabolic enzymes assessed by qRT-PCR. Gls: glutaminase, Chka: choline kinase α; Sdhb: succinate dehydrogenase b; Gln: glutamine; Glu: glutamate.

Figure 5. High expression in human breast cancers of metabolic enzymes characteristic of recurrent mouse mammary tumors is associated with decreased relapse-free survival in HER2-positive human breast cancer. (A) A heatmap showing expression levels of 6 profiled metabolic genes whose expression differed between primary and recurrent MTB/TAN tumors. qRT-PCR expression levels of these

genes were used to generate a metabolic gene expression signature. (B) Validation of the generated metabolic expression signature in an independent set of 10 primary and recurrent tumors showing that recurrent MTB/TAN tumors exhibit higher metabolic gene expression activity score. (C) Expression of metabolic enzymes characteristic of recurrent mouse mammary tumors is associated with decreased 5-year relapse-free survival in HER2-positive breast cancer patients. Ldhb: lactate dehyrdrogenase B; Gldc: glycine decarboxylase; Gls: glutaminase; Chka: choline kinase α; Sdhb: succinate dehydrogenase b; H.R.: hazard ratio.

3.7 Figures

Figure 1

A

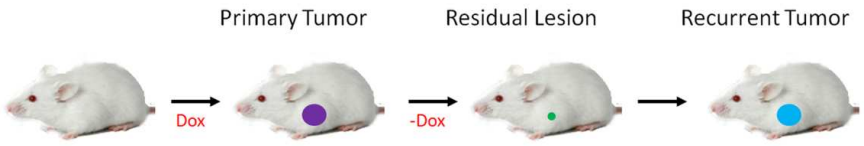

B

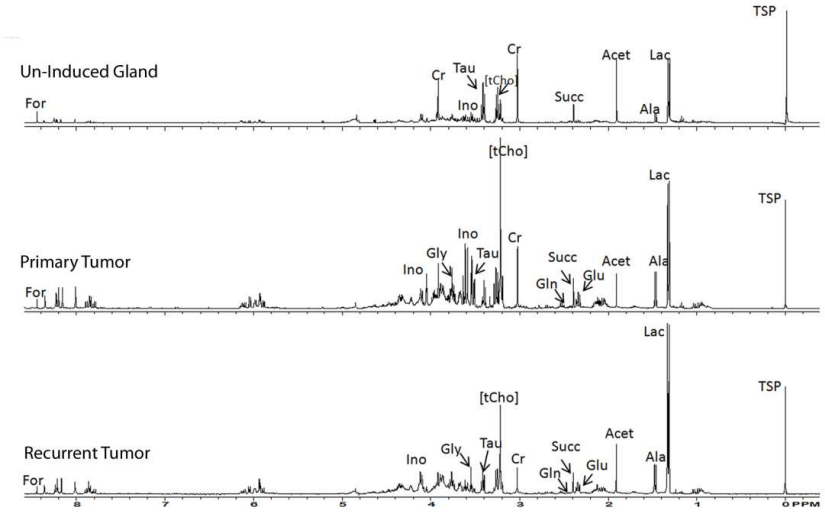

C

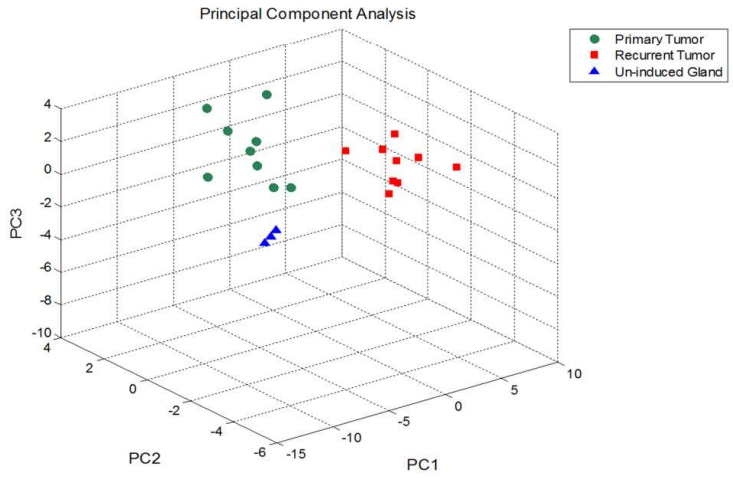

Figure 2

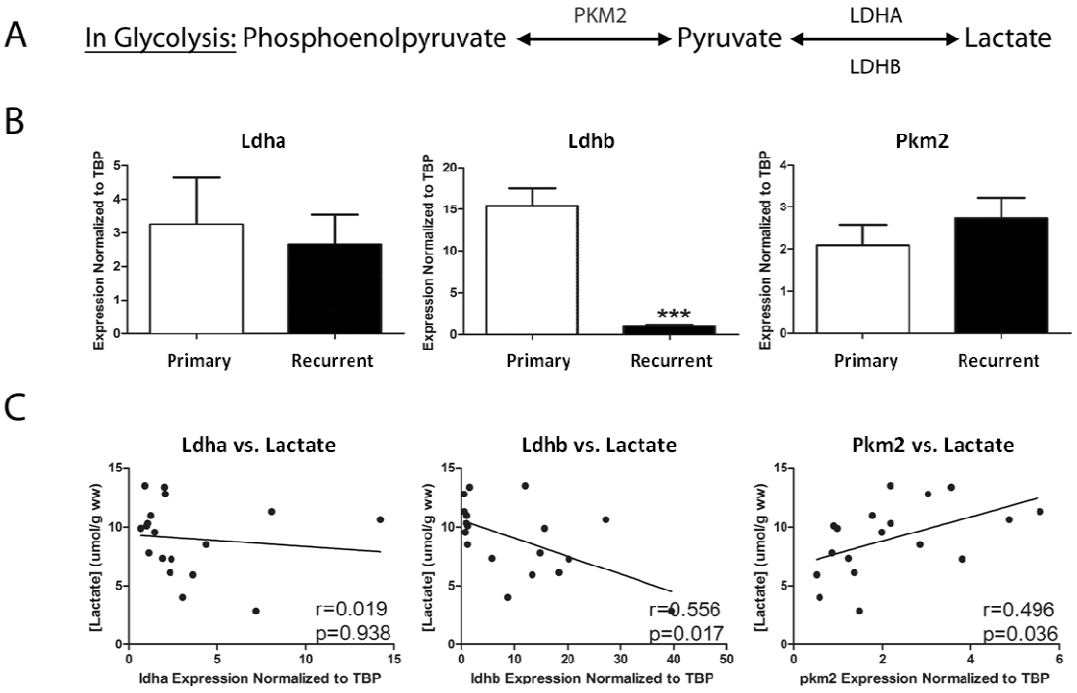
A
In Glycolysis: Phosphoenolpyruvate
PKM2
Pyruvate
LDHA
LDHB
Lactate
B
Ldha
Ldhb
Pkm2
Expression Normalized to TBP
***
Primary
Recurrent
C
Ldha vs. Lactate
Ldhb vs. Lactate
Pkm2 vs. Lactate
[Lactate] (umol/g ww)
r=0.019
p=0.938
r=-0.556
p=0.017
r=0.496
p=0.036
ldha Expression Normalized to TBP
ldhb Expression Normalized to TBP
pkm2 Expression Normalized to TBP

Figure 3

A
In Serine Pathway: 3-PG PHGDH 3-PHP Glycine GLDC CO2+NH3

B 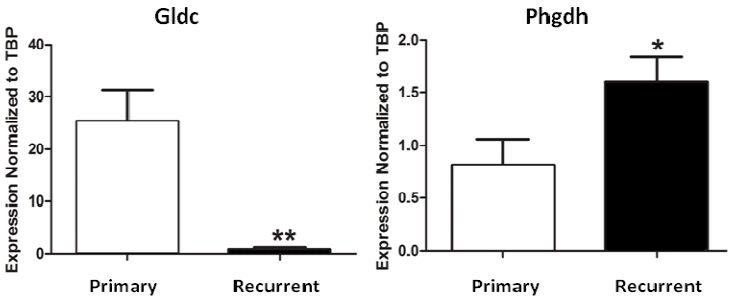
Gldc
Expression Normalized to TBP
40
30
20
10
0
**
Primary
Recurrent
Phgdh
Expression Normalized to TBP
2.0
1.5
1.0
0.5
0.0
*
Primary
Recurrent

C 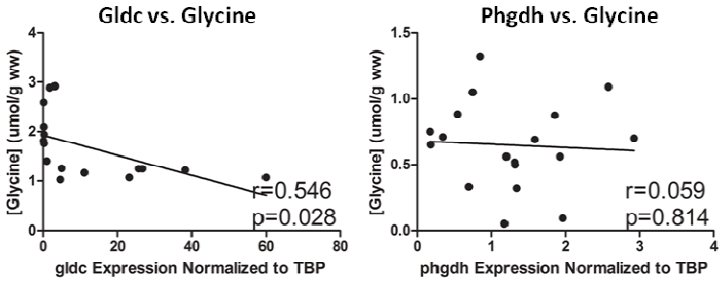
Gldc vs. Glycine
[Glycine] (umol/g ww)
4
3
2
1
0
r=0.546
p=0.028
0
20
40
60
80
gldc Expression Normalized to TBP
Phgdh vs. Glycine
[Glycine] (umol/g ww)
1.5
1.0
0.5
0.0
r=0.059
p=0.814
0
1
2
3
4
phgdh Expression Normalized to TBP

Figure 4

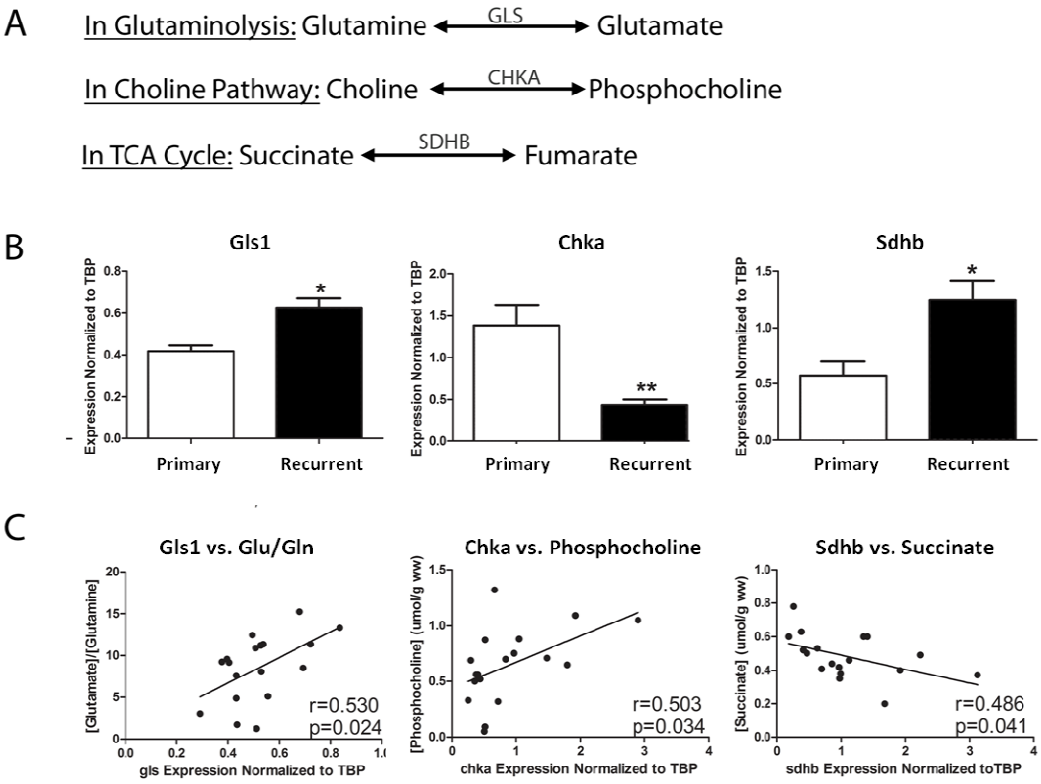
A
In Glutaminolysis: Glutamine GLS Glutamate
In Choline Pathway: Choline CHKA Phosphocholine
In TCA Cycle: Succinate SDHB Fumarate
B
Gls1
Chka
Sdhb
Expression Normalized to TBP
Primary
Recurrent
C
Gls1 vs. Glu/Gln
[Glutamate]/[Glutamine]
gls Expression Normalized to TBP
r=0.530
p=0.024
Chka vs. Phosphocholine
[Phosphocholine] (umol/g ww)
chka Expression Normalized to TBP
r=0.503
p=0.034
Sdhb vs. Succinate
[Succinate] (umol/g ww)
sdhb Expression Normalized toTBP
r=0.486
p=0.041

Figure 5

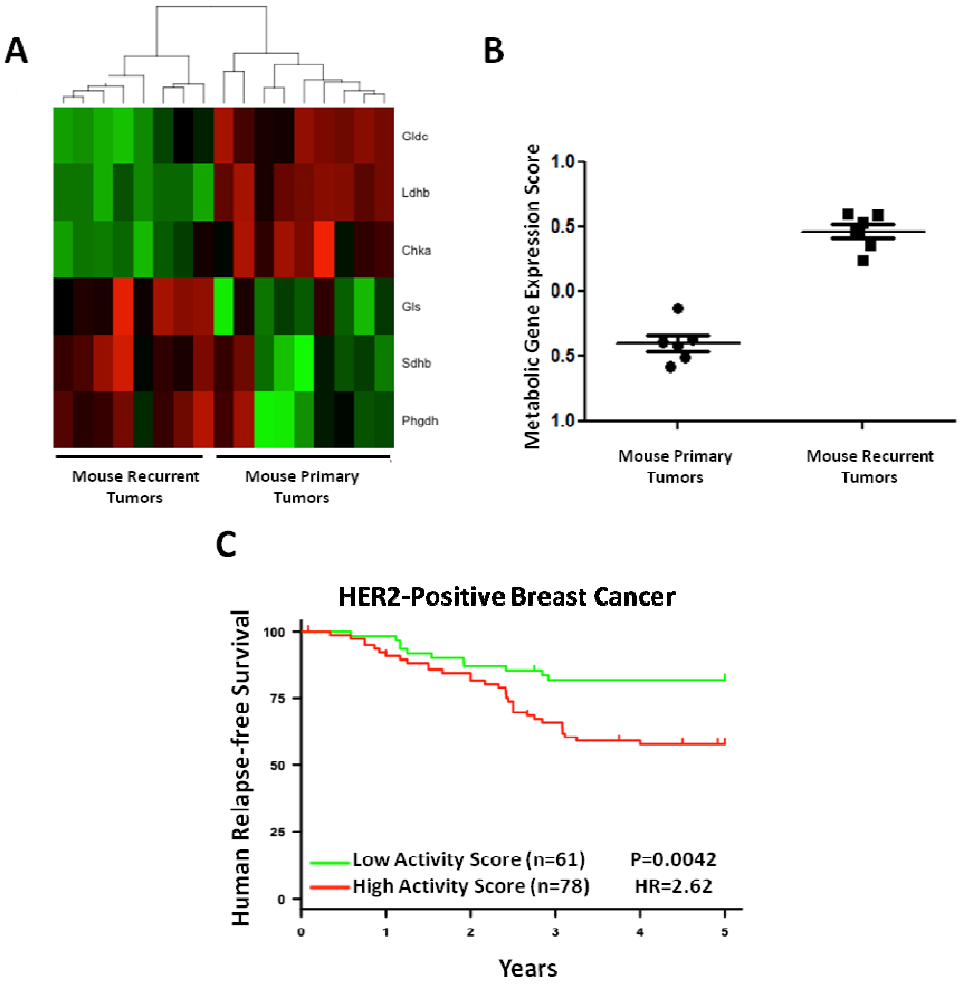
A
Gldc
Ldhb
Chka
Gls
Sdhb
Phgdh
Mouse Recurrent Tumors
Mouse Primary Tumors
B
Metabolic Gene Expression Score
1.0
0.5
0.0
0.5
1.0
Mouse Primary Tumors
Mouse Recurrent Tumors
C
HER2-Positive Breast Cancer
Human Relapse-free Survival
100
75
50
25
0
0
1
2
3
4
5
Years
Low Activity Score (n=61)
High Activity Score (n=78)
P=0.0042
HR=2.62

CHAPTER 4

Metabolic Reprogramming in Cancer: Unraveling the Role of Glutamine in Tumorigenesis

ABSTRACT

Increased glutaminolysis is now recognized as a key feature of the metabolic profile of cancer cells, along with increased aerobic glycolysis (the Warburg effect). In this chapter, we discuss the roles of glutamine in contributing to the core metabolism of proliferating cells by supporting energy production and biosynthesis. We address how oncogenes and tumor suppressors regulate glutamine metabolism and how cells coordinate glucose and glutamine as nutrient sources. Finally, we highlight the novel therapeutic and imaging applications that are emerging as a result of our improved understanding of the role of glutamine metabolism in cancer.

4.1 Introduction

Glutamine has long been recognized to play a unique role in the metabolism of proliferating cells, as compared to other amino acids[88, 89]. It is the most abundant amino acid in plasma, and most tumors consume and utilize glutamine at much higher rates than other amino acids[88]. Although glutamine is a non-essential amino acid in normal, non-dividing tissue, it is essential for the proliferation of most cells and the viability of some cancer cells that have become addicted to glutamine[170]. Glutamine metabolism contributes to the ability of cancer cells to continuously grow and proliferate by

supporting ATP production and biosynthesis of proteins, lipids, and nucleic acids. Glutamine also modulates redox homeostasis and can impact the activity of signal transduction pathways[90, 92].

Glutamine's involvement in oxidative mitochondrial metabolism in cancer cells was reported as early as the 1970s[171], and recent investigation has greatly expanded our understanding of the role and regulation of glutamine metabolism in cancer. In this article, we discuss the role of glutamine in supporting cellular proliferation and review current knowledge of how oncogenes and tumor suppressors regulate glutamine metabolism. We also discuss mechanisms through which metabolism of glutamine and glucose may be coordinated. Finally, we address the therapeutic and imaging applications that are emerging as a result of increasing recognition of the importance of glutamine metabolism in cancer.

4.2 Glutamine Metabolism Supports Cell Proliferation

Glutamine plays several important metabolic roles in the cell. It serves as a carbon source for energy production, contributes carbon and nitrogen to biosynthetic reactions, and regulates redox homeostasis (Figure 1). Glutamine availability and metabolism can also modulate activity of signal transduction pathways. As we discuss below, each of these functions of glutamine contributes to its ability to support cell growth and proliferation.

Glutamine: a Primary Carbon Source for Energy Production and Biosynthesis

Each of glutamine's fates in the cell serve important functions, although it is glutamine's role in supporting mitochondrial metabolism that is the primary reason that it is required in such large quantities. While non-proliferating cells can completely oxidize glucose-derived carbon in the TCA cycle to support their energy needs, proliferating cells use nutrients to support biosynthesis in addition to ATP production[74]. In proliferating cells, the TCA cycle metabolite citrate is exported out of the mitochondria to be used for generation of acetyl-CoA in the cytoplasm, which serves as a precursor for lipid biosynthesis. Because of the continual loss of citrate from the TCA cycle, replenishment of TCA intermediates (anaplerosis) is necessary, and glutamine serves as an important anaplerotic substrate in most proliferating cells. Citrate is generated from the condensation of acetyl-CoA and oxaloacetate, and ^{13}C labeling of glucose and glutamine in proliferating glioblastoma cells demonstrated that in these cells glutamine is a major source of oxaloacetate, whereas glucose carbon is the predominant source of acetyl-CoA[91]. Glutamine's role as a carbon source supporting TCA cycle function is critical for glutamine-addicted cancer cells. Cells expressing oncogenic levels of c-Myc die upon glutamine withdrawal, and viability can be restored by supplementing cells with TCA cycle intermediates, such as pyruvate, oxaloacetate, or alpha-ketoglutarate[97, 98, 172].

By contributing to citrate production, glutamine also supports *de novo* lipogenesis[91, 173]. While glutamine frequently plays a supporting role in lipogenesis by allowing transfer of glucose-derived acetyl-CoA from the mitochondria to the cytoplasm through citrate, glutamine carbon can also directly supply acetyl-CoA for lipogenesis. This can occur through two mechanisms. First, glutamine can contribute to lipogenesis through conversion of malate into pyruvate by malic enzyme, providing pyruvate that can

then re-enter the TCA cycle as acetyl-CoA[174, 175]. Second, glutamine, after conversion to alpha-ketoglutarate, can undergo reductive carboxylation to generate isocitrate, which is then converted into citrate[176-181]. The direct contribution of glutamine to *de novo* lipogenesis is particularly apparent under conditions of hypoxia or mitochondrial dysfunction, in which a number of cancer cell lines were shown to depend almost exclusively on the reductive metabolism of alpha-ketoglutarate to synthesize acetyl-CoA[177-179, 181]. Remarkably, HIF-alpha expression is sufficient to drive reductive carboxylation of alpha-ketoglutarate, even under normoxic conditions, indicating that "reversal" of the TCA cycle can be actively programmed[177, 178]. In lymphoma cells, on the other hand, Myc was shown to promote increased oxidation of glutamine, even under hypoxia[174]. Glutamine could in fact fully sustain the oxidative TCA cycle, even in the absence of glucose, in Myc-driven cells[174]. Recent estimates indicate that 10-25% of acetyl-CoA used for de novo lipogenesis comes from glutamine under normoxic conditions, and that up to 80% of acetyl-CoA for lipogenesis may come from glutamine in hypoxia[178]. Thus, the mechanism by which glutamine fuels lipid synthesis and proliferation is highly dependent on the oxygen and nutrient availability in the tumor environment, as well as oncogene expression, underlining the metabolic flexibility of cancer cells.

Glutamine: a Nitrogen Donor

In addition to the major function of glutamine in supplying carbon to mitochondria, glutamine serves as a nitrogen source. As depicted in Figure 1, the amido and amino groups of glutamine contribute to multiple biosynthetic pathways, including synthesis of non-essential amino acids, nucleotides, and hexosamines. Glutamine deprivation

causes growth arrest in most cell lines, and recent studies have highlighted glutamine's role as a nitrogen donor during proliferation. Supplementation of glutamine-starved Myc-driven cells with TCA intermediates was shown to rescue viability but not proliferation, suggesting that during proliferation, glutamine serves critical functions in addition to supporting the TCA cycle[172]. Indeed, rescue of proliferation during glutamine deprivation in Hep3B cells was more potent when cells were supplemented with alternate nitrogen sources such as alanine or asparagine than with alpha-ketoglutarate. Supplementation of alanine and alpha-ketoglutarate together produced a synergistic rescue[182].

In particular, glutamine's role in nucleotide biosynthesis, in which it is an obligate nitrogen donor for both purine and pyrimidine synthesis, has been implicated in ongoing support of proliferation. *K-ras* transformed fibroblasts cultured in glutamine-depleted media exhibit decreased cellular proliferation and abortive S phase entrance, which could be restored by addition of the four deoxyribonucleotides[183]. This result suggests that DNA synthesis may be particularly constrained by availability of glutamine and thus may inhibit proliferation when glutamine availability is limited. Interestingly, the expression of glutaminase (Gls1), an enzyme that catalyzes the conversion of glutamine to glutamate, is regulated during the cell cycle, with high expression during S phase that decreases as cells progress into G2/M. Glutamine consumption correlates with Gls1 expression, and following entry into S Phase, glutamine-deprived cells fail to progress to G2/M phases[184]. Thus, glutamine's function during DNA synthesis contributes to its role in supporting cell proliferation.

Role of Glutamine in Cell Signaling

In addition to its direct metabolic roles, glutamine has also been implicated in modulating cell signaling pathways to promote growth. Slc1a5 (ASCT2), a high-affinity L-glutamine transporter, is upregulated in multiple types of cancer and has been implicated in mediating net glutamine uptake in cancer cells[185]. Entry of glutamine into the cell through Slc1a5 plays a role in regulating mammalian target of rapamycin complex 1 (mTORC1) activity[185-187]. The mechanism for this was recently elucidated; glutamine uptake and subsequent rapid efflux through Slc7a5 (LAT1) in exchange for essential amino acids (EAA) allows EAA-dependent mTORC1 activation[186].

In addition to its role in promoting mTORC1 activation to support cell growth, some evidence suggests a possible role for glutamine in regulation of other signaling pathways. As a substrate for oxidative mitochondrial metabolism, glutamine may also influence signaling through regulation of mitochondrial ROS production[188]. For example, in IL-3-dependent hematopoietic progenitors, inhibition of glutamine metabolism with 6-diazo-5-oxo-L-norleucine (DON) blocks the sustained IL-3-dependent phosphorylation of Stat5[175]. Stat5 phosphorylation in DON-treated cells could be rescued by alpha-ketoglutarate, suggesting that mitochondrial metabolism of glutamine could modulate Stat5 phosphorylation. Antioxidant treatment inhibited glutamine-dependent Stat5 phosphorylation in this context, consistent with previous studies showing that Stat5 phosphorylation can be promoted under conditions in which reactive oxygen species (ROS) levels are elevated[189, 190]. In the context of oncogenic Kras, glutamine metabolism and mitochondrial ROS production was shown to contribute to cells' capacity to proliferate by promoting ERK signaling[191]. Through modulation of physiological ROS

production from the mitochondria, glutamine metabolism may participate in modulating multiple cell signaling pathways.

Glutamine in Regulation of Redox Homeostasis

In addition to glutamine metabolism contributing to mitochondrial ROS production through its oxidation in the TCA cycle, much recent evidence indicates that glutamine metabolism plays a key role in the maintenance of cellular redox homeostasis[98, 174, 192, 193]. This is due in large part to the role of glutamine in synthesis of glutathione, an endogenous antioxidant comprised of glutamate, cysteine, and glycine[194, 195]. As described above, glutamate derives in large part from glutamine taken up by the cell. Furthermore, glutamate can contribute to the uptake of cystine through the countertransporter Slc7a11[196]. In its antioxidant role, glutathione (GSH) donates electrons, becoming oxidized (GSSG). In order to restore glutathione to its reduced form, NADPH is required. Glutamine metabolism can also lead to increased production of NADPH, through its metabolism through malic enzyme[92]. Accordingly, glutamine metabolism was shown to promote an increased GSH/GSSG ratio in $p53^{+/+}$ cells (discussed further below)[192, 193].

4.3 Oncogenes Regulate Glutamine Metabolism

As outlined above, glutamine plays an important role in supporting cancer cell proliferation. Perhaps not surprisingly, data has emerged in recent years demonstrating that glutamine metabolism is directly regulated by oncogenes and tumor suppressors. Increased glutaminase activity was reported to correlate with tumor growth rate as early

as the 1960s [197, 198], and Myc has recently emerged as a critical regulator of glutamine metabolism and glutamine addiction in cancer cells[97, 98, 172]. A growing number of other tumor suppressors and oncogenes have also been implicated in regulating glutamine metabolism[100, 192, 193, 199].

Myc: Master Regulator of Glutamine Metabolism

Myc, a proto-oncogene and major regulator of cell proliferation, stimulates expression of multiple metabolic genes and is well known to promote glycolytic metabolism [200]. More recently, it has become clear that Myc also stimulates glutamine uptake and metabolism [97, 98]. Oncogenic levels of Myc cause glutamine addiction, and cells undergo apoptosis when deprived of glutamine[97, 172]. Myc stimulates glutamine metabolism both directly and indirectly. As a transcription factor, Myc directly binds the promoters and stimulates expression of glutamine metabolism genes, such as the transporter *Slc1a5*[97]. Myc also promotes glutaminase activity indirectly by repressing expression of miR-23a/b, which targets Gls1[98].

What functions of glutamine are critical for mediating cell survival in the context of oncogenic Myc? Viability in the absence of glutamine was rescued by supplementation with TCA cycle substrates[97, 98, 172], indicating that glutamine's anaplerotic role is critical for supporting cell survival in Myc-transformed cells. Furthermore, RNAi-mediated suppression of Gls1 also led to an increase in ROS levels and cell death, associated with diminished glutathione levels[98]. In Myc-driven cells, carbon derived from glutamine was shown to be preferentially used for glutathione

synthesis, in contrast to carbon originating from glycolysis[174]. These results suggest that glutamine's antioxidant roles are important for survival in Myc-driven cells.

Role of Rho GTPases in Glutamine Metabolism

Rho GTPases have also recently been reported to regulate glutamine metabolism [100]. Cancer cells dependent on Rho GTPase signaling display higher glutaminase activity, regulated in an NF-kB-dependent manner, and glutaminase activity is required for the transforming capability of at least three different Rho GTPases (Cdc42, Rac1 and RhoC)[100]. A small molecule inhibitor that impaired the growth and invasive potential of RhoGTPase-transformed fibroblasts and human cancer cells was found to target glutaminase, suggesting that glutamine metabolism could potentially be targeted in the context of Rho GTPase-driven tumorigenesis[100].

Ras Transformation and Glutamine

While Kras-mediated transformation has been reported to stimulate greater dependence on metabolism of glucose than glutamine, Kras-transformed cells nevertheless exhibit sensitivity to reduced glutamine conditions and fail to proliferate at levels of glutamine that can support growth of non-transformed cells[183]. Metabolic flux analysis provided evidence for both increased utilization of glutamine carbon to support the TCA cycle and contribution of glutamine's nitrogen to biosynthetic processes in Kras transformed cells[201]. Interestingly, mitochondrial metabolism was shown to promote proliferation in the context of oncogenic Kras through generation of ROS intermediates by the Q_o site of mitochondrial complex III. Glutamine-dependent ROS production promoted growth

through regulation of ERK signaling, and disruption of mitochondrial respiration led to decreased tumor formation in an *in vivo* mouse model of Kras-driven lung cancer[199].

Depending on ROS levels and cellular state, ROS can either have pro-proliferative effects in stimulating signal transduction or can cause damage and death [188, 202]. The role of glutamine in the regulation of ROS levels appears to be different depending on context[98, 174, 192, 193, 199]. Moreover, the complementing effects of glutamine in increasing oxidative mitochondrial metabolism and hence ROS production versus promotion of antioxidant defenses may balance differently and regulate different cell fates depending on cell type and/or oncogenic context.

p53: A tumor suppressor's role in glutamine metabolism

p53 is the first tumor suppressor to be shown to regulate glutamine metabolism. p53 induces the expression of *Gls2*, leading to increased mitochondrial oxidative phosphorylation and energy production from glutaminolysis. *Gls2* induction also increased glutathione levels and reduced ROS levels, conveying protection against oxidative stress-induced apoptosis. Induction of Gls2 was suggested to contribute to p53-dependent tumor suppression, since Gls2 expression was reduced in liver tumors and overexpression of Gls2 reduced tumor cell growth and colony formation [192, 193].

It is noteworthy that Gls1 and Gls2 seem to have contrasting effects in tumorigenesis. Myc induces the expression of *Gls1*, while p53 induces the expression of *Gls2*. Gls1 downregulation inhibits oncogenic transformation and cancer cell proliferation[100, 153, 154, 174] while overexpression of Gls2 is tumor suppressive[192, 193]. The two isoenzymes of glutaminase are known to have different structural and kinetic

properties, are subject to different regulation mechanisms, and exhibit different tissue-specific expression[203]. Notably, both enzymes have been implicated in regulating glutathione production and redox homeostasis, which is important for mediating cell survival in Myc-driven cells, as well as for protecting against p53-dependent apoptosis[98, 192, 193]. Hence, cellular context may be important for determining whether these enzymes act to promote or suppress tumorigenesis. It is also possible that alternate activities of these enzymes could also play a role in their divergent effects; for example, Gls2 was reported to interact with other proteins and to alter gene expression patterns in glioma cells[204, 205]. Further investigation is needed to understand the mechanisms underlying the different roles of Gls1 and Gls2 in tumorigenesis.

4.4 Mutations in Metabolic Enzymes and Glutamine Metabolism

As described above, a growing number of mutations in cancer have been reported to impact glutamine metabolism. Metabolic enzymes are also mutated in some cancers, including mutations in succinate dehydrogenase (*SDHA, SDHB, SDHC, SDHAF2*), fumarate hydratase (*FH*), and isocitrate dehydrogenase (*IDH1/2*). While the metabolic profiles of tumors bearing mutations in metabolic enzymes are unique based on the mutation, glutamine metabolism is also impacted in each of these circumstances.

IDH Mutations and Glutamine Metabolism

Mutations within IDH1 and IDH2 have been reported in low-grade gliomas, acute myeloid leukemias, and a number of other malignancies[206-212]. While wild type IDH1 and 2 interconvert alpha-ketoglutarate and isocitrate, these mutations result in a neomorphic

activity that catalyzes the conversion of alpha-ketoglutarate into 2-hydroxyglutarate (2-HG), a molecule described as an oncometabolite for its ability to independently induce metabolic changes similar to those associated with IDH mutations[213, 214]. 2-HG is thought to act by inhibiting certain alpha-ketoglutarate-dependent enzymes, including histone demethylases and Tet proteins, which can convert 5-methylcytosine into 5-hydroymethylcytosine and may participate in DNA demethylation[215-219].

Glutamine is the main source of alpha-ketoglutarate used by mutant IDH to produce 2-HG. Hence, the possibility that targeting glutamine metabolism could influence the activity of the mutant IDH enzyme was investigated[154]. Glutaminase inhibition indeed led to slowed proliferation of glioblastoma cells expressing mutant as compared to wild-type IDH1, and the growth suppression was rescued by alpha-ketoglutarate. However, despite reducing glutamate and alpha-ketoglutarate levels and suppressing growth in IDH1 mutant cells, 2-HG levels remained unaltered upon Gls inhibition[154]. The mechanism through which Gls inhibition selectively acts on cells expressing mutant IDH is not clear. Of note, metabolic profiling of IDH mutant cell lines indicates that broad metabolic changes occur in the presence of mutant IDH, including altered levels of TCA intermediates[220]; it is plausible that such alterations could play a role in sensitizing IDH mutant cells to suppression of glutaminase.

SDH and FH Mutations and Glutamine Metabolism

Mutations in the genes encoding the TCA cycle enzymes succinate dehydrogenase (SDH) and fumarate hydratase (FH) cause familial and sporadic paraganglioma and phaeochromocytoma (SDH mutations) or hereditary leiomyomatosis and renal cell carcinoma (*FH* mutations)[221, 222]. These mutations render the enzymes inactive, leading

to the accumulation of succinate and fumarate in the mitochondria. High levels of these metabolites can inhibit members of the prolyl hydroxylase family (PHDs), which are alpha-ketoglutarate dependent[223, 224]. This prevents the degradation of hypoxia inducible factor-1 (HIF-1α) and leads to a pseudohypoxic response and enhanced glycolysis. The pseudohypoxic response mediates the increased tumorigenicity induced by the loss of these mitochondrial tumor suppressors[223-225].

Two recent studies have investigated the metabolic changes that result from *FH* mutations that allow these cells to survive and proliferate. Metabolic modeling to assess pathways that allow cells to survive in the absence of FH, identified the heme biosynthesis pathway as synthetically lethal with FH mutations[226]. Glutamine carbon is diverted into heme biosynthesis from succinyl-CoA. This mechanism simultaneously allows generation of NADH by alpha-ketoglutarate dehydrogenase in order to fuel some ATP production by oxidative phosphorylation, as well as providing an outlet for glutamine carbon, from the impasse in the TCA cycle created by FH deficiency[226]. To generate acetyl-CoA to synthesize lipids, FH-deficient cells were shown to rely on reductive carboxylation of glutamine-derived alpha-ketoglutarate to provide citrate[181].

4.5 Coordinating Glutamine and Glucose Utilization in Cancer

As we have discussed, glutamine metabolism supports proliferation at several levels and its metabolism is directly regulated in many cancers. Together, glucose and glutamine serve as the primary nutrients to fuel cancer cell proliferation. Recent data indicate that the metabolism of these two nutrients is linked and that proliferating cells actively coordinate their metabolism (Figure 2). In cancer cells, oncogenic Myc puts into place gene expression programs to simultaneously increase the uptake and metabolism of

both glucose and glutamine, as has been discussed in recent reviews[200, 227, 228]. Cells presumably must also be able to detect and adapt to changing nutrient availability. Two distinct mechanisms, described in section 5.1, have recently been reported through which glucose or glutamine availability is sensed and used to regulate the metabolism of the other nutrient. On the other hand, recent data, discussed in section 5.2, indicates that some cancer cells also have the capacity to switch carbon source or compensate for reduced availability or metabolism of one nutrient by utilizing more of the other.

Metabolism of glucose and glutamine is coordinated

Recent data suggest that cells actively employ mechanisms to regulate metabolism of glucose or glutamine, dependent on the availability of the other (Figure 2). Glucose availability was recently shown in an IL-3-dependent hematopoietic cell line to modulate cellular uptake of glutamine through the hexosamine biosynthetic pathway[175], a branch of glucose metabolism that generates UDP-*N*-acetyl-D-glucosamine (UDP-GlcNAc), a donor substrate for glycosylation reactions[229, 230]. Glucose deprivation inhibited growth-factor-stimulated glutamine uptake, as a result of suppression of IL-3R surface expression and downstream signaling. IL-3R is N-glycosylated and supplementing cells with the GlcNAc, a hexosamine pathway metabolite, at least partially rescued IL-3R surface expression and IL-3-dependent glutamine uptake. Hence, glucose flux into the hexosamine biosynthetic pathway to support surface receptor glycosylation may serve as a metabolic checkpoint, though which cells can regulate growth-factor-dependent uptake of glutamine, in a glucose-dependent manner[175].

Reciprocally, a mechanism has been described through which glutamine availability can modulate glucose uptake, through the transcription factor MondoA.

MondoA is a member of the basic helix-loop-heliz zipper (bHLHZip) transcription factor family. Similar to Myc, MondoA interacts with Mlx, a Max-like bHLHZip protein, and binds to E-box sites on target genes[227]. The MondoA:Mlx complex is a glucose sensor present in the cytoplasm[231]. Upon glucose uptake, the MondoA complex detects elevations in glucose-6-phosphate levels and transits into the nucleus[232]. There, it stimulates expression of thioredoxin interacting protein (TXNIP), which constrains glucose uptake[232]. A recent study showed that glutamine availability inhibited transcriptional activation of TXNIP expression by recruiting a histone deacetylase-dependent co-repressor to the N-terminus of MondoA[233]. Reduced TXNIP expression led to enhanced glucose uptake, as well as cell growth and proliferation. Supplementation of cells with alpha-ketoglutarate could also promote transcriptional repression of TXNIP and the induction of glucose uptake, suggesting that glutamine-dependent anaplerosis modulates glucose uptake and cell growth through regulation of MondoA transcriptional activity[233].

Carbon source flexibility in cancer cells

Glucose and glutamine metabolism are regulated in a coordinated manner, and nutrient addiction can cause cancer cells to die in the absence of either glucose or glutamine. Cancer cells are notoriously resourceful, however, and two recent studies suggest that some cancer cells may be able to switch carbon sources. Using SF188 glioblastoma cells, which overexpress Myc, the effects of impairments in glucose availability on glutamine uptake and metabolism were assessed[93]. Glucose deprivation caused a large increase in the activity of glutamate dehydrogenase (GDH), and GDH was shown to be required for cells to survive impairments in glycolysis[93]. Reciprocally, impairment of

glutamine metabolism led cells to adapt to become fully reliant on glucose for mitochondrial metabolism[234]. Silencing of glutaminase suppressed growth, but cells were able to partially compensate by utilizing pyruvate carboxylase (PC) to allow use of glucose-derived carbon for anaplerosis[234]. Thus, glutamine and glucose metabolic pathways might be able to compensate for one another in some circumstances, a possibility that should be considered when developing cancer therapeutics targeting metabolism.

4.6 Glutamine Metabolism: Therapeutic and Imaging Implications

Therapeutic Targeting of Glutamine Metabolism

With the recognition that metabolic reprogramming is a key feature of transformed cells has come significant interest in targeting metabolism, including glutamine metabolism, as a cancer therapy. With glutamine participating in several key processes necessary for proliferation, as described in this article, there may be opportunities to interfere with glutamine metabolism at multiple points. Gls inhibition has shown promise in several models[100, 101, 153, 154, 174, 235]. Given the adaptability of cancer cells, inhibition of glutamine metabolism may potentially work best when combined with other therapies. Specific strategies for targeting glutamine metabolism in cancer cells have been recently reviewed in detail, to which the reader is referred for more information[92, 99, 236]. Targeting glutamine metabolism is an area of intense interest with much potential for future investigation and therapeutic benefit.

Glutamine Imaging: New Diagnostic Potential

Interest in imaging glutamine metabolism is also rising, in recognition of its potential to elucidate biologic characteristics of tumors exhibiting increased glutamine metabolism and to assess response to glutamine-targeted therapy[237]. Novel glutamine-based imaging techniques have emerged over the last few years, including positron emission tomography (PET) imaging and hyperpolarized magnetic resonance (MR).

Fluorinated glutamines have been synthesized for PET imaging, analogous to the commonly used fluorodeoxyglucose-(FDG)-PET used for imaging tumors that consume high levels of glucose. In particular, ^{18}F-(2S,4R)4-fluoroglutamine was shown to be taken up both by glutamine-dependent cancer cell lines and by tumors in mice, indicating the promise of this technology for imaging glutaminolytic tumors[238, 239]. Very recently, another glutamine PET tracer, l-[5-^{11}C]-glutamine, was described and has shown promise for the imaging of glutaminolytic cells and tumors, both *in vitro* and *in vivo*[240].

Magnetic resonance imaging has long been used as a technique allowing direct assessment of glutaminolytic intermediates. ^{1}H magnetic resonance spectroscopy (MRS) allows the quantification of both glutamine and glutamate and can be used to measure the steady-state concentrations of both of these metabolites *in vitro* and *in vivo*[169, 237, 241]. However, metabolism is a dynamic process and increased information can be gained from examining metabolic fluxes. Probing metabolic fluxes has been typically achieved by administering isotopically-labeled compounds (such as ^{13}C-labeled metabolites) to cells or animals and following the incorporation of the labeled nuclei (e.g. carbon) into downstream metabolites[91, 242, 243]. Yet, the biggest challenge with ^{13}C MRS

has long been the low signal-to-noise ratio (SNR) due to the low gyromagnetic ratio of the NMR-active carbon. Advances in MR imaging recently led to the introduction of a novel method, hyperpolarized MR, for real-time monitoring of single enzyme-catalyzed reactions of glutamine and glutamate metabolism. In hyperpolarized MR, a molecule is labeled with an NMR-active nucleus (typically ^{13}C) and that molecule is hyperpolarized using dynamic nuclear polarization (DNP). By dramatically increasing the fraction of targeted nuclei that are polarized (by as much of a factor of 10^5), DNP allows a large increase in the SNR for detection of the labeled metabolite compared to ^{13}C MR conducted at thermal equilibrium. This allows the user to observe the carbon transfer from substrate to product, as well as to compute the *in vivo* reaction rate of the conversion being observed. In the case of glutamine metabolism, this includes the ability to monitor and quantify the progressive conversion of glutamine into glutamate and glutamate into alpha-ketoglutarate. To date, successful hyperpolarization has been reported for [5-^{13}C]-glutamine, [1-^{13}C]-glutamate, and [5-^{13}C-4-$^{2}H_2$]-glutamine [244-246]. While these agents have been successfully used in cells, their implementation in animal models remains limited. The polarization tends to decay relatively rapidly following injection into living tissues minimizing the time frame during which the signal can be detected. For instance, the spin-lattice relaxation ($T_{1)}$ of the labeled carbon in [5-^{13}C]-glutamine is on the order of 16 seconds[245]. Strategies allowing improvements in polarization levels and T_1 prolongation of these agents might pave the way for wider *in vivo* implementation.

Overall, these techniques show significant promise for the monitoring of glutamine metabolism in vivo allowing improved diagnosis and monitoring of glutamine-dependent tumors.

4.7 Conclusion

Glutamine is one of the most versatile nutrients, contributing to many aspects of metabolism in cancer and proliferating cells. It is required in large quantities to support mitochondrial metabolism during proliferation, and its roles as a nitrogen donor and a regulator of cellular redox status and signal transduction also contribute to proper cell function, growth, and proliferation.

The uptake and metabolism of the other major carbon source supporting proliferation, glucose, has been a major research focus in several fields for years, and new details continue to emerge. Glucose uptake is highly complex and is regulated both through transcriptional control of the expression of glycolytic enzymes and signaling-dependent control of the trafficking of the glucose transporters themselves. By comparison, the regulation of glutamine metabolism is relatively poorly understood, though intense research into this topic is rapidly increasing our understanding of the role of glutamine in cancer. It is likely that additional complexities and levels of regulation will continue to emerge with further investigation. Better understanding of the signal transduction pathways that regulate glutamine metabolism, both in response to normal growth factor cues and oncogene activation, will be important. Understanding how cells adapt to inhibition of metabolic pathways will also be critical as more therapeutics targeting cancer cell metabolism are developed. Future investigation should also focus on *in vivo* study of glutamine metabolism, particularly as better imaging technologies emerge, with the ultimate goal of identifying strategies to most effectively target glutamine metabolism in cancer, likely in combination with other therapies.

4.8 Figure Legends

Figure 1. Glutamine metabolism in cancer cells. Glutamine contributes to bioenergetics and biosynthesis through reactions that use its α-nitrogen (green), γ-nitrogen (yellow) or carbon skeleton (pink). The γ-nitrogen from glutamine's amide group is a required nitrogen source for synthesis of nucleotides, hexosamines, and asparagine. During nucleotide synthesis, the alpha nitrogen is contributed in three independent enzymatic steps in purine synthesis and two reactions in pyrimidine synthesis. The alpha nitrogen can also be removed by glutaminase, which generates glutamate and ammonia. Ammonia has been previously shown to play a role in inducing autophagy. Glutamate carries most of glutamine's α-nitrogen and is a major nitrogen source for nonessential amino acid production in cells. Alanine aminotransferase (also known as glutamate: pyruvate transaminase; Gpt) and aspartate aminotransferase (also known as glutamate: oxaloacetate transaminase; Got) catalyze the transfer of glutamate's amino group directly into pyruvate and oxaloacetate to produce alanine and aspartate, respectively. Synthesis of other non-essential amino acids, including serine and the amino acids synthesized from serine, glycine and cysteine, requires the contribution of the amino group from glutamate. Glutamate is also a precursor for synthesis of arginine and proline. In addition to its role in amino acid synthesis, glutamate is an important component of the synthesis of glutathione, an endogenous antioxidant that protects cells against various forms of oxidative stress. The final major fate of glutamine, following its conversion to glutamate and then glutamate's conversion to alpha-ketoglutarate, is the oxidation of its carbon backbone in the mitochondria leading to energy production. Glutaminolysis contributes to production of mitochondrial NADH, which is used to support ATP production by oxidative phosphorylation.

Glutamine metabolism also contributes to production of NADPH and lipid and amino acid biosynthesis. The TCA cycle metabolite citrate can also exit the mitochondria to be used for generation of cytoplasmic acetyl-CoA, a precursor for fatty acid biosynthesis. Similarly, malate produced in the TCA cycle can exit the mitochondria and contribute to pyruvate and lactate production. gln: glutamine; glu: glutamate; gls: glutaminase; GSH: glutathione; OAA: oxaloacetate; Asp: aspartate; Pyr: pyruvate; Ala: alanine; Gpt: glutamate: pyruvate transaminase ; Got: glutamate: oxaloacetate transaminase; α-KG: α-ketoglutarate; glc: glucose.

Figure 2. Coordination of glutamine and glucose utilization during proliferation. Glucose and glutamine metabolism are linked and actively coordinated in cancer cells. Myc simultaneously increases the uptake and metabolism of both glucose and glutamine by regulating key transporters and enzymes involved in both pathways (shown in blue). Those targets highlighted in blue are transcriptionally activated by Myc, while those boxed in blue are regulated by Myc through other mechanisms. PKM2 expression is promoted by Myc through regulation of splicing factors and Gls1 is a target of miR23a/b, which is transcriptionally repressed by Myc. Two other mechanisms have been recently described that can contribute to cellular adaptation to nutrient availability. Glucose availability can control cellular uptake of glutamine through utilization of glucose in the hexosamine biosynthetic pathway (pathway shown in green). Glucose deprivation leads to a suppression of growth-factor-stimulated glutamine uptake, as a result of suppression of growth factor surface expression and downstream signaling in the absence of glucose. On the other hand, glutamine availability can be sensed by the cell to control uptake of glucose through the transcription factor MondoA (pathway shown in

pink). The MondoA complex is a glucose sensor present in the cytoplasm. Upon increase in glucose levels, MondoA detects elevation in glucose-6-phosphate levels and is translocated into the nucleus. There, it interacts with a MondoA transcriptional target, TXNIP, that induces a potent feedback circuit that restricts glucose uptake and cell growth. Glutamine availability inhibits activation of TXNIP and induces an increase in glucose uptake. Glut1: glucose transporter 1; HK2: Hexokinase 2; G6P: glucose-6-phosphate; F6P: fructose-6-phosophate; F-1,6-BP: fructose-1,6-biphosphate; PEP: phosphoenolpyruvate; PFK: phosphofructokinase; PKM2: pyruvate kinase isoform M2; Ldha: lactate dehydrogenase A; GF: growth factor; GlcNAc: N-acetyl-D-glucosamine; gls: glutaminase; Slc1a5 (ASCT2): a high-affinity L-glutamine transporter.

4.9 FIGURES

Figure 1

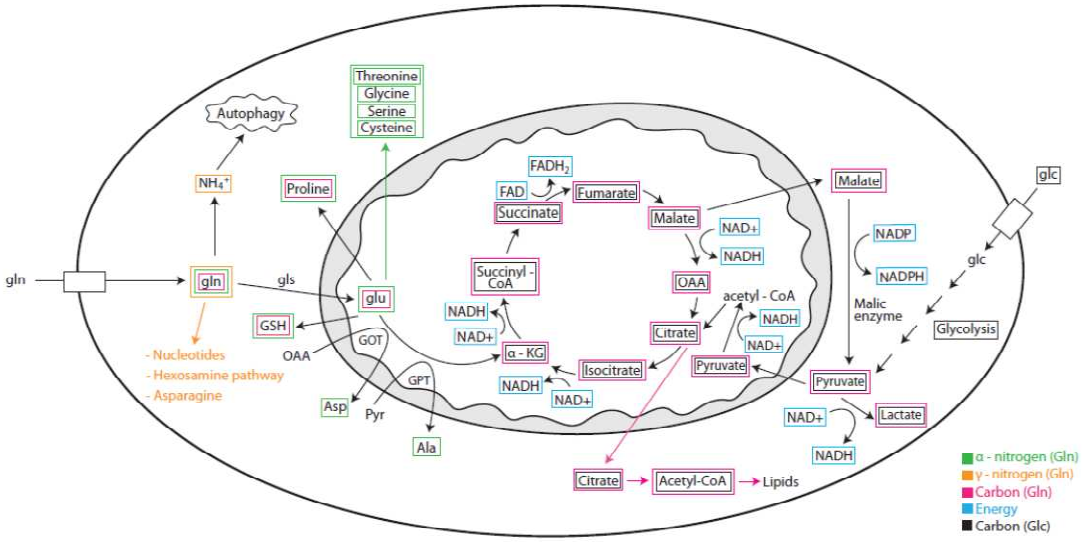

Figure 2

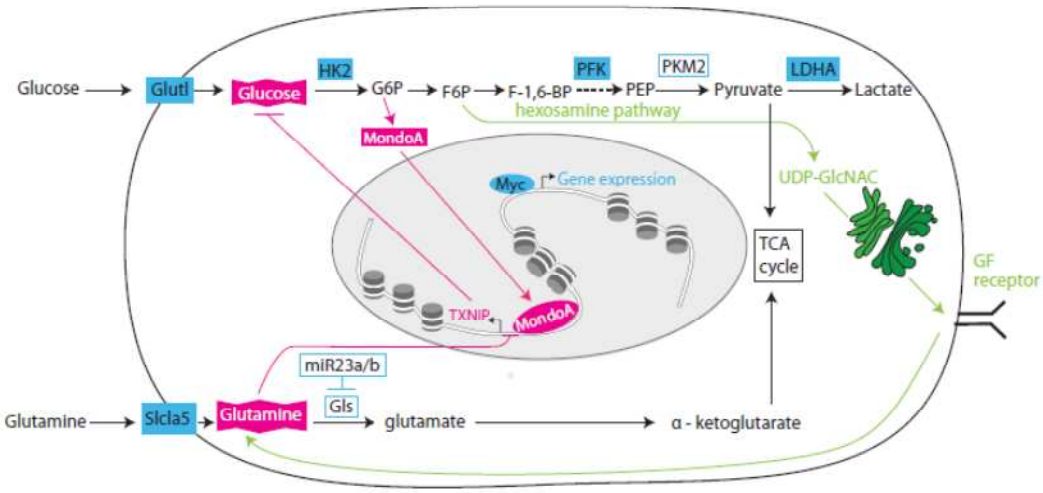
Glucose
Glut1
Glucose
HK2
G6P
F6P
F-1,6-BP
PFK
PEP
PKM2
Pyruvate
LDHA
Lactate
hexosamine pathway
MondoA
Myc
Gene expression
UDP-GlcNAC
TCA cycle
GF receptor
TXNIP
MondoA
miR23a/b
Gls
Glutamine
Slc1a5
Glutamine
glutamate
α - ketoglutarate

CHAPTER 5

Glutamine Addiction: A Targetable Hallmark of Breast Cancer Recurrence

ABSTRACT

Increased glutaminolysis has been increasingly recognized as a key feature of tumorigenesis. To date, no association has been established between glutamine metabolism and breast cancer progression. In this study, we investigate the glutaminolytic differences between primary and recurrent mammary tumors and assess their role as a potential therapeutic target. We use an MMTV-rtTa;TetO-HER2/*neu* doxycycline-inducible bitransgenic mouse model which accurately reproduces key features of the natural history of human breast cancer progression: primary tumor development, tumor dormancy and recurrence. We find that recurrent tumors exhibit higher glutamine uptake and glutamate production, when compared to primary tumors. ^{13}C-labeling experiments suggest increased glutaminolytic activity and increased reductive carboxylation in tumor recurrence. The observed increase in glutamine metabolism also seems to contribute to the tumorigenicity of recurrent mammary tumor cells. Recurrent, but not primary tumor cells are glutamine-addicted. The observed changes in the glutaminolytic profile are accompanied by increased expression of the glutamine transporter, Slc1a5, as well as increased expression of glutaminase (Gls1) in recurrent tumors. Both *Slc1a5* and *Gls1* expression are required for recurrent, but not primary tumor growth in vivo. Recurrent tumors also exhibit increased endogenous expression of the *Myc* oncogene. Myc was found to be required for *Slc1a5* and *Gls1* expression as well as increased glutamine uptake and glutamate production in recurrent tumor cells. Human association analysis reveals a statistically significant association

between *SLC1A5*, but not *GLS1* expression and increased recurrence risk in 11 human breast cancer datasets. Combined, our results suggest that recurrent HER2/*neu* mammary tumors are glutamine-addicted. Targeting glutamine metabolism might be a promising therapeutic strategy for the treatment of breast cancer recurrence.

5.1 Introduction

Breast cancer is the leading cause of cancer-related death and the most commonly diagnosed malignancy among women worldwide[247]. While advances in detection and therapy have led to improvements in the overall survival of women diagnosed with primary breast cancer, a substantial fraction of breast cancer survivors will ultimately relapse with recurrent breast cancer. Indeed, since recurrent breast cancer can be treated, but not cured, tumor recurrence remains the principal cause of mortality in this disease[66]. Nevertheless, despite its clinical importance, the molecular mechanisms underlying tumor recurrence remain poorly understood.

Dysregulated metabolism has long been known as a hallmark of human cancer, particularly aerobic glycolysis or the Warburg effect [74, 75]. More recently, increased utilization of glutamine has emerged as an important component of the altered metabolic profile of cancer cells[90-92, 99]. Since the 1950s, glutamine has been recognized as key nutrient for proliferating cancer cells[88, 89]. For example, glutamine is an obligate nitrogen donor for nucleotide and amino acid synthesis, contributes to bioenergetics, supports cell defenses against oxidative stress, and complements glucose metabolism[73, 75, 90-93]. Glutamine also influences a number of signaling pathways that contribute to tumor growth, most notably through maintaining activity of the mTOR kinase[186]. To date,

however, no association between changes in glutamine metabolism and cancer progression has been established.

In this study, we have investigated the changes in glutamine metabolism within the context of a genetically engineered mouse model for mammary tumorigenesis induced by the oncogene HER2/*neu* that accurately recapitulates key features of the natural history of human breast cancer progression, including minimal residual disease, tumor dormancy and recurrence[63, 66]. A member of the epidermal growth factor receptor family of tyrosine kinases, HER2/*neu* is amplified and overexpressed in ~20% of primary human breast cancers and its overexpression is associated with aggressive tumor behavior, high rates of recurrence and poor prognosis[51, 55, 57, 123]. Supporting the critical role of HER2/*neu* signaling in human breast cancer, therapies such as trastuzumab and lapatinib that target this molecule are effective in treating both early stage and advanced breast cancers[248-251]. In addition, HER2/*neu* activation results in downstream activation of the PI3K-AKT signaling pathway, an important regulator of cellular metabolism[67, 68, 71].

Our in vivo and in vitro studies reveal increased glutaminolysis in mammary tumor recurrence. ^{13}C labeling experiments in vivo also reveal higher rates of reductive carboxylation in recurrent tumors. These metabolic observations are accompanied by Myc-driven increased expression levels of both *Slc1a5* and *Gls1*. Slc1a5 is a glutamine transporter and Gls1 expresses the glutaminase enzyme, the enzyme that catalyzes the conversion of glutamine to glutamate at the beginning of the glutaminolytic pathway. Slc1a5 and Gls1 are found to be required for recurrent, but not primary tumor growth. SLC1A5 expression levels are also positively correlated with reduced 10-year recurrence-free risk in human breast cancer patients.

5.2 Methods

Animals, cell culture and recurrence assays

The MMTV-rtTa;TetO-HER2/*neu* (MTB/TAN) doxycycline-inducible bitransgenic mouse model has previously been described[63, 132]. All mice were housed and treated in accordance with protocols approved by the Institutional Animal Care and Use Committee at the University of Pennsylvania. *MTB/TAN* mice were bred, housed, induced with 2 mg/ml doxycycline, monitored for tumor development and recurrence, and sacrificed as previously described[66].

Tumor cells from primary mammary tumors arising in *MTB/TAN* mice maintained on doxycycline were isolated and cultured in the presence of doxycycline as described[66], as were tumor cells from recurrent mammary tumors arising in *MTB/TAN* mice bearing tumors that had fully regressed following doxycycline withdrawal and HER2/*neu* downregulation, and had then subsequently recurred spontaneously in the absence of doxycycline or HER2/*neu* transgene expression. Primary and recurrent tumor cells were transduced with retroviruses expressing either shRNAs targeting genes of interest and puromycin was used to select stably-transduced polyclonal cells.

Glutamine addiction assay

To assess the glutamine addiction phenotype of tumor cells, 300,000 primary or recurrent tumor cells were plated in triplicate in complete tumor media and incubated for 24 hr. Culture media was then removed and replaced with fresh tumor media, fresh tumor media lacking glutamine (Invitrogen), or fresh tumor media lacking glutamine but supplemented with 7 mM alpha-ketoglutarate (Sigma-Aldrich). Following incubation for 96 hr, cell viability was quantified by trypan blue exclusion using a Vi-CELL Cell Viability Analyzer (Beckman Coulter).

Slc1a5, Gls1 and Myc knockdown

For in vivo experiments, *Slc1a5* and *Gls1* expression were knocked down using retroviruses expressing commercially available shRNA constructs targeting these genes (Applied Biosystems). Five shRNA-expressing constructs were tested for each gene. The two shRNA's yielding the greatest knockdown for each gene were used for subsequent experiments. An shRNA targeting renilla luciferase was used as a negative control. *Slc1a5* and *Gls1* expression knockdown was confirmed by qRT-PCR.

For in vitro experiments, knockdown of c-Myc expression in recurrent tumor cells was performed using commercially available siRNAs (Ambion). Two different siRNAs exhibiting *c-Myc* knockdown were employed. A scrambled siRNA was used as a negative control (Ambion). siRNA transduction was performed according to manufacturer's instructions and cells were incubated with siRNAs for 48 hr. *Myc* knockdown was confirmed by qRT-PCR.

Orthotopic tumor assays

Orthotopic tumor growth assays were performed in athymic nude mice (*nu/nu*) purchased from Taconic (Germantown, NY). Cells were injected into the inguinal mammary fat pads of 10-12 *nu/nu* mice for each experimental group. Experiments were performed in parallel with five experimental arms, including one experimental arm for each of the *Slc1a5* or *Gls1* shRNA contructs, as well as a control arm for the renilla luciferase shRNA. Each of the number four mammary fat pads of each mouse was injected with 500,000 tumor cells.

For primary orthotopic tumor growth assays, HER2/*neu* expression in transplanted cells was induced by administering 2 mg/mL doxycycline in drinking water. Mice injected with recurrent tumor cells were maintained on water without doxycycline.

Tumor size was measured 2-3 times per week and tumor volume was determined by caliper measurements for each injected site using the following formula: Tumor volume = (smallest diameter^2 * largest diameter)/2. Tumors were followed until they reached a size of approximately 15x15 mm. Mean tumor growth rate (MGR) was calculated for each tumor as described[252].

RNA Isolation and qRT-PCR

RNA extraction was performed on snap-frozen primary and recurrent mammary tumor tissue and cell samples as described[253]. Samples were homogenized and RNA isolation was carried out using the RNeasy RNA isolation kit (Qiagen) according to manufacturer's instructions. Reverse transcription was performed from 2 µg of RNA using the cDNA High Capacity Reverse Transcriptase Kit (Applied Biosystems) according to the manufacturer's instructions. qRT-PCR analysis for *Slc1a5* and *Gls1* mRNA levels was performed on the Applied Biosystems 7900 HT Fast Real-Time PCR system using 6-carboxyfluorescein–labeled Taqman probes (Applied Biosystems). Expression levels of each gene were normalized to TBP.

Western blotting

Mammary tumors and cultured cell were homogenized in T-PER protein lysis buffer (Thermo Scientific). Primary antibodies were obtained from Abcam (anti-Slc1a5 and anti-Gls1), or Santa Cruz (anti-c-Myc). Horse radish peroxidase-conjugated secondary antibodies (Jackson Laboratories) were used to probe membranes incubated with the anti-c-Myc antibody. The enhanced chemiluminescent system (ECL; Amersham) was used to detect the bound secondary antibodies. Anti-Slc1a5 and Gls primary antibodies were detected using Alexa-Fluor-conjugated secondary antibodies (Molecular Probes).

The Odyssey V3.0 system (Li-COR Biosciences) was used to visualize and quantify proteins of interest.

Glutamine and glutamate level determination in culture

Ex vivo tumor culture experiments were performed following a procedure similar to that described by Banerjee et al.[254]. Briefly, a total of 4 primary and 4 recurrent mammary tumors that had reached a size of 12x12 mm were dissected using sterile technique, diced to yield fragments approximately 2x2 mm in diameter, weighed and equally distributed between 3 wells containing tumor culture media. Samples were maintained in a tissue culture incubator in 5% CO_2 at 37^{o}C for 96 hr, after which tumor tissue was collected, re-weighed, and the culture media harvested for determination of metabolite levels. Concentrations of glutamine and glutamate in culture media were determined using a 7100 Multiparameter Bioanalytical System (YSI life Sciences). The amount of each metabolite consumed or produced by tumor tissue samples was computed as the difference between the level of that metabolite in conditioned media from cultured tumor fragments compared to its level in control media incubated without tissue, and then normalized to the average weight of cultured tumor in that well. Positive values denote metabolite production, whereas negative values denote metabolite consumption. Samples from each tested condition were run in triplicate and statistical significance was determined using a Student's t-test.

A similar procedure for metabolite level determination was used for cell culture studies. 300,000 cells were plated and incubated in cell culture media for 96 hours. Glutamine consumption and glutamate production levels were determined using a 7100 Multiparameter Bioanalytical System (YSI life Sciences). Measured metabolite levels were normalized to the number of cultured cells in each well.

PET imaging

A total of 6 mice, 3 bearing primary mammary tumors and 3 bearing recurrent tumors, were each injected with 508±13 µCi of L-[5-^{11}C]-Glutamine prepared as described[255]. Dynamic PET imaging was performed on a small-animal Mosaic PET scanner (Philips, Inc.). For each mouse, 12 frames were acquired at 5-min intervals. Tumor segmentation and uptake quantification were performed at each frame for each mouse using the AMIDE software[256]. Uptake values were normalized according to the injected dose and the weight of each mouse and the area under each uptake curve (AUC) was computed. Differences in AUC values between primary and recurrent tumors were assessed using a Student's t-test.

^{13}C-labeling experiments

A total of 8 mice, 4 bearing primary tumors and 4 bearing recurrent mammary tumors, were infused through a tail vein catheter with an 8 mM solution of L-[3-^{13}C]-glutamine (Isotec) over a period of 45 minutes. At the end of the infusion period, tumors were dissected and clamp-frozen in liquid nitrogen. Perchloric acid extraction was performed as described[128]. NMR spectroscopy was performed at 9.4T on an Avance III 400 wide-bore spectrometer (Bruker). Carbon spectra were acquired overnight with a 5 mm BBO probe under the following conditions: pulse width of 45 degrees, TR 1.4s, 24 kHz spectral width, 64K data points and 35,000 – 40,000 scans. Spectral analysis was performed using the NMR NUTS software (Acorn, Inc.). Statistical significance was determined using a Student's t-test.

Measurement of ^{13}C isotopomers was performed on a Triple Quad 6410 mass spectrometer combined with an LC 1290 Infinity mass selective detector (Agilent), as described[257]. Briefly, samples were first purified by passage through either AG-1 or AG-

50 cation exchange columns (Biorad) and then converted into t-butyldimethylsilyl derivatives. Isotopic enrichment of glutamine was monitored using ions at 431, 432, 433, 434, 435, 436 and 437 m/z for M0, M+1, M+2, M+3, M+4, M+5 and M+6, respectively. Isotopic enrichment of ^{13}C-glutamate was monitored using ions at 432, 433, 434, 435, 436 and 437 m/z for M0, M+1, M+2, M+3, M+4 or M+5, respectively. Isotopic enrichment of ^{13}C-aspartate was monitored using ions at 418, 419, 420, 421 and 422 m/z for M0, M+1, M+2, M+3 and M+4, respectively. Isotopic enrichment of ^{13}C-succinate was monitored using ions at 289, 290, 291, 293 and 294 m/z for M0, M+1, M+2, M+3 and M+4, respectively. Isotopic enrichment of ^{13}C-lactate was monitored using ions at 261, 262, 263 and 264 m/z for M0, M+1, M+2 and M+3, respectively. Isotopic enrichment of ^{13}C-malate was monitored using ions at 419, 420, 421, 422 and 423 m/z for M0, M+1, M+2, M+3 and M+4, respectively. Isotopic enrichment of ^{13}C-citrate was monitored using ions at 459, 460, 461, 462, 463, 464 and 465 m/z for M0, M+1, M+2, M+3, M+4, M+5 and M+6, respectively.

^{13}C-enrichment is reported in molar percent enrichment (MPE), reflecting the mol fraction (%) of analytes containing ^{13}C atoms in excess of natural abundance, where MPE (M+i) = % $A_{M+i}/[A_M + \Sigma A_{M+i}]$, and A_M and A_{M+i} represent the peak area from MS ions corrected for natural abundance and corresponding to the unlabeled (M0) and ^{13}C-labeled (M+i) mass isotopomers, respectively.

Human breast cancer microarray data analysis

Meta-analysis of the association between relapse-free survival and the expression of SLC1A5 and GLS was performed using microarray and clinical data from 11 human breast cancer data sets. Data were obtained from NCBI GEO or authors' websites[258-261]. Microarray data were converted to base 2 log scale if the original data were on a

different scale. Affymetrix microarray data were normalized using Robust Multi-array Average (RMA) when .CEL files were available. For situations in which multiple microarray features mapped to the same gene on a single platform, the feature with the highest median absolute deviation (for two-color arrays), or the probe set with "_at" suffix and highest median expression (for Affymetrix arrays) was chosen to represent the target gene.

Within each data set, the effect size of the association between mRNA expression for a given gene and 10-year relapse-free survival was estimated using two different methods: 1) hazard ratio from Cox proportional hazards regression in which gene expression was modeled as a continuous variable; and 2) the concordance index (c-index). Each type of effect size estimate was combined across data sets by meta-analysis using the inverse-variance weighting method. For data sets in which relapse-free survival information was not available, but distant metastasis-free survival information was available, metastasis-free survival was used for survival analysis.

Between-study homogeneity of survival association was tested using chi-squared test on Cochran's Q statistic, for which a p-value of less than 0.1 was interpreted as evidence of significant heterogeneity. In the presence of significant heterogeneity, the random-effect model was used for meta-analysis. In the absence of significant heterogeneity, the fixed-effect model was used. Cox proportional hazards regression, concordance index analysis, and meta-analysis were performed using the "coxph" function in the "survival" package, the "survConcordance" function in the "survival" package and the "metagen" function in the "meta" packages in R 2.15.0. The precision of the meta-analysis p-values was verified using Monte Carlo permutation tests by randomly permuting sample labels and repeating the above meta-analyses 10,000 times.

5.3 Results

Recurrent mammary tumors exhibit increased glutamine consumption and glutamate production

To better define the molecular and cellular events that contribute to breast cancer recurrence, we have developed a doxycycline-inducible transgenic mouse model that displays key features of human breast cancer progression, including minimal residual disease, tumor dormancy and recurrence. In this model, the reverse tetracycline-inducible transactivator (rtTA) is specifically expressed within the epithelial compartment of the mammary gland under the control of the mouse mammary tumor virus (MMTV) promoter[132] in mice bearing the *MMTV-rtTA* transgene (*MTB*), and expression of the HER2/*neu* oncogene is driven by the *tet* operator[63] in mice bearing the *TetO-HER2/neu* transgene (*TAN*). Following the administration of doxycycline to *MMTV-rtTA;TetO-HER2/neu* (*MTB/TAN*) bitransgenic mice in drinking water, doxycycline-bound rtTA in mammary epithelial cells binds to the *tet* operator and induces expression of the HER2/*neu* oncogene[132]. Doxycycline induction of HER2/*neu* in bitransgenic animals results in the development of epithelial hyperplasias, focal atypical hyperplasias and, ultimately, invasive mammary adenocarcinomas in a manner that is highly penetrant, mammary-specific, and absolutely dependent on transgene induction by doxycycline.

Importantly, the inducible nature of these transgenic models permits the complete downregulation of the HER2/*neu* oncogenic stimulus following tumor formation. Surprisingly, we have found that virtually all HER2/*neu*-induced mammary tumors regress to a non-palpable state following oncogene downregulation, suggesting that tumors become “addicted” to the oncogenic signaling pathways that led to their formation[63, 66]. However, analogous to the phenomena of tumor recurrence in women with breast cancer, many fully regressed tumors in *MTB/TAN* mice spontaneously recur

over periods of up to a year, ultimately resulting in the death of the animal[66]. As such, this model parallels the natural history of human breast cancer and enables mechanistic approaches to elucidating the mechanisms that underlie tumor recurrence.

To begin to investigate whether changes in glutamine metabolism occur during the process of mammary tumor recurrence in vivo, we used the L-[5-^{11}C]-glutamine tracer to perform dynamic positron emission tomography (PET) on *MTB/TAN* bitransgenic mice bearing either primary or recurrent mammary tumors. Both primary and recurrent mammary tumors exhibited L-[5-^{11}C]-glutamine uptake higher than that of non-tumor tissues, however L-[5-^{11}C]-glutamine uptake in recurrent tumors appeared to be higher than that of primary tumors (Fig. 1A). Quantification of normalized L-[5-^{11}C]-glutamine tumor uptake over time revealed higher uptake over time for recurrent tumors compared to primary mammary tumors (AUC_{mean}= 313.4±34.4 vs. 242.5 ±8.92; p=0.007) (Fig. 1B). This suggested the possibility that glutaminolysis is up-regulated during the process of mammary tumor recurrence in vivo.

To further explore this potential difference in glutamine metabolism, we conducted tumor culture experiments in which explanted primary and recurrent mammary tumors from *MTB/TAN* mice were dissected, minced and cultured for 96 hours. Differences in glutamine uptake and glutamate production were determined. Concentrations of glutamine and glutamate in culture media were determined using a 7100 Multiparameter Bioanalytical System and the amount of each metabolite consumed or produced by each tumor sample was computed as the difference between the level of that metabolite in conditioned media from cultured tumor fragments compared to its level in control media incubated in the absence of tumor tissue. Results were normalized by weight of cultured tumor tissue.

In accordance with our in vivo PET studies using L-[5-^{11}C]-glutamine, this analysis revealed that recurrent mammary tumors exhibited a 3.4-fold higher level of glutamine uptake compared to primary tumors (Fig. 1C; p=0.001). Consistent with this, recurrent tumors also displayed a 1.7-fold increase in glutamate production compared to primary tumors (Fig. 1D; p=0.004). Together with our findings using L-[5-^{11}C]-glutamine PET, these results suggest that recurrent mammary tumors in *MTB/TAN* mice exhibit higher glutamine uptake and metabolism than primary mammary tumors in this same model.

Recurrent tumors display higher glutaminolytic flux and increased reductive carboxylation

To investigate the differences in glutaminolytic activity between primary and recurrent mammary tumors, we next performed ^{13}C-glutamine labeling experiments. Mice bearing primary and recurrent tumors were infused with a solution containing L-[3-^{13}C]-glutamine. Metabolism of the ^{13}C- labeled tracer was followed using magnetic resonance spectroscopy (MRS) and mass spectrometry.

Using MRS, we found that primary and recurrent mammary tumors displayed clear differences in the concentrations of 3-^{13}C-glutamine (Gln-3) and3-^{13}C-glutamate (Glu-3) (Fig. 2A). Specifically, the integral ratio of labeled Glu-3 to labeled Gln-3 was 2.8-fold higher in recurrent tumors compared to primary tumors (Fig. 2B; p<0.001). This suggests that recurrent tumors exhibit greater conversion of glutamine to glutamate than primary tumors.

Assessment of metabolite isotopomers from this experiment using mass spectrometry revealed higher mole percent excess (MPE) in recurrent tumors compared to primary tumors for all tested intermediates of the glutaminolytic pathway downstream

of glutamine (Fig. 2C). Specifically, glutamate, aspartate, succinate, malate, citrate and lactate each exhibited higher ^{13}C-labeling amounts in recurrent tumors than in primary tumors. Conversely, glutamine displayed lower labeling in recurrent tumors compared to primary tumors, which would be consistent with higher consumption of the ^{13}C-glutamine label in recurrent tumors.

Interestingly, assessment of metabolite isotopomers from this experiment also revealed higher overall labeling of citrate compared to succinate in both primary and recurrent mammary tumors. This suggests the possibility that active reductive carboxylation may occur in each of these tumor types in vivo. This effect, however, was more pronounced in recurrent tumors, as evidenced by higher MPE that were observed for each if the metabolites considered. In aggregate, these results are compatible with a model in which recurrent tumors exhibit increased glutaminolytic flux as well as reductive carboxylation.

Recurrent, but not primary, tumor cells are glutamine-addicted

To begin to assess the functional significance of the increase in glutaminolysis that we observed in recurrent mammary tumors, we next sought to determine the effect of glutamine deprivation on the viability and growth of primary and recurrent mammary tumor cells in vitro. Primary and recurrent mammary tumor cell lines derived from tumor-bearing *MTB/TAN* mice were plated in control media containing glutamine, growth factors and serum and then shifted to control media, to media lacking glutamine, or to media lacking glutamine but supplemented with alpha-ketoglutarate.

When grown in control media containing glutamine, both primary and recurrent tumor cells became fully confluent 96 hours post plating (Fig. 3A). In contrast, culturing cells in glutamine-deprived media led to marked cell death in recurrent, but not primary,

tumor cells. This effect on recurrent tumor cells was rescued by supplementing glutamine-deprived media with alpha-ketoglutarate.

Consistent with these observations, quantification of cell viability by trypan blue exclusion revealed an 47% reduction in cell viability, when recurrent tumor cells were cultured in media lacking glutamine, compared to recurrent tumor cells cultured in control media containing glutamine (Fig. 3B; p=0.002). In contrast, no difference was observed in the viability of primary tumors cells cultured in media containing or lacking glutamine. The loss of cell viability observed in recurrent tumor cells subjected to glutamine deprivation was fully and efficiently rescued by the addition of alpha-ketoglutarate to the medium, indicating that the carbon backbone of glutamine is required for recurrent tumor cell growth. Together, these observations are consistent with a model in with recurrent, but not primary, mammary tumors cells are glutamine-addicted.

Slc1a5, Gls1 and glutamine metabolism are up-regulated in recurrent tumors in a c-Myc-dependent manner

During glutaminolysis, glutamine can first be taken up by cancer cells through the sodium-dependent neutral amino acid transporter, Slc1a5. Glutamine is subsequently converted to glutamate by glutaminase, a reaction reported to be the rate-limiting step in glutamine metabolism[262, 263]. In an effort to identify the underlying molecular determinants for the increase in glutamine uptake observed in recurrent tumors, we first measured expression of the glutamine transporter Slc1a5 by qRT-PCR and immunoblotting, since we had observed increased uptake of glutamine by PET in vivo as well as increased uptake of glutamine from culture medium in vitro. Slc1a5 is known to be a key neutral amino acid transporter in cells and its inhibition reduces glutamine

uptake in vitro[186]. This analysis revealed that recurrent mammary tumors exhibit 2.8-fold higher steady-state levels of *Slc1a5* than primary tumors, at the mRNA level (Fig. 4A; p=0.002). Immunoblotting also revealed higher Slc1a5 at the protein level (Fig. 4B).

Analogous to our findings with Slc1a5, our observation that recurrent tumors exhibit higher levels of glutamate production compared to primary tumors, led us to investigate whether glutaminase (Gls1) is upregulated in recurrent tumors, since Gls1 expresses the glutaminase enzyme which is known to catalyze the conversion of glutamine into gltuamate. We found that recurrent tumors express a 1.8-fold higher level of *Gls1* expression than primary tumors at the mRNA level (p=0.024) (Fig. 5A). Immunoblotting also revealed higher Gls1 at the protein level (Fig. 5B).

In light of the upregulation of glutamine metabolism that we observed in recurrent tumors, as well as the known regulatory role of the proto-oncogene *c-Myc* and glutamine metabolism, we considered the possibility that c-Myc was responsible for the observed upregulation of Slc1a5 and Gls1 in recurrent mammary tumors. Myc has been previously shown to regulate *Slc1a5* level by binding to its promoter, as well as modulate Gls1 levels through mir23a/b[97, 98]. Consistent with this prediction, immunoblotting revealed Myc upregulation in recurrent mammary tumors (Fig. 7A). Myc upregulation was accompanied by increased expression of the downstream Myc targets *Odc1*, *Ccnb1*, *Mthfd2*, *Nap1l1*, *Col1a1*, and *Pmp22* (Fig. 7B).

Consistent with the supposition that c-Myc upregulation contributes to the observed upregulation of Slc1a5 and Gls1 in recurrent tumors, downregulation of *c-Myc* expression in recurrent tumor cell lines using siRNA approaches resulted in downregulation of *Slc1a5* and *Gls1* (Fig. 7C). In addition, *c-Myc* downregulation by either of two siRNAs also led to a decrease in glutamine consumption as well as a decrease in glutamate production in recurrent tumor cells (Fig. 7D). Together, these

findings suggest that c-Myc upregulation in recurrent mammary tumors is responsible for the observed increases in Slc1a5 and Gls1 expression, as well as for increased glutamine metabolism.

Slc1a5 is required for recurrent, but not primary, tumor growth

Our observations to this point suggested the possibility that the growth of recurrent, but not primary mammary tumors is dependent upon the c-Myc-induced upregulation of glutamine transport and metabolism. To begin to test this hypothesis, we asked whether upregulation of Slc1a5 contributed to the higher levels of glutamine uptake observed in recurrent tumors, as well as recurrent tumor growth. To this end, we knocked down expression of *Slc1a5* in primary and recurrent tumor cells using retrovirally transduced shRNAs (Fig. 4C, E). As anticipated, Slc1a5 downregulation was accompanied by decreased glutamine uptake in both primary and recurrent tumor cells.

Primary and recurrent tumor cells with and without *Slc1a5* knockdown were then implanted orthotopically into the mammary glands of *nu/nu* mice in order to assess the effect of Slc1a5 knockdown on the rate of orthotopic tumor growth. Slc1a5 downregulation did not alter the growth rate of primary orthotopic tumors as tumors formed by primary tumor cells expressing either of two *Slc1a5* shRNAs grew at the same rate as tumors formed by primary tumor cells expressing a control hairpin (Fig. 4D). In contrast, orthotopic tumors formed by recurrent tumor cells expressing shRNAs directed against *Slc1a5* grew 3.5 to 4.6-fold more slowly than tumors formed by recurrent tumor cells expressing a control hairpin (Fig. 4F; 23.36±12.82 $MGR_{control}$ vs. MGR_{shRNA1}=6.71±2.35, MGR_{shRNA2}=5.03±1.34; $p_{shRNA1}<0.001$, $p_{shRNA2}<0.001$). These findings indicate that while Slc1a5 is required for efficient glutamine uptake in both

primary and recurrent mammary tumor cells, Slc1a5 is required for the growth of recurrent, but not primary, mammary tumors.

Gls1 is required for recurrent, but not primary, tumor growth

To investigate the functional consequences of Gls1 upregulation on tumor growth, we knocked down expression of *Gls1* in primary as well as recurrent tumor cells using two different shRNAs (Fig. 5C, E). As anticipated, *Gls1* downregulation was accompanied by reduced glutamate production in both primary and recurrent tumor cells.

Primary and recurrent tumor cells with and without Gls1 knockdown were next implanted orthotopically into the mammary glands of *nu/nu* mice in order to assess the effect of Gls1 knockdown on the rate of orthotopic tumor growth. As observed for *Slc1a5, Gls1* downregulation did not alter the growth rate of primary orthotopic tumors as tumors formed by primary tumor cells expressing either of two *Gls1* shRNAs grew at the same rate as tumors formed by primary tumor cells expressing a control hairpin (Fig. 5D). In contrast, orthotopic tumors formed by recurrent tumor cells expressing shRNAs directed against *Gls1* grew 3.9 to 4.2 fold more slowly than tumors formed by recurrent tumor cells expressing a control hairpin (Fig. 5F; 23.36±12.82 $MGR_{control}$ vs. MGR_{shRNA1}=6.30±1.98, MGR_{shRNA2}=5.23±0.99; $p_{shRNA1}<0.001$, $p_{shRNA2}<0.001$). These findings indicate that while Gls1 is required for efficient glutamate production in both primary and recurrent mammary tumor cells, Gls1 is required for the growth of recurrent, but not primary mammary tumors.

Elevated Slc1a5 expression is associated with an increased risk of recurrence in women with breast cancer

Our observations in mice that glutaminolysis is up-regulated in recurrent mammary tumors, that recurrent mammary tumor cells are glutamine-addicted, and the both Slc1a5 and Gls1 are differentially required for recurrent tumor growth, we considered the possibility that expression *Slc1a5* or *Gls1* in primary tumors might be associated with recurrence-free survival in women with breast cancer. Based on the above data, we hypothesized that if upregulation of glutaminolysis functionally contributes to tumor recurrence in humans, that women with primary breast cancers expressing higher levels of *Slc1a5* or *Gls1* might relapse at a faster rate than women whose breast cancers express lower levels of *Slc1a5* or *Gls1*.

To test this hypothesis, we collected unique patient profiles from 11 published human primary breast cancer microarray data sets, each of which contained at least 50 patients in addition to information on relapse-free survival. For each data set, the effect size of the association between *Slc1a5* or *Gls1* mRNA expression and relapse-free survival was estimated using Cox proportional hazard regression in which *Slc1a5* or *Gls1*expression were modeled as continuous variables; and 2) the concordance index (c-index). To derive an overall estimate and statistical significance of the association between mRNA expression and relapse-free survival while accounting for the heterogeneity among data sets, effect size estimates were combined across data sets by meta-analysis using the inverse-variance weighting method. In the presence of significant heterogeneity (p-value for Cochran's Q statistic < 0.1), a random-effect mode was used for meta-analysis. Otherwise, a fixed-effect model was used.

When considering all patients encompassed by the 11 data sets, a significant positive association was observed between elevated *SLC1A5* expression and risk of

relapse in breast cancer patients within 10 years of diagnosis (H.R. = 1.41 [1.18-1.67], p=0.00012; Fig. 6A). In contrast, no significant association was observed between *GLS1* expression and relapse-free survival (Fig. 6B). These results suggest an overall association between *SLC1A5* expression and the risk of tumor recurrence and breast cancer patients.

5.4 Discussion

Since the 1950s, glutamine has been recognized as an important nutrient for proliferating cancer cells[88]. Glutamine acts as a carbon and nitrogen source supporting energy production as well as contributing to biosynthesis reactions and redox homeostasis[74, 91, 173, 182, 191]. In this study, we have shown that recurrent mammary tumors that spontaneously arise in genetically engineered mice following HER2/*neu* downregulation and primary tumor regression exhibit increased glutaminolysis and are glutamine-addicted. While several studies have demonstrated significantly reduced viability of a number of human cancer cell lines following glutamine withdrawal[97, 98, 172, 199], to our knowledge no study has demonstrated a shift from glutamine independence to glutamine addiction during the course of cancer progression in vivo in an autochthonous tumor model. Our results highlight the potential importance of glutaminolysis beyond its previously reported role in primary tumor growth.

In this study we have demonstrated that recurrent mammary tumors that arise in a HER2/*neu*-induced mammary tumor model exhibit increased glutamine uptake and glutamate production, as well as increased reductive carboxylation, compared to primary tumors. This observed increase in glutaminolysis was accompanied by increased

expression of the glutamine transporter, Slc1a5, as well as the glutaminase enzyme, Gls1. Moreover, we found that upregulation of *Slc1a5* and *Gls1* was driven by c-Myc, which was itself upregulated in recurrent tumors and shown to be required for their observed glutaminolytic phenotype. Finally, consistent with the glutamine-addicted nature of recurrent mammary tumor cells, we found that Slc1a5 and Gls1 are each preferentially required for the growth of recurrent, but not primary, mammary tumors. Combined, these results suggest an important role of glutamine metabolism in the recurrence of HER2/*neu*-induced mammary tumors.

In this study, we report the spontaneous upregulation of both Slc1a5 and Gls1 during the process of recurrence of HER2/*neu*-induced primary mammary tumors induced to regress by HER2/*neu* pathway downregulation. We also find that Slc1a5 and Gls1 are each required in vivo for the growth of recurrent, but not primary, tumors. Gls1 has previously been reported to be required for tumor growth in some primary tumors in the context of xenografted tumors from cell lines[100, 101, 153, 262, 263]. To our knowledge, however, a requirement for Slc1a5 in tumor growth has not been previously demonstrated. Indeed, while the conversion of glutamine to glutamate catalyzed by glutaminases is a known rate-limiting step in glutamine metabolism, transport of glutamine by Slc1a5 is not. As such, our results provide some of the first evidence to support an important functional role for Slc1a5 in tumor growth, as well as functional role for Slc1a5 and Gls1 in tumor progression.

While many studies have established a key role for Slc1a5 in glutamine transport in cancer cells[185, 186], Slc1a5 can transport a number of small neutral amino acids other than glutamine. As such, it is possible that the functional effect of Slc1a5 knockdown on tumor growth could be due to differential transport of a neutral amino acid other than glutamine. Nevertheless, given the tight association that we observe in our model

between spontaneous Slc1a5 upregulation and increased glutamine metabolism, as well as shRNA-mediated *Slc1a5* knockdown and downregulation of glutamine uptake, we favor the possibility that the effects of Slc1a5 in recurrent tumor cells are indeed mediated by its transport of glutamine.

To date, a number of oncogenes have been reported to regulate glutamine metabolism[97, 98, 191, 192]. Among those, Myc is known to be a key regulater of glutaminolysis in cancer cells[264]. Oncogenic levels of Myc have been shown to directly induce glutamine addiction as well as apoptosis following glutamine withdrawal[97, 172]. In our model, we observe the spontaneous upregulation of *Myc* expression, as well as the expression of Myc transcriptional targets, during the spontaneous recurrence of HER2/*neu*-induced mammary tumors. Moreover, we find that Myc upregulation is responsible for the observed glutaminolytic phenotype of recurrent tumors by virtue of its ability to positively regulate the expression of *Slc1a5* and *Gls1*. Myc has been previously shown to transcriptionally regulate a number of genes involved in metabolism, including *Slc1a5*[97], and is known to regulate glutaminase activity indirectly by repressing the expression of miR23a/b[98]. Our findings that glutamine metabolism in recurrent tumors is regulated by *Myc* expression provides further in vivo confirmation of these reports and highlight an important role of Myc in cancer recurrence. This, in turn, suggests the potential utility of blocking downstream metabolic effectors of the Myc pathway, particularly those involved in glutamine metabolism, in human cancers.

Glutamine carbon is known to support de novo lipogenesis, which can occur through the conversion of glutamine-derived α-ketoglutarate to citrate through reductive carboxylation followed by acetyl-coA production[176-181]. Previous studies have reported this finding in vitro. Our findings provide evidence for increased reductive carboxylation in vivo in recurrent mammary tumors, compared to primary tumors, manifested as high

citrate labeling from glutamine. It has been suggested that the "reverse" TCA cycle accompanying active reductive carboxylation is most pronounced under hypoxic conditions and within the context of mitochondrial dysfunction[177-179, 181]. We speculate that the increase in reductive carboxylation that we observe in recurrent tumors may result from increased hypoxic conditions within these tumors. However, direct demonstration that this is the case will require further investigation.

Finally, our analysis of relapse-free survival in breast cancer patients revealed a significant positive association of SLC1A5, but not GLS1, expression levels with an increased risk of recurrence. Consistent with our findings in genetically engineered mouse models for breast cancer recurrence, patients with primary tumors expressing elevated levels of *SLC1A5* exhibited higher 10-year relapse rates when compared to women whose cancers expressed lower levels of *SLC1A5*. These results are in agreement with reports in the literature indicating that of high *SLC1A5* levels are associated with reduced survival in some human cancers, including colorectal[265] and prostate adenocarcinomas[266]. To our knowledge, however, no studies have established an association between *GLS1* expression levels and survival in human cancer patients. Additional work will be needed to determine, by multivariate analysis, whether either of these genes is associated with patient outcome independent of currently used clinicoprognostic factors.

In conclusion, our findings provide direct evidence for an evolving metabolic phenotype of breast cancers during the course of tumor progression, as well as support for a role for glutamine metabolism as a potentially targetable feature in recurrent breast cancers. While additional studies will be required to assess the translational potential of our findings. Glutamine addiction, a newly identified hallmark of breast cancer recurrence, can be further exploited to establish potential early tumor recurrence

diagnotic markers of increased glutamine uptake; targeted anti-recurrence therapies against Slc1a5 and Gls1; and finally breast cancer prognostic markers through *SLC1A5* expression profiling in individual tumors.

5.5 Figure Legends

Figure 1. Recurrent tumors exhibit increased glutamine metabolism (A) L-[5-^{11}C]-Glutamine PET imaging reveals higher tracer uptake in recurrent tumors relative to primary tumors. (B) Quantification of the L-[5-^{11}C]-Glutamine dynamic PET measurements shows higher mean area under the curve (AUC) in recurrent tumors, when compared to primary tumors. Uptake values at each timeframe were normalized to the injected dose and the weight of each mouse. (C) Tumor culture experiments reveal higher glutamine uptake in recurrent tumors. (D) Tumor culture experiments show increased glutamate production in recurrent tumors. The measured metabolite levels in the tumor culture experiments were normalized to the wet weight of the cultured tumors.

Figure 2. Recurrent tumors exhibit higher glutaminolytic flux and increased reductive carboxylation (A) Assessment of L-[3-^{13}C]-glutamine metabolism using ^{13}C-magnetic resonance spectroscopy (MRS) reveals increased labeled glutamate production from glutamine in recurrent tumors relative to primary tumors. Representative spectra from 2 of the tumors examined are shown. Glu-3: 3-^{13}C-glutamate; Gln-3: 3-^{13}C-glutamine. (B) Quantification of the integral ratio of the Glu-3 peak to the Gln-3 peak in all the primary and recurrent tumors examined reveals statistically significant higher ratios in recurrent tumors. (C) Assessment of metabolite isotopomers using mass spectrometry reveals higher mole percent excess levels of glutamate, aspartate, succinate, malate, citrate and lactate in recurrent tumors when compared to primary tumors. Glutamine labeling was lower in recurrent tumors

indicating higher label consumption. Gln: glutamine; Glu: glutamate; Asp: aspartate; Succ: sucinate; Mal: malate; Citric: citrate; Lac: lactate.

Figure 3. Recurrent tumor cells are glutamine-addicted (A) Primary tumors cells cultured in control media and media lacking glutamine exhibit similar growth characteristics. Recurrent tumor cells cultured in media lacking glutamine exhibit decreased growth and increased cell death compared to those cultured in control media. The observed glutamine-addiction phenotype displayed by recurrent tumor cells can be rescued by media supplementation with α-ketoglutarate. (B) Quantification of cell viability by trypan blue reveals decreased viability of recurrent tumor cells cultured in media lacking glutamine. All other conditions exhibited similar viability levels. Gln: glutamine; α-kg: α-ketoglutarate.

Figure 4. Slc1a5 is upregulated in recurrence and is required for tumor growth (A) qRT-PCR profiling of primary and recurrent tumors reveals higher expression levels of *Slc1a5* at the mRNA level. (B) Recurrent tumors exhibit higher protein levels in recurrent tumors. (C) Confirmation of Slca15 knockdown in primary tumor cells was assessed by qRT-PCR. 2 shRNA constructs were used. Ctrl: Control. (D) *Slc1a5* knockdown does not affect the mean growth rate of primary tumors *in vivo*. (E) Confirmation of *Slc1a5* knockdown in recurrent tumor cells was performed by qRT-PCR. 2 shRNA constructs were used. (F) *Slc1a5* downregulation in recurrent tumors leads to statistically significant lower mean growth rate of recurrent tumors *in vivo*. Mean tumor growth rate was calculated from bi-weekly caliper measurement of tumor dimensions.

Figure 5. Gls1 is upregulated in recurrence and is required for tumor growth (A) Recurrent tumors exhibit higher expression of *Gls1* levels relative to primary tumors at the mRNA level. Gene expression levels were assessed using qRT-PCR. (B) Gls1 has higher expression at the protein level in recurrent tumors. (C) Confirmation of *Gls1* knockdown in primary tumor cells by qRT-PCR. 2 shRNA constructs were used. (D) *Gls1* downregulation does not affect primary tumor mean growth rate *in vivo*. (E) Confirmation of *Gls1* knockdown in recurrent tumor cells. 2 shRNA constructs were used. (F) *Gls1* knockdown results in a marked decrease in mean tumor growth rate in recurrent tumors *in vivo*. Mean tumor growth rate was calculated from bi-weekly caliper measurement of tumor dimensions.

Figure 6. *SLC1A5*, but not *GLS1* expression is associated with recurrence risk in human breast cancer (A) Cox proportional hazard regression of 11 human datasets reveals a statistically significant association between high *SLC1A5* expression and 10-year cancer relapse risk. When all datasets are considered, the random effect model yields a hazard ratio of 1.58 (p=0.0067). HR: hazard ratio; CI: confidence interval. (B) Examination of the same human datasets does not reveal a statistically significant association between *GLS1* expression and 10-year relapse risk. The combined hazard ratio was 0.96 (p=0.56). This analysis was conducted using a meta-analysis-based algorithm.

Figure 7. Myc is upregulated in recurrence and drives *Slc1a5* and *Gls1* upregulation (A) Myc exhibits increased expression in recurrent tumors on the protein level. (B) Myc upregulation is accompanied by increased expression of a number of known downstream Myc targets. Target expression level was assessed using qRT-

PCR. (C) Downregulation of *Myc* expression in recurrent tumor cells is accompanied by decreased expression of *Slc1a5* and *Gls1*. *Myc* downregulation was achieved with *Myc*-targeted siRNAs. Gene expression levels were assessed using qRT-PCR. (D) *Myc* downregulation was also accompanied by decreased glutamine consumption and decreased glutamate production. Negative values correspond to metabolite consumption and positive values correspond to metabolite production. Metabolite measurements were normalized to the average number of cells in each well.

5.6 Figures

Figure 1

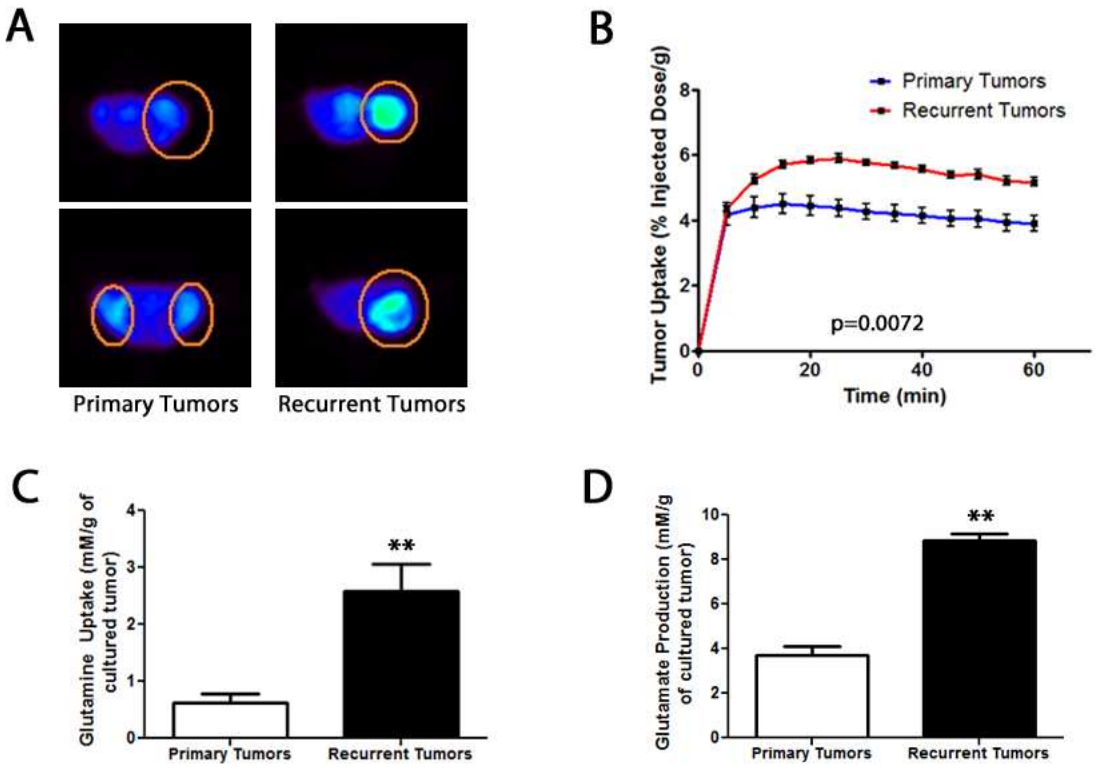

Figure 2

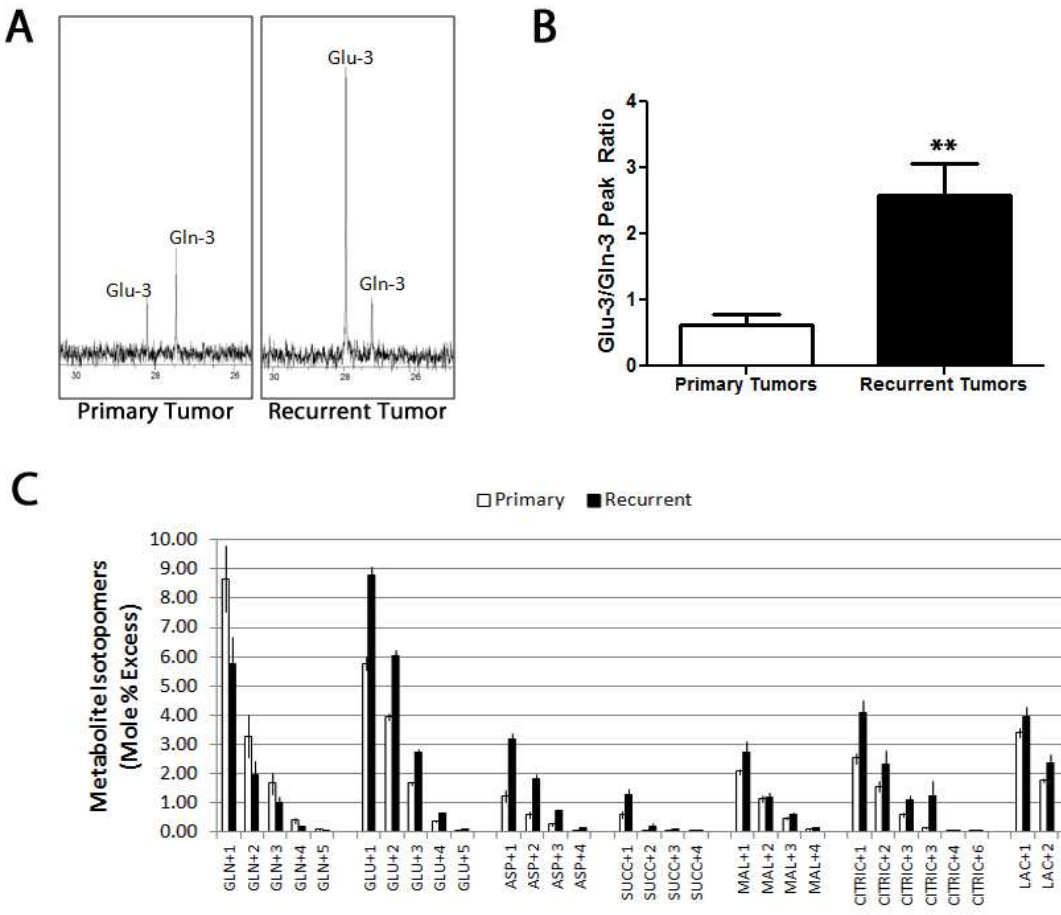
A
Glu-3
Gln-3
Glu-3
Gln-3
Primary Tumor
Recurrent Tumor
B
Glu-3/Gln-3 Peak Ratio
**
Primary Tumors
Recurrent Tumors
C
Primary
Recurrent
Metabolite Isotopomers (Mole % Excess)
GLN+1
GLN+2
GLN+3
GLN+4
GLN+5
GLU+1
GLU+2
GLU+3
GLU+4
GLU+5
ASP+1
ASP+2
ASP+3
ASP+4
SUCC+1
SUCC+2
SUCC+3
SUCC+4
MAL+1
MAL+2
MAL+3
MAL+4
CITRIC+1
CITRIC+2
CITRIC+3
CITRIC+4
CITRIC+6
LAC+1
LAC+2
LAC+3

Figure 3

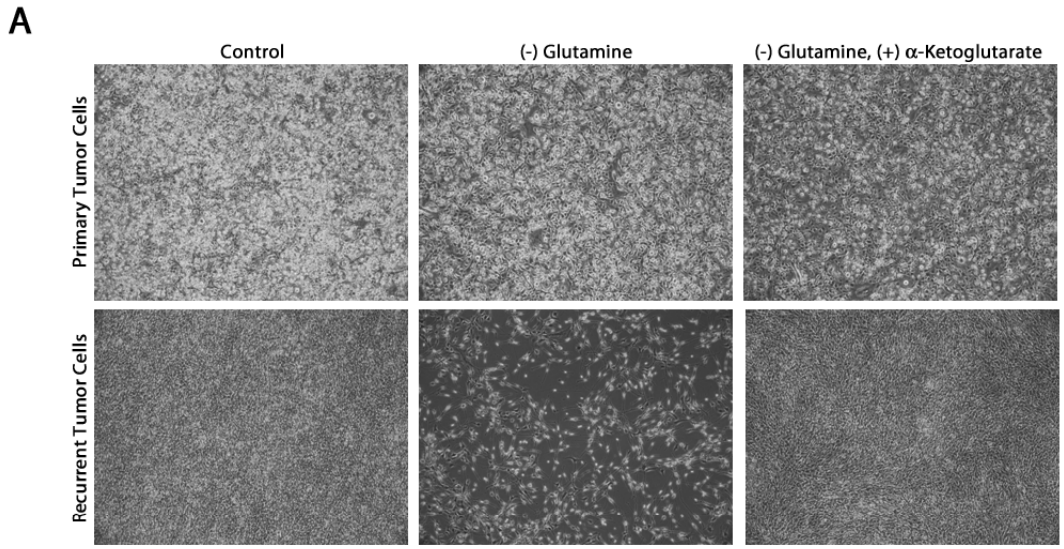
A
Control
(-) Glutamine
(-) Glutamine, (+) α-Ketoglutarate
Primary Tumor Cells
Recurrent Tumor Cells

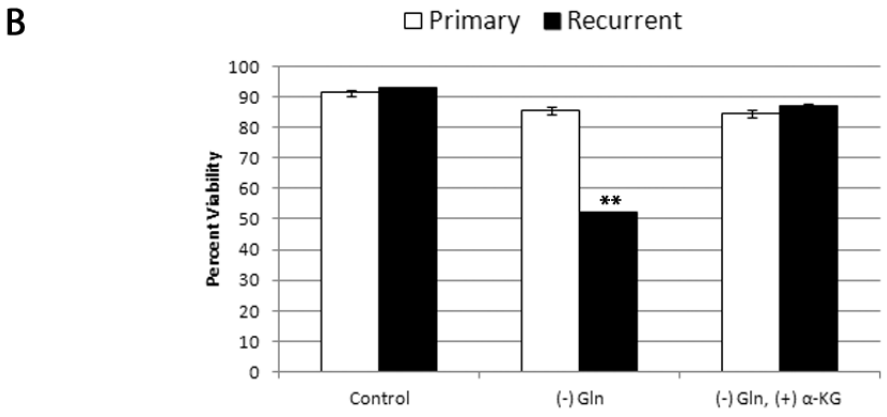
B
Primary
Recurrent
Percent Viability
100
90
80
70
60
50
40
30
20
10
0
**
Control
(-) Gln
(-) Gln, (+) α-KG

Figure 4

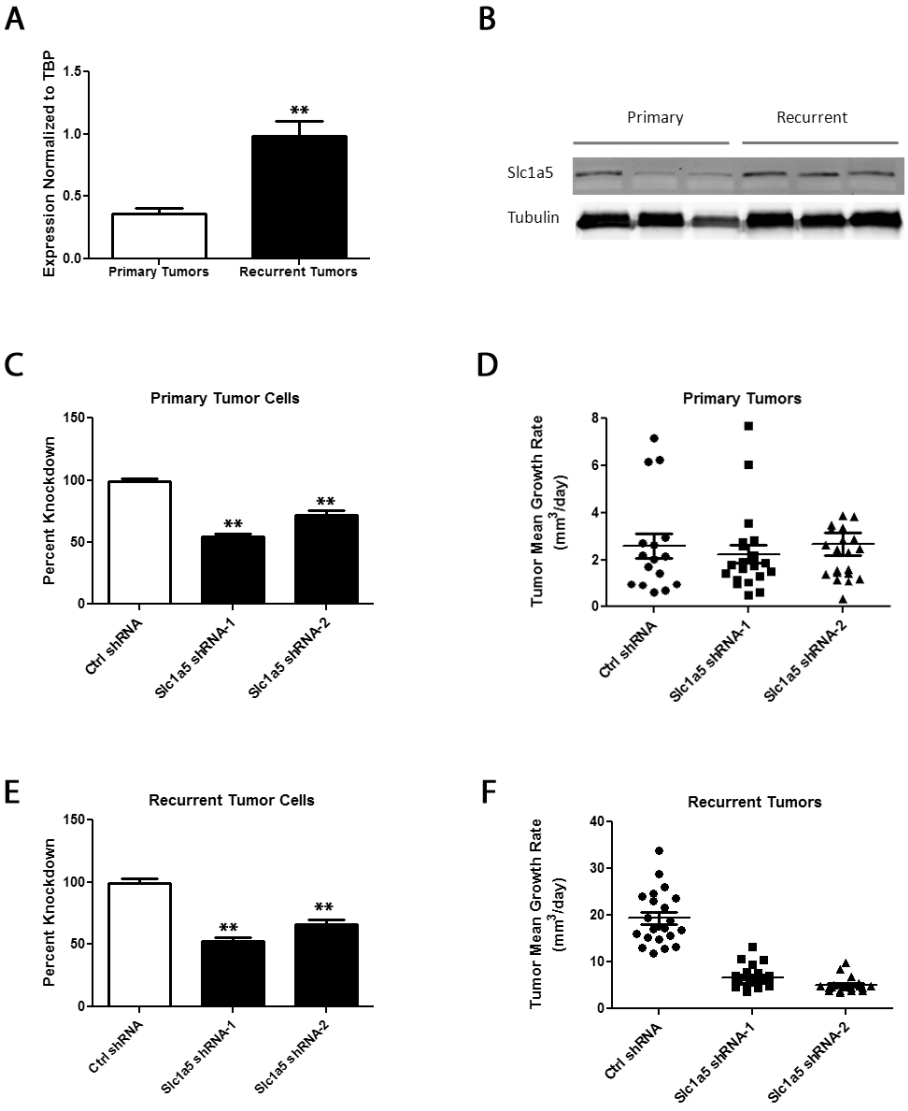
A
Expression Normalized to TBP
1.5
1.0
0.5
0.0
**
Primary Tumors
Recurrent Tumors
B
Primary
Recurrent
Slc1a5
Tubulin
C
Primary Tumor Cells
Percent Knockdown
150
100
50
0
**
**
Ctrl shRNA
Slc1a5 shRNA-1
Slc1a5 shRNA-2
D
Primary Tumors
Tumor Mean Growth Rate
(mm3/day)
8
6
4
2
0
Ctrl shRNA
Slc1a5 shRNA-1
Slc1a5 shRNA-2
E
Recurrent Tumor Cells
Percent Knockdown
150
100
50
0
**
**
Ctrl shRNA
Slc1a5 shRNA-1
Slc1a5 shRNA-2
F
Recurrent Tumors
Tumor Mean Growth Rate
(mm3/day)
40
30
20
10
0
Ctrl shRNA
Slc1a5 shRNA-1
Slc1a5 shRNA-2

Figure 5

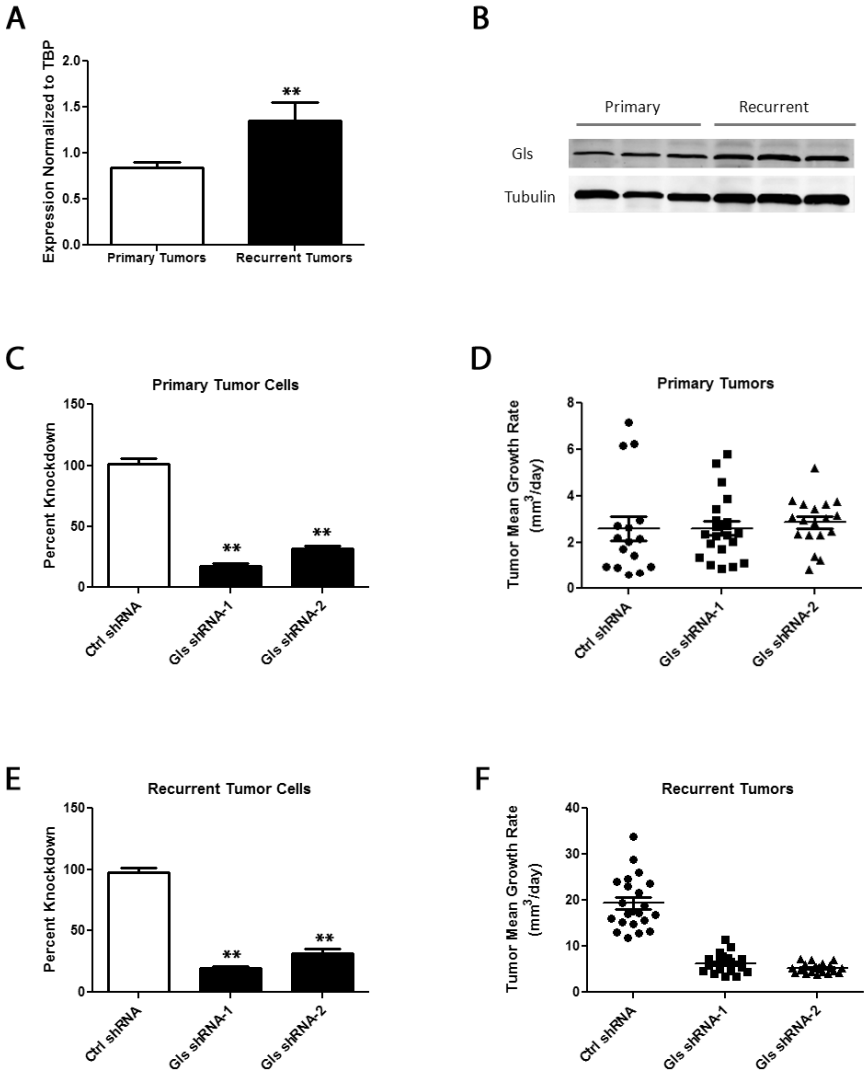
A
Expression Normalized to TBP
2.0
1.5
1.0
0.5
0.0
**
Primary Tumors
Recurrent Tumors
B
Primary
Recurrent
Gls
Tubulin
C
Primary Tumor Cells
Percent Knockdown
150
100
50
0
**
**
Ctrl shRNA
Gls shRNA-1
Gls shRNA-2
D
Primary Tumors
Tumor Mean Growth Rate (mm3/day)
8
6
4
2
0
Ctrl shRNA
Gls shRNA-1
Gls shRNA-2
E
Recurrent Tumor Cells
Percent Knockdown
150
100
50
0
**
**
Ctrl shRNA
Gls shRNA-1
Gls shRNA-2
F
Recurrent Tumors
Tumor Mean Growth Rate (mm3/day)
40
30
20
10
0
Ctrl shRNA
Gls shRNA-1
Gls shRNA-2

Figure 6

A

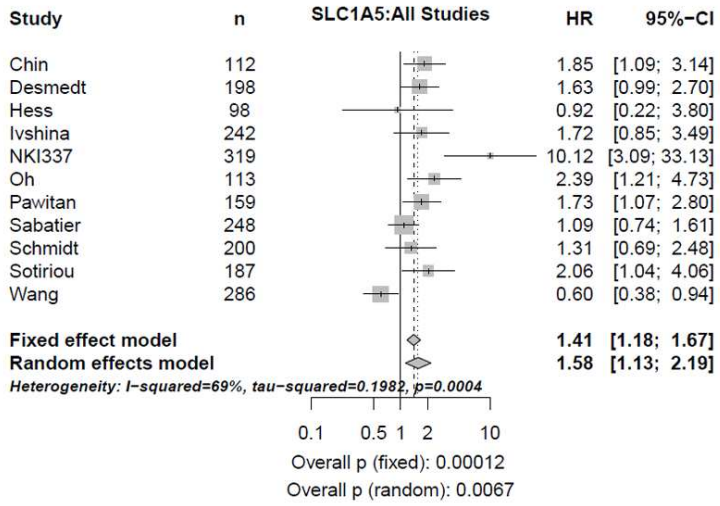
Study
n
SLC1A5:All Studies
HR
95%−CI
Chin 112 1.85 [1.09; 3.14]
Desmedt 198 1.63 [0.99; 2.70]
Hess 98 0.92 [0.22; 3.80]
Ivshina 242 1.72 [0.85; 3.49]
NKI337 319 10.12 [3.09; 33.13]
Oh 113 2.39 [1.21; 4.73]
Pawitan 159 1.73 [1.07; 2.80]
Sabatier 248 1.09 [0.74; 1.61]
Schmidt 200 1.31 [0.69; 2.48]
Sotiriou 187 2.06 [1.04; 4.06]
Wang 286 0.60 [0.38; 0.94]
Fixed effect model 1.41 [1.18; 1.67]
Random effects model 1.58 [1.13; 2.19]
Heterogeneity: I−squared=69%, tau−squared=0.1982, p=0.0004
0.1 0.5 1 2 10
Overall p (fixed): 0.00012
Overall p (random): 0.0067

B

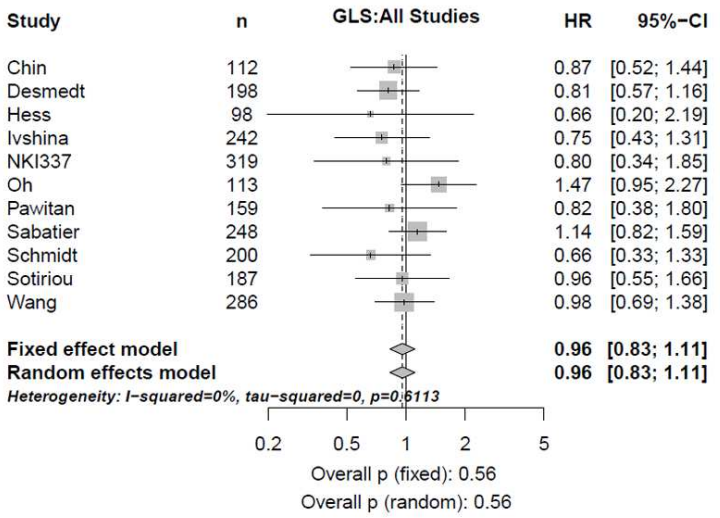
Study
n
GLS:All Studies
HR
95%−CI
Chin 112 0.87 [0.52; 1.44]
Desmedt 198 0.81 [0.57; 1.16]
Hess 98 0.66 [0.20; 2.19]
Ivshina 242 0.75 [0.43; 1.31]
NKI337 319 0.80 [0.34; 1.85]
Oh 113 1.47 [0.95; 2.27]
Pawitan 159 0.82 [0.38; 1.80]
Sabatier 248 1.14 [0.82; 1.59]
Schmidt 200 0.66 [0.33; 1.33]
Sotiriou 187 0.96 [0.55; 1.66]
Wang 286 0.98 [0.69; 1.38]
Fixed effect model 0.96 [0.83; 1.11]
Random effects model 0.96 [0.83; 1.11]
Heterogeneity: I−squared=0%, tau−squared=0, p=0.5113
0.2 0.5 1 2 5
Overall p (fixed): 0.56
Overall p (random): 0.56

Figure 7

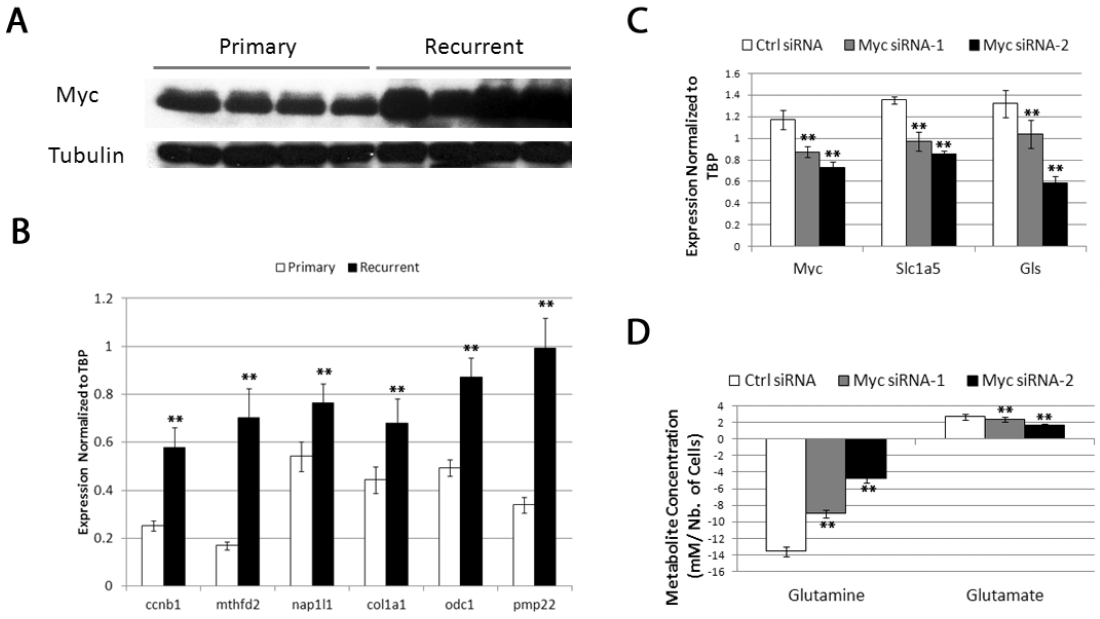
A
Primary
Recurrent
Myc
Tubulin
B
Primary
Recurrent
Expression Normalized to TBP
ccnb1
mthfd2
nap1l1
col1a1
odc1
pmp22
C
Ctrl siRNA
Myc siRNA-1
Myc siRNA-2
Expression Normalized to TBP
Myc
Slc1a5
Gls
D
Ctrl siRNA
Myc siRNA-1
Myc siRNA-2
Metabolite Concentration (mM/ Nb. of Cells)
Glutamine
Glutamate

CHAPTER 6

Ldhb Downregulation by Sirt3 Contributes to the Warburg Effect and Promotes Breast Cancer Recurrence

ABSTRACT

Tumor recurrence is the principal cause of mortality in women with breast cancer. Despite its clinical importance, little is known about the mechanisms underlying breast cancer recurrence. Increased lactate levels have been shown to be a poor prognostic marker in cancer patients and have been proposed to be a characteristic feature of metastatic and recurrent tumors. In this study, we assess changes in lactate metabolism during breast cancer progression in a genetically-engineered mouse model of HER2/*neu*-induced breast cancer that recapitulates key features of the natural history of breast cancer progression including primary tumor development, tumor dormancy and recurrence. We find that recurrent mammary tumors exhibit increased lactate levels, compared to primary tumors, and that downregulation of *Ldhb* in recurrent tumors was responsible for this change. Ldhb, a subunit of the LDH enzyme, favors the conversion of lactate to pyruvate. Consequently, decreased *Ldhb* expression in recurrent tumors favors the accumulation of lactate due to a reduced ability to oxidize this metabolite. We further determined that *Ldhb* downregulation plays a functional role in tumor recurrence as *Ldhb* knockdown in primary tumor cells was sufficient to promote tumor recurrence in orthotopic mouse experiments. Consistent with a role for *Ldhb* downregulation in human breast cancer progression, low *Ldhb* was associated with reduced recurrence-free survival in breast cancer patients, particularly those whose tumors exhibited HER2/*neu*

amplification. *Ldhb* downregulation in recurrent tumors was due to downregulation of the NAD-dependent mitochondrial deacetylase, Sirt3, an effect that was mediated by Hif1-α. Taken together, our results suggest a functional role for *Ldhb* downregulation in promoting breast cancer recurrence and suggest potential clinical applications of *Ldhb* expression as a prognostic factor in human breast cancer.

6.1 Introduction

Breast cancer is the most commonly diagnosed malignancy in women and is the second leading cause of cancer-related death in women in the U.S.[2, 5]. Among women with breast cancer, tumor recurrence represents the principal cause of mortality[17]. Nevertheless, little is known about the molecular mechanisms by which breast cancer cells survive therapy and recur. In particular, while dysregulated metabolism has long been recognized as a key feature of cancer development, the metabolic changes accompanying cancer recurrence are largely unexplored. Progress in this area has been greatly hindered by the lack of models for breast cancer recurrence. To address this gap, our laboratory has developed a series of inducible bitransgenic mouse models that accurately recapitulate human breast cancer progression, including primary tumor development, minimal residual disease, tumor dormancy and recurrence[63-65]. In this study, we explore the changes in lactate metabolism that accompany breast cancer progression and identify their underlying causes and potential functional role in tumor recurrence.

Increased lactate production in tumors has generally been associated with advanced disease in cancer patients. For example, high lactate levels have been

reported in metastatic recurrent tumors in human cervical cancers, head and neck cancers, lung cancers and colorectal cancers[145, 267-271]. In addition, lactate accumulation in the plasma of cancer patients has also been found to be positively correlated with tumor burden[82]. These results provide evidence for a potential role of increased lactate metabolism in cancer progression.

The tendency of cancer cells to produce large amounts of lactate, despite the presence of oxygen, was first observed by Otto Warburg in the 1930s[76]. Today, aerobic glycolysis, or the Warburg effect, is recognized as one of the most characteristic features of the metabolic profile of cancer cells. In the presence of oxygen, cancer cells metabolize most of the glucose they uptake and convert it to lactate. At the end of the glycolytic pathway, lactate dehydrogenase catalyzes the interconversion of pyruvate to lactate. Lactate dehydrogenases consist of homo- and hetero- tetramers of M and H proteins encoded by the *Ldha* and *Ldhb* genes respectively[85]. Five iso-enzymes, with different activity levels, have been described: LDH1 (4H), LDH2 (3H1M), LDH3 (2H2M), LDH4 (1H3M) and LDH5 (4M)[85]. LDH5, which consists of 4 Ldha subunits, is known to favor the conversion of pyruvate to lactate[85]. To date, differential lactate production in cancer cells has mainly been ascribed to changes in Ldha[84, 272]. More recently, cancer cells were found to preferentially express the embryonic isoform of pyruvate kinase, Pkm2[273], which increases lactate levels in tumors[273]. In addition, both Ldha and Pkm2 appear to be required for tumor growth[83, 274]. In contrast, at present, little is known about the role of Ldhb in tumorigenesis.

In this study, we investigate changes in lactate metabolism during breast cancer progression and characterize the functional role of these changes on tumorigenesis. In doing so, we establish a novel role for *Ldhb* downregulation in promoting cancer

recurrence in genetically engineerd mice and identify the mechanism behind the observed changes in mammary tumorigenesis and tumor recurrence. Consistent with a role in human breast cancer progression, *Ldhb* downregulation was associated with reduced recurrence-free survival in breast cancer patients.

6.2 Methods

Animals, cell culture and recurrence assay

The MMTV-rtTa;TetO-HER2/*neu* (MTB/TAN) doxycycline-inducible bitransgenic mouse model has been described[63, 132]. All mice were housed and treated in accordance with protocols approved by the Institutional Animal Care and Use Committee at the University of Pennsylvania. MTB/TAN mice were bred, housed, induced with 2 mg/ml doxycycline, monitored for tumor development and recurrence, and sacrificed as described[66].

Tumor cells from primary mammary tumors arising in MTB/TAN mice maintained on doxycycline were isolated and cultured in the presence of doxycycline as described[66]. Primary tumor cells were transduced with retroviruses expressing shRNAs targeting genes of interest and were selected in puromycin for stably-transduced polyclonal populations.

Magnetic resonance spectroscopy

PCA extraction was performed on 4 primary and 4 recurrent flash-frozen tumor samples using 12% perchloric acid. Extracted samples were lyophilized and dissolved in 0.6 ml D_2O. ^1H NMR spectroscopy was performed at 400MHz on a Bruker Avance DMX 400

wide-bore spectrometer. Fully relaxed proton spectra were acquired with a 5 mm inverse probe using the following conditions: PW 45º, TR 8s, water saturation during the relaxation delay, 6775 Hz SW, TD 64k and 64 scans. An external standard made of trimethylsilylpropionic acid (TSP) was introduced in the NMR tube and used as a chemical shift reference and as a quantification standard. Metabolite resonance assignments were made based on previously published spectra in breast cancer tissue[133]. Analysis of collected NMR spectra was performed using NUTS (Acorn NMR Inc).

^{13}C-labeling experiments and mass spectrometry

Three primary tumor-bearing mice and three recurrent mammary tumor-bearing mice, were infused through a tail vein catheter with a 200 mM solution of D-[1,2-^{13}C]-glucose (Isotec) over a period of 45 minutes. Six additional mice, 3 bearing primary tumors and 3 bearing recurrent tumors were infused through a tail vein catheter with a 40 mM solution of L-[U-^{13}C]-lactate for 45 minutes. At the end of the infusion period, tumors were dissected and clamp-frozen in liquid nitrogen. Perchloric acid extraction was performed as described[128].

Measurement of ^{13}C isotopomers was performed on a Triple Quad 6410 mass spectrometer combined with an LC 1290 Infinity mass selective detector (Agilent), as described[257]. Briefly, samples were first purified by passage through either AG-1 or AG-50 cation exchange columns (Biorad) and then converted into t-butyldimethylsilyl derivatives. Isotopic enrichment of lactate, alanine, citrate, glutamate, malate and aspartate were monitored. ^{13}C-enrichment was computed as molar percent enrichment

(MPE), reflecting the mol fraction (%) of analytes containing ^{13}C atoms in excess of natural abundance, where MPE (M+i) = % $A_{M+i}/[A_M + \Sigma A_{M+i}]$, and A_M and A_{M+i} represent the peak area from LC-MS ions corrected for natural abundance and corresponding to the unlabeled (M0) and ^{13}C-labeled (M+i) mass isotopomers, respectively. To reflect the amount of each labeled metabolite pool relative to the total available metabolite amount in the tissue, results are presented as the Σ ^{13}C- labeled Metabolite: Σ(^{13}C- labeled Metabolite) = [Metabolite Concentration] x Σ(MPE).

In vitro metabolite level quantification

300,000 cells were plated and incubated in cell culture media for 96 hours. Lactate and glucose levels present in the media at 96 hours were determined using a 7100 Multiparameter Bioanalytical System (YSI life Sciences). The amount of each metabolite consumed or produced by cells in each well was computed as the difference between the level of that metabolite in conditioned media from cultured cells compared to its level in control media incubated without cells, and then normalized to the average number of cultured cells in that well. Positive values denote metabolite level increase, whereas negative values denote metabolite level decrease. Samples from each tested condition were run in triplicate and statistical significance was determined using a student's t-test.

RNA isolation and qRT-PCR

RNA extraction was performed on snap-frozen primary and recurrent mammary tumor tissue and cell samples as described[253]. Samples were homogenized and RNA isolation

was carried out using the RNeasy RNA isolation kit (Qiagen) according to manufacturer's instructions. Reverse transcription was performed from 2 µg of RNA using the cDNA High Capacity Reverse Transcriptase Kit (Applied Biosystems). qRT-PCR analysis for mRNA levels was carried out on an Applied Biosystems 7900 HT Fast Real-Time PCR system using 6-carboxyfluorescein–labeled Taqman probes (Applied Biosystems). Expression levels were normalized to TBP.

Western blotting

Mammary tumors were homogenized with a sonicator in TPER protein lysis buffer (Thermo Scientific). Primary antibodies were obtained from Abcam (anti-Ldhb and anti-Ldha), or Cell Signaling (anti-Pkm2, anti-Sirt3 and anti-Hif1). Horse radish peroxidase-conjugated secondary antibodies (Jackson Laboratories) were used to probe membranes incubated with the anti-Pkm2, anti-Hif1 and anti-Sirt3 antibodies. The enhanced chemiluminescent system (ECL; Amersham) was used to detect the bound secondary antibodies. Anti-Ldha and Ldhb primary antibodies were detected using Alexa-Fluor-conjugated secondary antibodies (Molecular Probes). The Odyssey V3.0 system (Li-COR Biosciences) was used to visualize and quantify proteins of interest.

Hif1 gene pathway activity

A hypoxia gene expression signature was generated from a dataset obtained from the NCBI GEO website (GSE3188). Cyber-T analysis was performed to identify differentially regulated genes in breast cancer cells under hypoxic conditions. A p-value

cutoff of 0.01 and a fold change cutoff of 2 generated a 288-gene hypoxia gene signature. The generated signature was used to assess hypoxic pathway activity in microarray data of mouse tumors using a scoring system described previously[134].

Pkm1 and Pkm2 isoform quantification

We designed 5' and 3' oligonucleotide primers (ACACGAAGGTCGACATCCTC and CAAGGGGACTACCCTCTGG) for the *Pkm* gene. Using RNA extracted from primary and recurrent tumor samples, *Pkm1* and *Pkm2* were amplified using PCR. Equivalent amounts of amplified *Pkm1* and *Pkm2* fragments were digested with *Pst1*, *Econ1* restriction enzyme, both enzymes or neither enzymes. *EcoN1* is specific for *Pkm1* and *Pst1* is specific for the *Pkm2*. Following digestion, products were electrophoresed on a non-denaturing polyacrylamide gel. The gel was stained with ethidium bromide prior to UV imaging.

LDH activity determination

LDH was extracted from primary and recurrent tumor samples using the Biovision LDH Activity Quantification kit (Biovision, Inc.) according to manufacturer's instructions. Protein amounts were quantified in each of the extracted samples and the same amount of protein was loaded in each well prior to activity measurements. Enzyme activity is presented as amount of lactate converted into pyruvate in nmol/min/ml.

Zymography

To separate the different LDH isoenzymes, aliquots from the same samples extracted for LDH activity assays were subjected to a non-denaturing polyacrylamide gel for electrophoresis. Following electrophoresis, gels were placed in a staining solution containing NAD^+, lactate and Syber Gold. NADH produced during the conversion of lactate to pyruvate reacts with Syber Gold thereby reflecting the activity of each of the LDH isoenzymes.

Ldhb shRNA constructs

Oligonucleotides targeted against *Ldhb* were designed using RNAi Central (http://katahdin.cshl.org/siRNA/RNAi.cgi?type=shRNA). The following sequences were used: *Ldhb* shRNA-1: TGCTGTTGACAGTGAGCGCCCTCATCGAGTCCATGCTGAA-

TAGTGAAGCCACAGATGTATTCAGCATGGACTCGATGAGGTGCCTACTGCCTCGG; and *Ldhb* shRNA-2: TGCTGTTGACAGTGAGCGAACAGACAATGACAGTGAGAACTA-

GTGAAGCCACAGATGTAGTTCTCACTGTCATTGTCTGTCTGCCTACTGCCTCGGA. Oligonucleotides were cloned into the MLP vector and retroviral vectors and supernatants were generated as described[253].

siRNA experiments

Knockdown of *Sirt3* and *Hif1* expression in primary tumor cells was performed using commercially available siRNAs (Ambion). A scrambled siRNA was used as a negative control (Ambion). siRNA transduction was performed according to manufacturer's instructions and cells were incubated with siRNAs for 48 hrs. *Sirt3* and *Hif1* knockdown were confirmed by qRT-PCR.

Orthotopic tumor assay

Orthotopic tumor assays were performed in athymic nude mice (*nu/nu*) (Taconic, Germantown, NY). Cells were injected into the inguinal mammary fat pads of 10-12 *nu/nu* mice for each experimental group. Experiments were performed in parallel with three experimental arms, including one experimental arm for each of the *Ldhb* shRNA contructs, as well as an arm for a control shRNA. Cells expressing an empty MLP vector were used in the control group. 1 million tumor cells were injected into the number four mammary fat pads of each mouse.

For primary orthotopic tumor growth assays, HER2/*neu* expression in transplanted cells was induced by administering 2 mg/mL doxycycline in drinking water. Tumor size was measured 2-3 times per week and tumor volume was determined by caliper measurements for each injected site using the following formula: Tumor volume = (smallest diameter^2 * largest diameter)/2. Tumors were followed until they reached a size of approximately 15x15 mm. Mean tumor growth rate (MGR) was calculated for each tumor as described[252].

For orthotopic recurrence assays, mice were maintained on doxycycline until primary tumors reached a size of 3x3 mm. Doxycycline was then withdrawn and tumors were followed for regression. The incidence and latency of tumor recurrence was assessed from biweekly measurements. Kaplan-Meier curves were generated for recurrence-free survival following doxycycline withdrawal and compared between the two cohorts using a logrank test.

Human association analysis

Microarray data sets[135, 137, 138] profiled using the Affymetrix HG-U133A platform were downloaded from Gene Expression Omnibus and individually RMA-normalized. 943 lymph node-negative patients who did not receive any systemic adjuvant therapy were identified according to available clinical information. Microarray data were mean-centered by gene within each data set and combined into one data set. HER2-positive status was approximated by inspection of the rank plot of HER2 mRNA levels, and defined as samples having mean-centered log2 expression greater than 1. Patients were assigned to high- or low-scoring classes based on their metabolic gene expression signature scores. The cutoff between high- and low-scoring classes was determined by an outcome-oriented approach[140]. Differences in 5-year relapse-free survival between the two classes were assessed by p-value from the log-rank test and hazard ratio from Cox proportional hazards regression. To guard against high false-positive rates resulted from multiple testing, a corrected p-value was also calculated as part of the cut-point determination step[140]. Analyses were performed specifically for the HER2-positive subset of patients. All data analyses were performed in the R environment[141].

6.3 Results

To assess the differences in lactate metabolism between primary and recurrent tumors, we made use of a previously described doxycycline-dependent genetically engineered mouse model for HER2/*neu*-induced mammary tumorigenesis[63, 66]. In this model, activation of HER2/*neu* results in mammary epithelial hyperplasia and the eventual development of primary mammary tumors that are addicted to HER2/*neu* expression[63]. When doxycycline is withdrawn, the resulting acute downregulation of HER2/*neu* pathway activity results in the regression of mammary tumors to a non-palpable state. This mimics the effect of therapy in women with HER2/*neu*-amplified breast cancers who are treated with a targeted agent that blocks HER2/*neu* activity[63]. Akin to human breast cancer patients, primary mammary tumors that regress to a non-palpable state following doxycycline withdrawal subsequently recur with stochastic kinetics following a variable latent period that mimics human tumor dormancy[66]. Recurrent mammary tumors in this system do not re-activate the HER2/*neu* transgene, but rather escape their dependence on HER2/*neu* signaling by activating alternate growth and survival pathways[66].

Recurrent tumors exhibit higher lactate levels than primary tumors

We used ^{1}H magnetic resonance spectroscopy (MRS) to evaluate lactate levels in primary and recurrent mammary tumors. Metabolic profiling of primary and recurrent mammary tumors revealed several metabolites whose concentrations differed between primary and recurrent tumors, including lactate whose levels were 30% higher levels in recurrent tumors ($p=0.002$) (Figure 1A). These results were confirmed with mass spectrometry where in metabolite quantification in primary and recurrent tumors also revealed 40% higher lactate levels in recurrent tumors ($p=0.014$) (Figure 1B).

To further characterize the source of the higher lactate levels observed in recurrent tumors, we used ^{13}C-labeled compounds and determined their isotopic labeling at specific metabolic steps. Since increased lactate levels in cancer cells have primarily been attributed to the Warburg effect, we tested the hypothesis that increased lactate levels in recurrent tumors result from increased glycolytic flux. To achieve this end, we infused [1,2-^{13}C]-glucose into primary as well as recurrent tumor-bearing mice. The total amount of ^{13}C-labeled metabolite was used as a readout of glucose carbon contribution to each of the assessed metabolites. Surprisingly, this analysis revealed that glucose exhibited a lower ^{13}C-labled carbon contribution to lactate in recurrent tumors compared to primary tumors ($p=0.004$) (Figure 1C). This suggested that the increased lactate levels observed in recurrent tumors might not simply be the product of increased glucose metabolism.

We next sought to determine whether increased lactate concentrations in recurrent tumors might result from lactate accumulation in the tumors driven by reduced lactate metabolism. To test this hypothesis, we infused [3-^{13}C]-lactate into primary tumor-bearing mice and recurrent tumor-bearing mice. Assessment of isotopic labeling and quantification of the total amount of available metabolite revealed a higher total amount of labeled lactate in recurrent tumors compared to primary tumors ($p=0.01$) (Figure 1D). Consistent with our hypothesis, recurrent tumors displayed lower levels of total labeled alanine from lactate, potentially reflecting reduced lactate uptake and metabolism in recurrent tumors (Figure 1D).

Recurrent tumors exhibit similar Ldha and Pkm2 but lower Ldhb levels

To identify the underlying molecular determinants responsible for the observed differences in lactate levels, we used qRT-PCR to quantify the mRNA expression levels of *Ldha* and *Ldhb*. Expression profiling in primary and recurrent tumors revealed similar *Ldha* expression levels (p=0.151), but a 5-fold decrease in *Ldhb* expression levels as tumors progressed from the primary to recurrent stage (p=0.016) (Figure 2A). These results were confirmed at the protein level where Ldha levels were similar in primary and recurrent tumors and Ldhb levels were decreased in recurrent tumors (Figure 2B).

Another enzyme implicated in contributing to increased lactate levels in cancer is the embryonic isoform of pyruvate kinase, Pkm2. To assess whether differences in Pkm2 levels, or differences in the Pkm2/Pkm1 ratio, might be responsible for the observed change in lactate level, we examined *Pkm2* expression at the mRNA and protein levels and compared them to those of Pkm1, the adult isoform of pyruvate kinase. Since Pkm1 and Pkm2 result from alternative splicing of the *Pkm* gene transcript (Figure 2C), we designed primers to amplify both *Pkm1* and *Pkm2* and sought to quantify each isoform using restriction enzymes specific to each amplified fragment. Our results revealed that primary and recurrent tumors exhibited similar levels of *Pkm1* and *Pkm2* (Figure 2C). This was further confirmed by western blotting which revealed similar levels of Pkm2 protein in primary and recurrent tumors (Figure 2D).

In summary, our results indicate that primary and recurrent mammary tumors exhibit similar Ldha and Pkm2 levels, but lower levels of Ldhb, suggesting that reduced Ldhb levels might contribute to the elevated levels of lactate observed in recurrent tumors.

Ldhb downregulation levels result in lower LDH activity and reduced lactate metabolism in recurrent tumors

To further characterize the metabolic effects of Ldhb downregulation, we evaluated the distribution of LDH isoforms in primary and recurrent tumors. The LDH enzyme is a tetramer consisting of different numbers of Ldha and Ldhb subunits, which manifests as five different enzyme isoforms. The LDH5 isoform consists of four Ldha subunits whereas the LDH1 isoform consists of four Ldhb subunits. Zymography performed on protein lystes prepared from primary and recurrent tumors revealed a shift in the distribution of the LDH isoforms as tumors recur. While primary tumors expressed all five isoforms of LDH, recurrent tumors only expressed LDH4 and LDH5, and lacked LDH isoforms containing two or more subunits of Ldhb (isoforms 1, 2 and 3) (Figure 3A).

As Ldhb is known to favor the conversion of lactate into pyruvate, we sought to quantify any differences in the rate of this reaction between primary and recurrent tumors. Profiling of LDH enzymatic activity in primary and recurrent tumors revealed 40% lower LDH activity converting lactate to pyruvate in recurrent tumors compared to primary tumors ($p=0.014$) (Figure 3B).

To directly address whether reduced Ldhb levels contributed to the high lactate levels observed in recurrent tumors, we downregulated expression of *Ldhb* in a recurrent tumor cell line (Figure 3C), incubated these *Ldhb* knockdown cells in media containing lactate and quantified the amount of lactate present in the media at 96 hours. These studies revealed that shRNA-mediated *Ldhb* downregulation resulted in signficant increase in the amount of lactate present in the media at 96 hours compared to the cells expressing a control shRNA ($p<0.05$) (Figure 3D). Similar results were obtained with

two different shRNA constructs. These findings suggest Ldhb downregulation in recurrent tumor cells could contribute to higher lactate levels that we observed in the recurrent tumors in vivo.

Lower Ldhb levels promote tumor recurrence in mice and are correlated with lower recurrence-free survival in human breast cancer

To assess the functional effect of Ldhb downregulation on breast cancer progression, we employed an orthotopic tumor assay in which we genetically manipulated the expression of *Ldhb* in primary tumor cells derived from MMTV-rtTa;TetO-HER2/*neu* mice in which a HER2/*neu* transgene was expressed in a doxycycline-inducible manner (Figure 3C) prior to injecting them in the mammary fat pad of *nu/nu* mice. In this assay, primary tumor growth was induced by doxycycline administration to *nu/nu* mice whose mammary fat pads had been injected with primary tumor cells that had been transduced with an *Ldhb* shRNA or control shRNA. When those tumors reached a size of 3x3 mm, doxycycline was withdrawn to induce tumor regression then monitored for the appearance of recurrent tumors (Figure 4A). Our results revealed that primary tumors derived from cells in which *Ldhb* had been knocked down recurred at a significantly faster rate compared to primary tumors derived from cells transduced with a control shRNA (Figures 4B and 4C). These results were reproduced with two different shRNA constructs (HR1=0.2755, p1=0.001 and HR2=0.21, p2<0.001). This indicates that Ldhb downregulation in primary tumor cells is sufficient to promotoe tumor recurrence.

To further assess the effect of *Ldhb* knockdown on tumorigenesis, we investigated the effect of *Ldhb* knockdown on primary tumor growth. Primary tumor cells

expressing either a control shRNA or an shRNA directed against *Ldhb* were injected into the mammary fat pads of *nu/nu* mice. Tumor growth was induced by the administration of doxycycline to induce HER2/*neu* transgene expression and was followed biweekly until tumors reached a size of 15x15 mm. Quantification of mean tumor growth rate did not reveal any differences in primary tumor growth between control tumors and those with Ldhb knockdown (p1=0.932, p2=0.743) (Figure 4D).

To investigate the potential clinical relevance of our findings, we assessed the association between *Ldhb* gene expression levels and the risk of tumor recurrence in a cohort of breast cancer patients with HER2-positive, node-negative tumors. Consistent with our findings in mice, this analysis revealed that tumors with lower levels of *LDHB* expression were associated with reduced 5-year metastasis-free survival (HR=-2.88 and p=0.0158).

In aggregate, our results indicate that *Ldhb* downregulation is sufficient to promote tumor recurrence, but has no effect on primary tumor growth. Moreover, reduced *LDHB* levels were associated with reduced recurrence-free survival in breast cancer patients.

Ldhb downregulation is caused by Sirt3 downregulation

Sirt3 is an NAD-dependent mitochondrial deacetylase known to regulate glycolytic activity through Hif1-α destabilization[275]. We hypothesized that the reduced levels of *Ldhb* expression that we observed in recurrent tumors was due to a decrease in expression of *Sirt3*. To begin to address this hypothesis, we assessed Sirt3 levels in primary and recurrent tumors. qRT-PCR experiments revealed lower expression of *Sirt3*

at the mRNA level in recurrent tumors (p=0.038) (Figure 5A). These results were further confirmed by western blotting which revealed lower expression of Sirt3 at the protein level in recurrent tumors (Figure 5B).

Next, we used siRNAs targeted against *Sirt3* to directly address whether Sirt3 was capable of modulating *Ldhb* levels in recurrent tumor cells. siRNA-mediated downregulation of *Sirt3* resulted in downregulation of *Ldhb*, but not *Ldha* (Figure 5C). Similar results were obtained with two different siRNAs.

Consistent with this, assessment of changes in metabolite levels in the media 48 hours post-transfection revealed higher lactate levels in the media of cells with siRNAs targeted against *Sirt3* (Figure 5D). These findings suggest that *Sirt3* downregulation in recurrent tumors contributes to the observed decrease in *Ldhb* levels as well as the accompanying increase in lactate levels observed in recurrent tumors.

Downregulation of Ldhb is mediated through Hif1

To further characterize the mechanism responsible for *Ldhb* downregulation, we investigated whether the effect of Sirt3 was mediated through Hif1, a previously-described downstream effector of Sirt3. First, we assessed whether recurrent tumors exhibited higher levels of Hif1-α stabilization. Western blotting revealed higher levels of Hif1 in recurrent tumors compared to primary tumors (Figure 6A). These results were confirmed by assessing Hif1 pathway activity using a gene expression signature incorporating known Hif1 targets. Consistent with our immunoblotting results, Hif1 pathway activity was higher in recurrent tumors compared to primary tumors (p=0.022) (Figure 6B).

To address whether the effect of Sirt3 downregulation on *Ldhb* expression is mediated through Hif1, we used siRNAs targeted against both *Hif1* and *Sirt3* in recurrent tumor cells. Again, downregulation of *Sirt3* expression led to a reduction in *Ldhb* levels as previously ($p=0.003$). However, simultaneous downregulation of both *Sirt3* and *Hif1* abrogated the effect of *Sirt3* dowregulation on *Ldhb* expression (Figure 6C). *Ldha* levels were unaffected by *Sirt3* or *Hif1* downregulation.

Consistent with these findings, assessing changes in lactate levels in the media in which the cells were incubated revealed that *Sirt3* downregulation resulted in higher lactate levels in the media, whereas simultaneous downregulation of both *Sirt3* and *Hif1* abrogated the effect of Sirt3 downregulation on lactate compared to control cells (Figure 6D). These results suggest that the effect of Sirt3 on *Ldhb* expression and lactate levels is mediated through Hif1.

6.4 Discussion

In this work, we provide evidence for increased lactate levels as tumors progress from primary to recurrent stage. Our findings further suggest that this increase in lactate results from decrease in the expression of *Ldhb*, which encodes the LDH subunit that favors the conversion of lactate to pyruvate. Consistent with this, recurrent tumors exhibited a shift in the LDH isoforms that they express towards homo- and heterodimers containing fewer subunits of Ldhb which would be expected to result in a reduction in the conversion of lactate to pyruvate. Notably, this reduction in *Ldhb* expression was also associated with a functional effect on tumorigenesis, as *Ldhb* knockdown in primary tumors accelerated the appearance of recurrent tumors indicating that *Ldhb*

downregulation is sufficient for tumor recurrence. In contrast, *Ldhb* downregulation had no effect on primary tumor growth. Mechanistically, *Ldhb* downregulation could be ascribed to downregulation of the NAD-dependent deacetylase, Sirt3, which was observed in recurrent tumors. Finally, we find that the effect of Sirt3 on Ldhb and lactate levels was mediated through Hif1. Together, our findings suggest that Ldhb downregulation plays a rate-limiting role in tumor recurrence.

High intratumoral lactate levels have previously been associated with poor patient prognosis and increased risk for metastasis and recurrence in human cervical cancers, head and neck cancers and lung cancers[145, 267-270]. Increased lactate levels are also associated with increased tumor invasion, metastasis and tumor burden and have been directly linked to tumor avoidance of immunosurveillance[82, 276, 277]. In this regard, it has been postulated that high lactate levels in the extracellular space lead to an acidic environment that results in more aggressive tumor behavior[82]. High lactate levels also inhibit lactate export from T cells in the tumor microenvironment, significantly reducing their function in tumor recognition[276]. Results from our study suggest that increased lactate levels are associated with tumor progression and breast cancer recurrence.

While most metabolism models suggest that net increased lactate production in cancer cells results from the Warburg effect, several studies suggest that exogenous lactate can act as a carbon source for oxidative metabolism[278-280]. Specifically, evidence exists suggesting a symbiosis between oxygenated and hypoxic cells within tumors, wherein hypoxic cells use glucose as their major energy source while oxygenated cells use lactate generated by hypoxic cells to maintain their metabolic activity[280-282]. Our findings are compatible with this model in that we find that primary tumors, in our model, do indeed uptake and metabolize lactate. In fact, in primary tumors, lactate was a

significant precursor of alanine and glutamate carbon compared to glucose, consistent with observations in rat C6 glioma cells[278]. Our findings also suggest differential lactate metabolism by primary and recurrent tumors. In light of the increased lactate levels that we observed in recurrent tumors, we had initially expected to find increased glycolytic flux and increased lactate production in recurrent tumors. Surprisingly, we found that recurrent tumors exhibited reduced glucose metabolism as well as reduced lactate oxidation, despite the higher net amount of lactate found in those tumors. These findings suggest a potential metabolic shift away from lactate oxidation toward lactate accumulation in recurrent tumors, which might underlie their aggressive behavior.

Previous reports have implicated Ldha levels in regulating lactate production and in contributing to the ability of tumors to proliferate under hypoxic conditions[272, 274]. Similarly, cancer cells have recently been found to exhibit an isoform switch in pyruvate kinase whereby tumors preferentially express high levels of the embryonic form Pkm2 compared to normal tissues, which primarily express Pkm1[273]. This isoform switch modulates lactate production and plays a functional role in tumorigenesis, in that Pkm2 is required for tumor growth[273]. In our study, however, both Ldha and Pkm2 were expressed at similar levels in primary and recurrent tumors, and were therefore unlikely to be responsible for the increased levels of lactate observed in recurrent tumors. Rather, we found that the ldhb subunit of LDH that preferentially converts lactate to pyruvate, was markedly downregulated during the course of tumor recurrence. While some reports have suggested a potential association between Ldhb downregulation and increased metastasis in some human cancers[87, 149, 283], our findings provide the first direct evidence for a functional role for Ldhb downregulation in tumor recurrence.

Downregulation of Ldhb in recurrent tumors results in a reduction in LDH isoforms 1-4 such that these tumors primarily express LDH5, an isoform that consists of 4 Ldha subunits. LDH5 has the highest efficiency of converting pyruvate to lactate. As such, recurrent tumors exhibiting Ldhb dowregulation primarily produce and secrete lactate while exhibiting a reduced ability to uptake and metabolize lactate. This would be anticipated to result in lactate accumulation, as we observed in recurrent tumors.

A limited number of studies have suggested an association between decreased Ldhb expression and increased metastasis and invasive tumor behavior. A laser microdissection study in colorectal tumors found a significant reduction in *LDHB* in the infiltrative edges of the tumors, in the absence of changes in *LDHA* expression[271]. Other studies have shown LDHB downregulation in metastatic human prostate cancer samples when compared to benign prostate tissue[87]. These results are in agreement with our findings that Ldhb is downregulated as tumors progress to the stage of recurrence, and that LDHB downregulation is associated with reduced recurrence-free survival in human breast cancer patients, primarily those exhibiting HER2-positive breast cancer.

In this study, we have established a direct functional link between Ldhb downregulation and reduced recurrence-free survival in an animal model that faithfully recapitulates key features of breast cancer progression. Using an orthotopic tumor assay, we demonstrated that *Ldhb* downregulation is sufficient to promote tumor recurrence. To our knowledge, this is the first evidence identifying a functional role for Ldhb in tumor progression. Reduced Ldhb expression contributes to lactic acid accumulation by reducing lactate uptake and metabolism within tumors. This, in turn, leads to decreased pH in the tumor microenvironment, thereby stimulating tumor

invasion while impairing immunogenicity. A role for increased lactate levels in inducing and selecting for a stem-like phenotype in cancer cells has also been suggested. Moreover, Kennedy et al. have reported increased expression of the transcriptional repressor Snail and epithelial-to-mesenchymal transition (EMT) in breast cancer cells chronically subjected to high lactate levels[284]. As our laboratory has previously reported increased Snail expression and EMT in recurrent tumors[66], we speculate that tumor recurrence driven by elevated lactate levels could facilitate induction of a stem-like phenotype and EMT in a subset of tumor cells. Such cells might persist following regression of the primary tumor and could give rise to recurrent tumors at a later time.

Sirtuins have recently emerged as important regulators in cancer metabolism. In particular, Sirt3, an NAD-dependent mitochondrial deacetylase has been reported to repress glycolytic activity and proliferation in breast cancer cells and to modulate lactate levels[275]. While Sirt3 has principally been found to affect *Ldha* expression[275], we found that Sirt3 was downregulated in recurrent tumors and demonstrated that *Sirt3* downregulation in primary tumor cells led to a reduction in *Ldhb* expression. To our knowledge, this is the first evidence that Sirt3 regulates Ldhb expression.

As lactate levels are also significantly influenced by hypoxia, we investigated the link between Sirt3, hypoxia and Ldhb expression. Previous studies have established that the ability of Sirt3 to regulate glycolytic activity is dependent upon Hif1-α destabilization[275]. Consistent with this, we found higher Hif1-α protein levels in recurrent tumors compared to primary tumors. Moreover, while *Sirt3* downregulation led to a reduction in *Ldhb* levels, siRNA-mediated Hif1 dowregulation abrogated the effect of Sirt3 on Ldhb expression consistent with a model in which Sirt3 regulates Ldhb through Hif1. Of note, Hif1 controls the expression of target genes by binding to the hypoxia

response element (HRE) thereby inducing upregulation of target genes[285]. To our knowledge, few reports exist suggesting that Hif1-α stabilization induces downregulation of gene expression. As such, the impact of Hif1 on Ldhb downregulation might be mediated by a Hif1 target. In addition, some studies have suggested that the *Ldhb* promoter is hypermethylated in human cancers[87, 283]. It is possible that promoter hyperpmethylation might play an additional role in regulating the expression of Ldhb. Interestingly, *Ldha* levels did not change during tumor recurrence despite Hif1-α stabilization.

In summary, our findings provide direct evidence for a functional role for Ldhb downregulation in tumor recurrence. *Ldhb* downregulation was sufficient to accelerate tumor recurrence and was sufficient to induce lactate accumulation within tumors. These changes were driven by Sirt3 downregulation and mediated by changes in Hif1 stabilization. Our findings suggest that Ldhb expression may serve as a useful prognostic marker for breast cancer patients and that modulating LDH activity may have therapeutic utility.

6.5 Figure Legends

Figure 1. Recurrent tumors exhibit higher lactate levels than primary tumors. (A) ^{1}H MRS reveals differences in selected metabolites between primary and recurrent tumors. 30% higher steady-state lactate levels were observed in recurrent tumors. Results are shown from a total of 4 primary and 4 recurrent tumors arising in MTB/TAN mice. (B) Higher lactate levels in recurrent tumors confirmed by mass spectrometry analysis in the same mice as in (A). Lactate levels are normalized to mg of total protein (TP) in the analyzed tissue samples. (C) ^{13}C-labeled glucose infusion of tumor-bearing mice reveals lower production of labeled lactate from glucose in recurrent tumors relative to primary tumors. Results represent the amount of labeled metabolite from the total available metabolite pool. White bars represent primary tumors and black bars represent recurrent tumors. (D) Labeled lactate infusion of tumor-bearing mice reveals higher accumulation of labeled lactate and less lactate oxidation in recurrent tumors compared to primary tumors. Results represent the total amount of labeled metabolite pool. White bars represent primary tumors and black bars represent recurrent tumors. (** indicates $p<0.05$).

Figure 2. Recurrent tumors exhibit lower Ldhb expression levels. (A) Recurrent tumors exhibit lower *Ldhb* expression but similar *Ldha* expression at the mRNA level compared to primary tumors. Expression levels were assessed by qRT-PCR in 4 primary and 4 recurrent tumors. Expression was normalized to TBP. (B) Recurrent tumors exhibit lower Ldhb, but similar Ldha protein levels compared to primary tumors. Tubulin is shown as a loading control. (C, D) Recurrent tumors exhibit similar *Pkm1* and

Pkm2 expression levels. Pkm1 and Pkm2 are the product of differential splicing of the *Pkm* gene. *Pkm1* and *Pkm2* were amplified from RNA extracted from primary and recurrent tumor samples. Relative expression was assessed by electrophoresis of digested or undigested amplification products on a non-denaturing polyacrylamide gel. EcoN1 is a restriction enzyme specific for Pkm1 and Pst1 is specific for Pkm2. (E) Recurrent tumors exhibit similar Pkm2 protein levels compared to primary tumors. Tubulin is shown as a loading control.

Figure 3. *Ldhb* downregulation results in higher lactate levels (A) Zymography reveals that recurrent tumors lack LDH isoenzymes LDH1, LDH2 and LDH3. Protein was extracted from 3 primary and 3 recurrent tumors and electrophoresed on a non-denaturing polyacrylamide gel. (B) Assessment of the conversion of lactate to pyruvate reveals reduced LDH activity in catalyzing that conversion compared to primary tumors. Results are for LDH extracted from 3 primary and 3 recurrent tumors. (C) shRNA knockdown of *Ldhb* in primary tumor cells compared to controls. Expression levels were assessed in primary tumor cells by qRT-PCR and normalized to TBP. (D) Conditioned media from primary tumor cells with Ldhb knockdown exhibit higher lactate levels compared to control cells. Results were normalized to the average number of cultured cells in each well. (* indicates $p<0.05$).

Figure 4. *Ldhb* downregulation promotes tumor recurrence in mice and is associated with reduced recurrence-free survival in human breast cancer. (A) Schematic of orthotopic tumor recurrence assay consisting of injecting genetically-

engineered primary-tumor derived cells into the mammary fat pad of *nu/nu* mice, inducing tumor growth by doxycycline administration, withdrawing doxycycline treatment to induce tumor regression to a non-palpable state followed by the stochastic appearance of recurrent tumors following a latency period. (B,C) *Ldhb* knockdown in primary tumors promotes recurrence in the MTB/TAN mouse model using two different shRNA constructs. Results are from 24 injected sites in each experimental group. (D) Primary tumors with *Ldhb* knockdown grow at a similar rate compared to control tumors. Tumor growth was assessed by computing the mean growth rate (MGR) as tumors increased in size from 5x5 mm to 15x15 mm. Results are from 20 injected sites in each experimental group. (E) *Ldhb* knockdown is associated with reduced recurrence-free survival in HER2-positive human breast cancer among patients with node-negative disease who did not receive adjuvant therapy. (H.R.: Hazard Ratio; p: p-value).

Figure 5. *Sirt3* downregulation reduces *Ldhb* levels in recurrence. (A) Recurrent tumors exhibit low *Sirt3* mRNA levels compared to primary tumors. Expression levels were assessed by qRT-pCR and normalized to TBP. Results are from 4 primary and 4 recurrent tumors. (B) Recurrent tumors exhibit lower Sirt3 protein levels relative to primary tumors. Tubulin is shown as a loading control. (C) Downregulation of Sirt3 in primary tumor cells leads to downregulation of *Ldhb* levels without affecting *Ldha* levels. Sirt3 knockdown was achieved by siRNA transfection. Expression levels were assessed by qRT-PCR and normalized to TBP. (D) Sirt3 knockdown results in increased lactate levels in the culture media. Results were normalized to the average number of cultured cells in each well.

Figure 6. Sirt3 downregulation of *Ldhb* is mediated through Hif1. (A) Recurrent tumors exhibit Hif1-α protein stabilization. Tubulin is used as a loading control. (B) Recurrent tumors exhibit higher Hif1-α pathway activity. Pathway activity was assessed by considering expression of known Hif1 targets. The EPS algorithm used outputs a pathway activity score based on the combined expression of target genes present in the signature. (C) Simultaneous downregulation of *Sirt3* and *Hif1* abrogates the effect of Sirt3 on *Ldhb* expression levels. While *Sirt3* downregulation leads to a decrease in *Ldhb* levels, simultaneous downregulation of *Sirt3* and *Hif1* abrogates the effect of Sirt3 on *Ldhb* expression. Sirt3 and Hif1 were downregulated in primary tumor cells using siRNAs targeted to those genes. Expression levels were assessed by qRT-PCR and normalized to TBP. (D) Simultaneous downregulation of *Sirt3* and *Hif1* in primary tumor cells does not change lactate levels in culture media. Results were normalized to the average number of cultured cells in each well. (** indicates $p<0.05$).

6.6 Figures

Figure 1

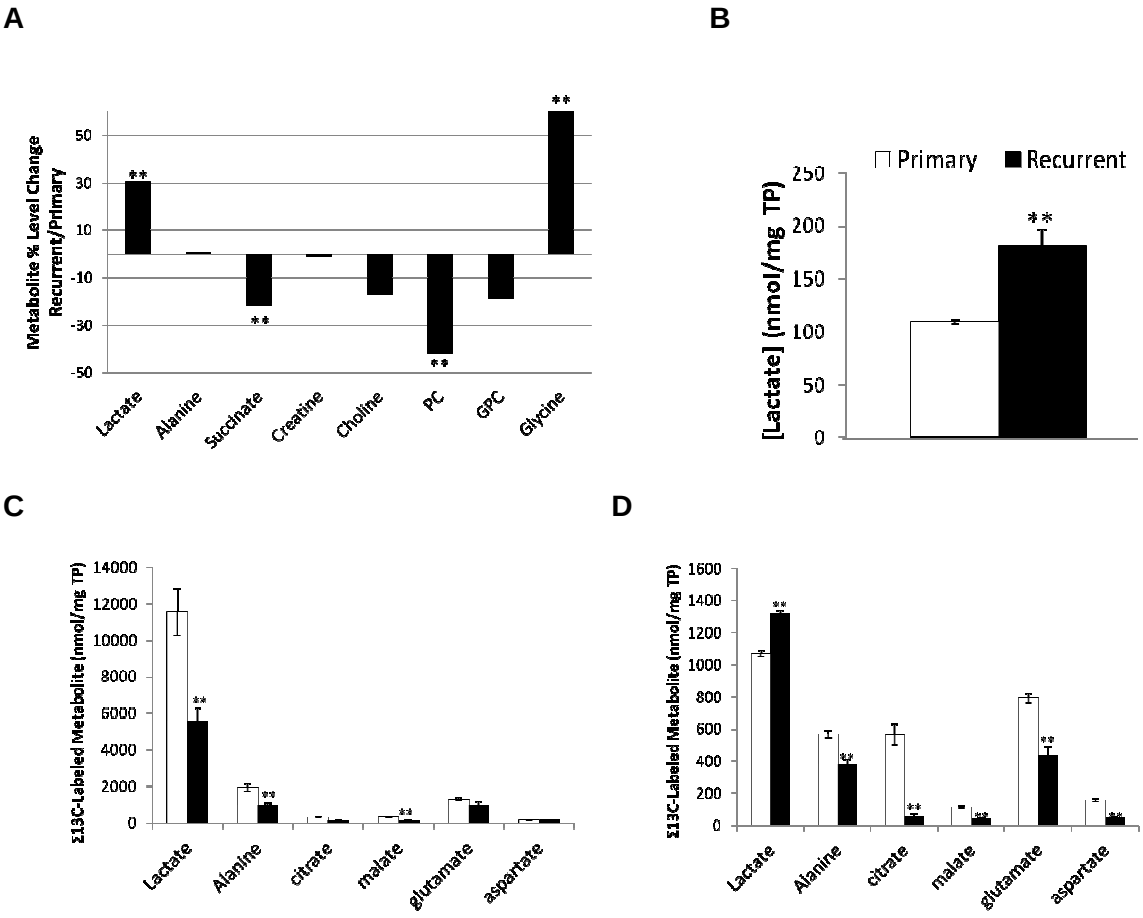

Figure 2

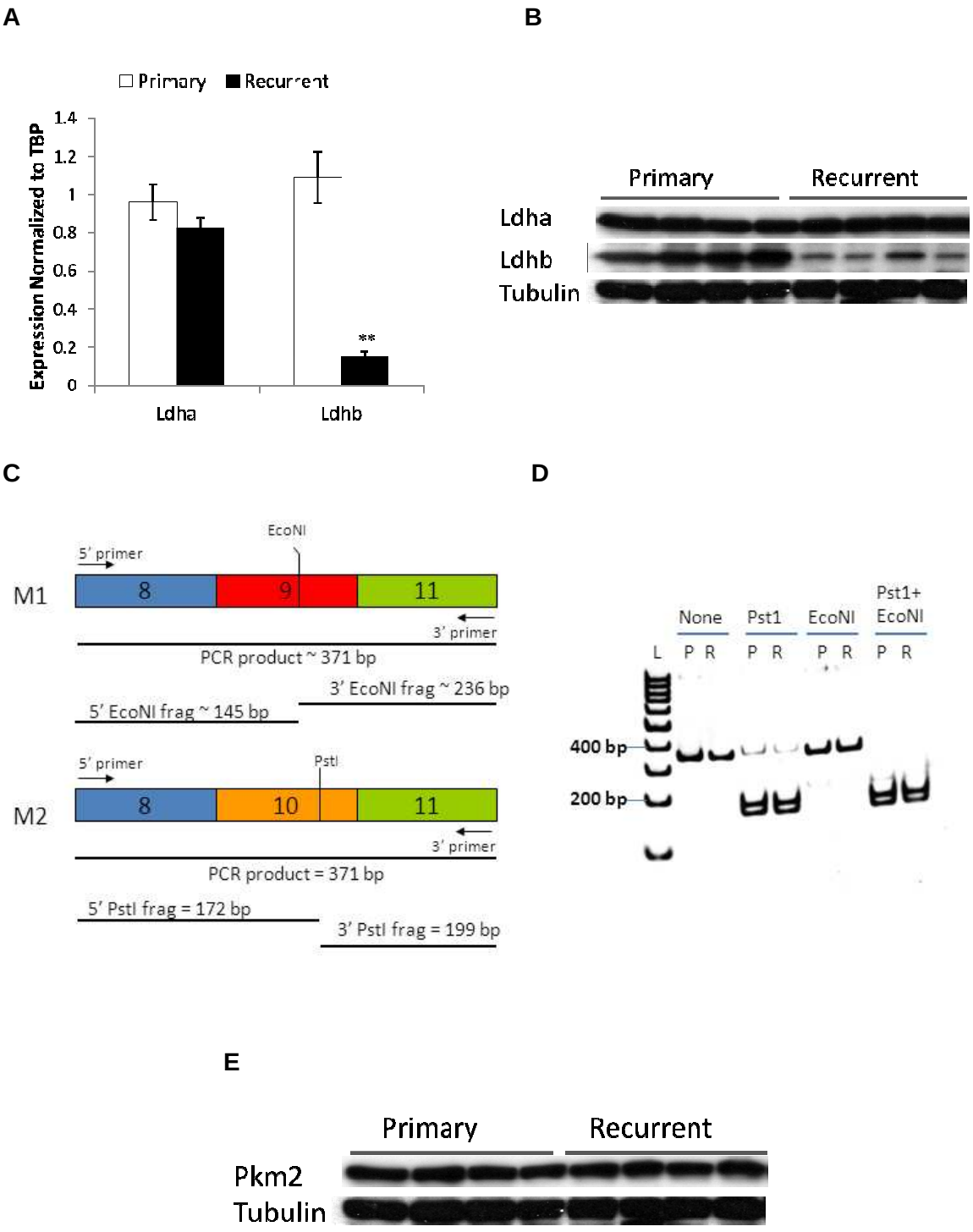
A
Primary
Recurrent
Expression Normalized to TBP
1.4
1.2
1
0.8
0.6
0.4
0.2
0
**
Ldha
Ldhb
B
Primary
Recurrent
Ldha
Ldhb
Tubulin
C
EcoNI
5' primer
M1
8
9
11
3' primer
PCR product ~ 371 bp
3' EcoNI frag ~ 236 bp
5' EcoNI frag ~ 145 bp
5' primer
PstI
M2
8
10
11
3' primer
PCR product = 371 bp
5' PstI frag = 172 bp
3' PstI frag = 199 bp
D
None
Pst1
EcoNI
Pst1+ EcoNI
L
P R
P R
P R
P R
400 bp
200 bp
E
Primary
Recurrent
Pkm2
Tubulin

Figure 3

A

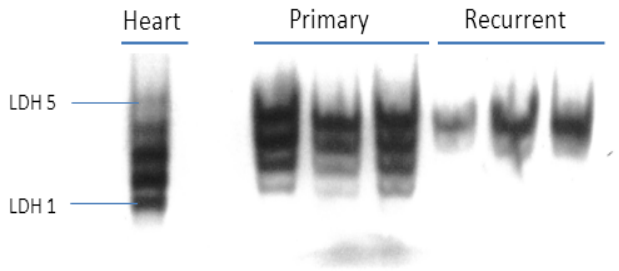

B

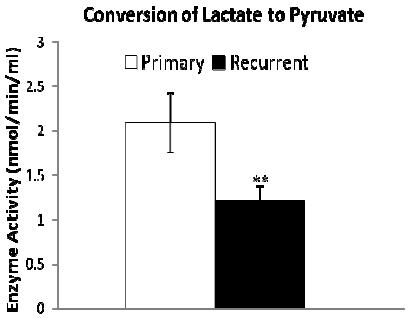

C

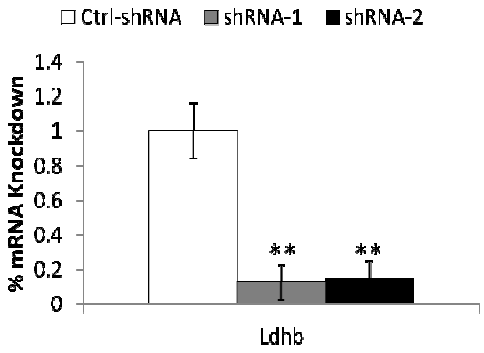

D

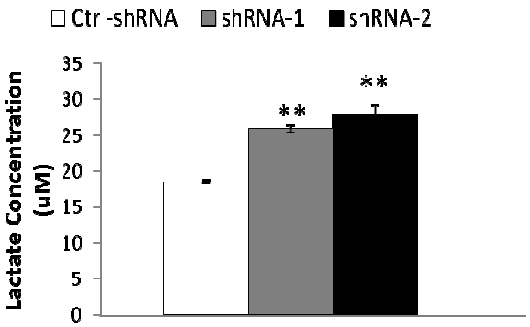

Figure 4

A

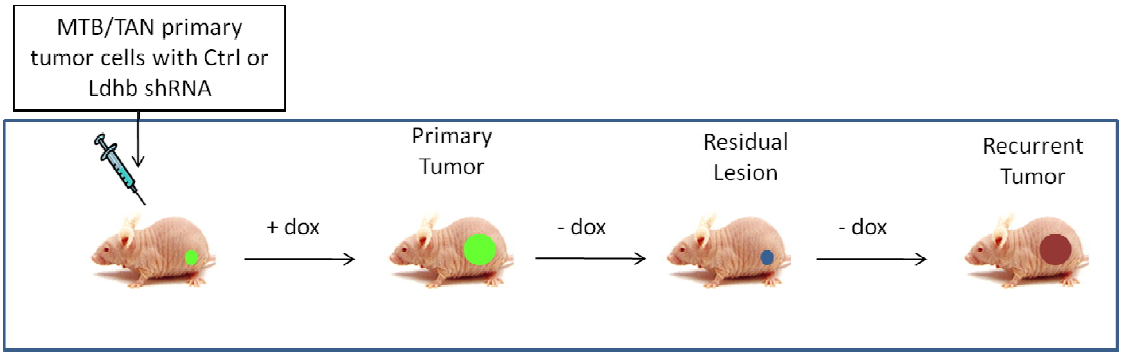

B

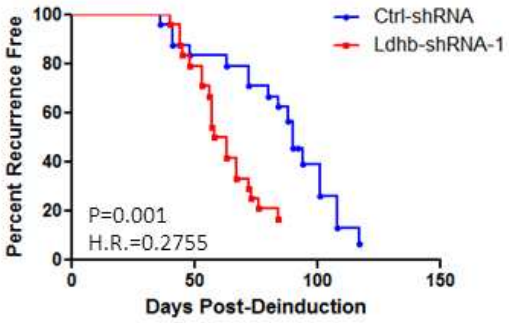

C

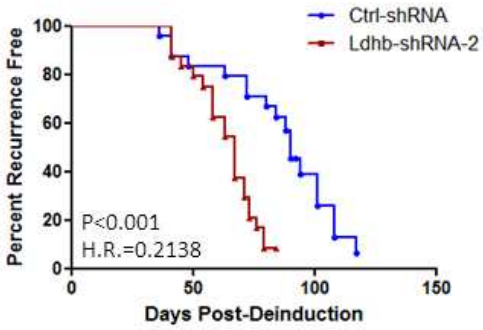

D

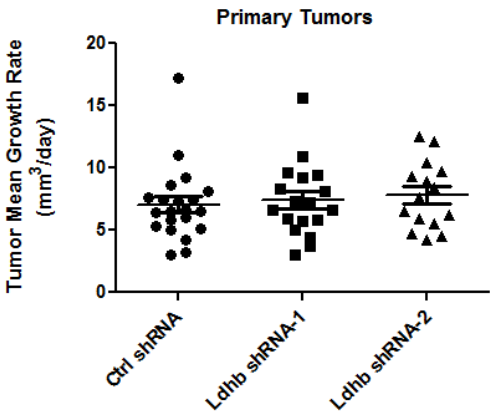

E

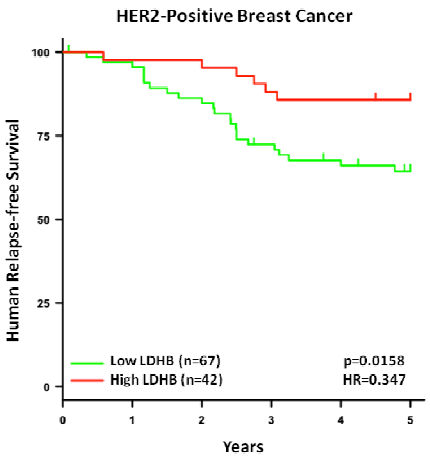

Figure 5

A

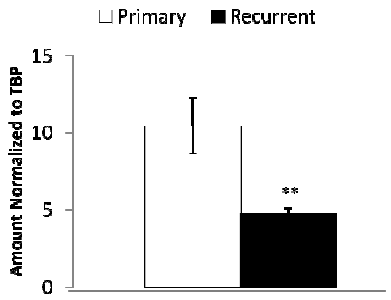

B

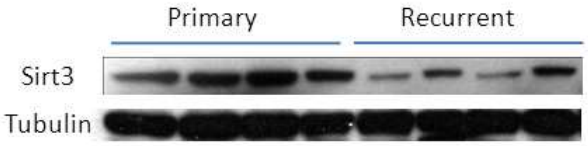

C

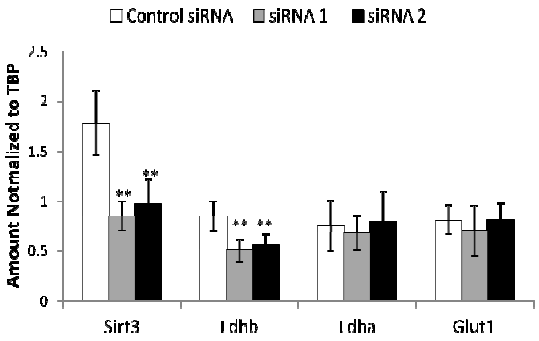

D

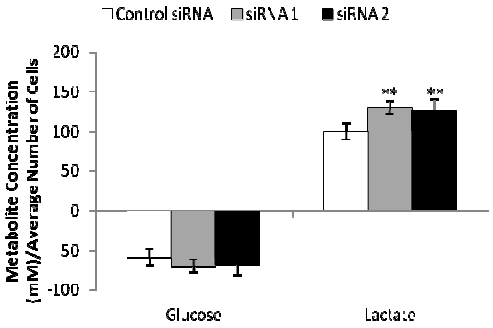

Figure 6

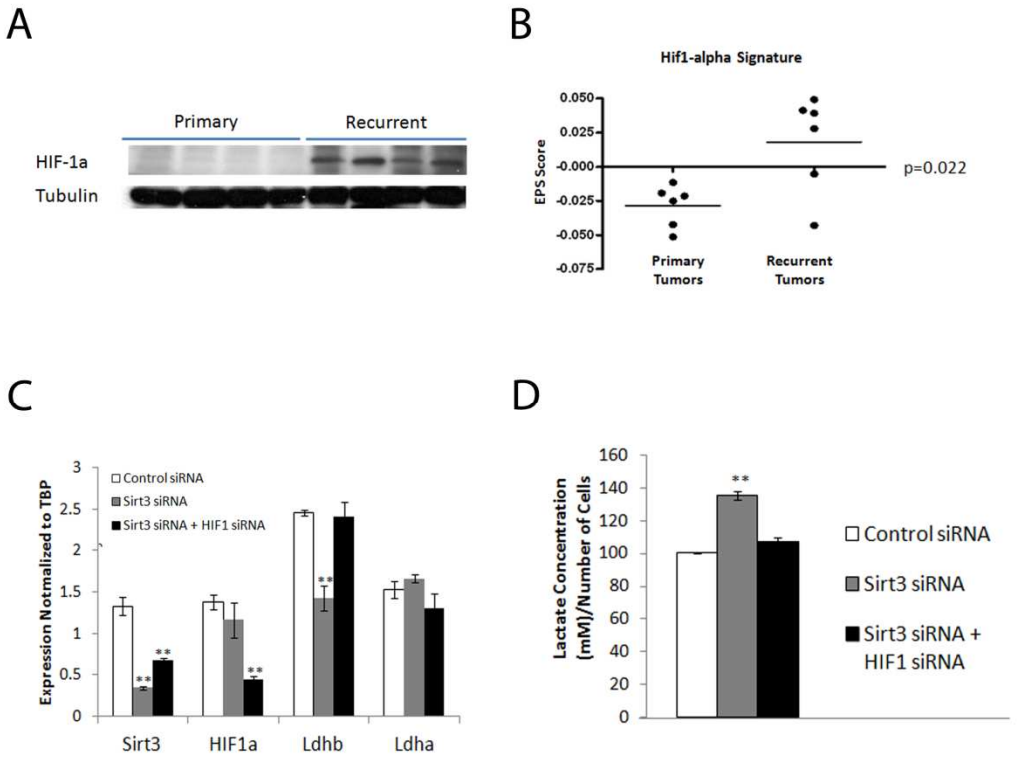
A
Primary
Recurrent
HIF-1a
Tubulin
B
Hif1-alpha Signature
EPS Score
0.050
0.025
-0.000
-0.025
-0.050
-0.075
p=0.022
Primary Tumors
Recurrent Tumors
C
Control siRNA
Sirt3 siRNA
Sirt3 siRNA + HIF1 siRNA
Expression Notmalized to TBP
3
2.5
2
1.5
1
0.5
0
**
Sirt3
HIF1a
Ldhb
Ldha
D
Lactate Concentration (mM)/Number of Cells
160
140
120
100
80
60
40
20
0
**
Control siRNA
Sirt3 siRNA
Sirt3 siRNA + HIF1 siRNA

CHAPTER 7

Conclusions and Future Directions

7.1 Thesis Summary

In this work, we present evidence for an evolving metabolic phenotype within breast cancers during the course of tumor recurrence. We speculate that metabolic reprogramming could be a mechanism by which tumors escape therapy and recur. A better understanding of the basis for the metabolic changes that accompany tumor recurrence might allow for the development of more effective approaches to preventing and treating recurrent breast cancers.

Using a systems engineering approach, we have designed and implemented a process-based system aimed at increasing our understanding of the metabolic and genetic regulation of breast cancer recurrence. Magnetic resonance-based metabolic profiling of primary and recurrent tumors allows for broad identification of potential metabolic pathways that exhibit differential activity in recurrent tumors compared to primary tumors in a mouse model of mammary tumor recurrence. The identified metabolic changes are further characterized with ^{13}C-labeling infusion experiments in vivo. Mass spectrometry analysis and ^{13}C magnetic resonance spectroscopy are used for pathway-focused assessment allowing the detection of changes in metabolic flux or the identification of key dysregulated steps in a given pathway. Once potential dysregulated metabolic steps are identified, we proceed to identify the underlying genetic determinant(s) of those changes and assess the functional role of those in

tumorigenesis as well as their effect on tumor recurrence. If a gene is found to exhibit a functional effect on tumor recurrence, the potential for clinical translation of our findings is assessed using microarray and outcome data from human breast cancer patients. The top-down process-based system of:

1. identifying potential dysregulated metabolic pathways using magnetic resonance spectroscopy in a mouse model of mammary tumor recurrence,
2. identifying the specific affected metabolic steps using ^{13}C-labeling experiments,
3. connecting those to their underlying molecular determinants,
4. characterizing their functional effect in tumorigenesis,
5. assessing their translational potential using human microarray data

forms the basis of our magnetic resonance-based integrative metabolomics approach that we propose and implement here as a mean to better understand the metabolic and genetic regulation of breast cancer recurrence. This approach was implemented and validated in two metabolic pathways, glutaminolysis and lactate metabolism, which exhibited differences between primary and recurrent tumors in ^{1}H magnetic resonance studies.

^{1}H magnetic resonance profiling of primary and recurrent tumors led to the identification of a number of metabolites whose levels exhibited statistically significant differences between primary and recurrent tumors. Recurrent tumors displayed higher lactate levels, lower succinate levels, higher glutamate to glutamine ratio, lower phosphocholine levels and higher glycine levels than primary tumors. Higher levels of *Sdhb* and *Gls* expression as well as lower levels of *Chka, Gldc* and *Ldhb* in recurrence

can potentially explain the observed succinate, glu/gln, phosophocholine, glycine and lactate metabolite level changes, respectively. The identified changes might have translational potential for human breast cancer prognosis prediction. A metabolic gene expression signature based on the metabolic changes observed in recurrent tumors in mice successfully predicted 5-year recurrence risk in human breast cancer patients with HER2-positive disease. Two of the identified differences in this study, increased lactate levels and increased glutamate to glutamine ratio, were further pursued using the process-based system proposed above to further characterize their contribution to breast cancer recurrence.

The first pathway we chose to assess was glutaminolysis with this pathway known to be a key feature of tumorigenesis. ^{13}C-labeling experiments suggested increased glutaminolytic activity and increased reductive carboxylation in tumor recurrence. The observed changes in the glutaminolytic profile were accompanied by increased expression of the glutamine transporter, Slc1a5, as well as increased expression of glutaminase (Gls1) in recurrent tumors. Both *Slc1a5* and *Gls1* expression were required for recurrent, but not primary tumor growth in vivo. Recurrent tumors also exhibited increased endogenous expression of the *Myc* oncogene. Myc was found to be required for *Slc1a5* and *Gls1* expression as well as increased glutamine uptake and glutamate production in recurrent tumor cells. Human association analysis further revealed a positive correlation between *Slc1a5* expression levels and recurrence-free survival in human breast cancer patients.

The second pathway that we chose to further characterize was lactate metabolism. The Warburg effect, consisting of increased aerobic glycolytic flux and increased lactate production, is one of the most fundamental observations in cancer

metabolism. Interestingly, ^{13}C-labeling experiments showed that recurrent tumors do not exhibit increased glycolytic flux but rather seem to accumulate lactate and display reduced oxidation of this metabolite. Molecular profiling experiments identified downregulation of *Ldhb* in recurrent tumors as the potential underlying molecular determinant of the differential lactate levels between the two tumor stages. This translated into recurrent tumors lacking LDH isozymes 1,2 and 3. Ldhb is found to be regulated by the NAD-dependent mitochondrial deacetylase Sirt3; and this effect is mediated through Hif1. Functional experiments further suggested a role for *Ldhb* downregulation in promoting tumor progression and recurrence. Furthermore, we found that *Ldhb* downregulation in human breast cancer patients, particularly in those with HER2-positive disease, is correlated with reduced recurrence-free survival.

Combined, our findings validate our proposed process-based system for understanding the metabolic and genetic regulation of breast cancer recurrence. Our findings further provide evidence for metabolic reprogramming in breast cancer progression and suggest a role for increased glutaminolysis and lactate metabolism in promoting recurrence. The identified molecular determinants, *Slc1a5, Gls1* and *Ldhb* might potentially serve as therapeutic targets as well as prognostic markers that could aid in the clinical management of breast cancer patients.

7.2 Future Directions

From the Genome to the metabolome and back: how do metabolic changes drive tumor recurrence?

In chapter 6, we provided evidence that *Ldhb* downregulation, which results in increased lactate levels, promote tumor recurrence. The mechanism by which this process takes

place remains to be investigated. Here, we propose a potential pathway that might be underlying this phenomenon.

In this work, our findings suggest that *Ldhb* downregulation is induced by *Sirt3* downregulation. In a separate experiment, we also found evidence that *Sirt3* levels were modulated by changes in *Myc* levels (Figure 1A). To our knowledge, this is the first evidence of Myc regulating *Sirt3* expression. With *Sirt3* downregulation, tumors exhibit increased lactate levels due to the associated Ldhb level changes. The accumulation of lactate and the reduced conversion of lactate to pyruvate are accompanied by reduced amounts of NADH, a key product of this reaction. High availability of NAD has been found to correlate with increased expression and activation of another NAD-dependent deacetylase, Sirt1[286]. Interestingly, increased Sirt1 levels and activity are correlated with increased p53 deacetylation[287]. This, in turn, is associated with pro-survival signaling and evasion of apoptosis. A schematic of this proposed pathway is shown in Figure 1B.

We speculate that increased Myc levels are the initiating genetic event that triggers a number of downstream metabolic changes, one of which is increased lactate. The increased lactate, in turn, might promote epigenetic changes by affecting p53 acetylation providing a survival advantage to some tumor cells and allowing them to evade apoptosis. The tumor cells where this phenomenon takes place might be potentially persisting following HER2/*neu* downregulation and recurring at a later time.

In terms of the glutaminolytic changes that accompany breast cancer progression, we speculate that a subset of cells in the primary tumors upregulate glutamine metabolism and that those cells escape HER2/*neu* downregulation and persist as a result of the ammonia generated from increased glutamine uptake and breakdown. Ammonia is released as glutamine is converted into glutamate. Increased ammonia levels in tumors have been associated with autophagy[288], a mechanism that tumor cells

might use to become dormant. It is possible that during dormancy, most of the increased glutamine uptake is diverted into ammonia to maintain autophagy. This can be achieved by tumor cells maintaining low expression levels of enzymes that typically allow the entry of glutamine carbon into the TCA cycle, such as Gls1 or Glud1. As tumors escape from dormancy, cells might upregulate these genes allowing glutaminolysis to support increased growth and energy production and leading to the appearance of a recurrent tumor. We speculate that during dormancy, *Myc* upregulation induces increased glutamine uptake and conversion into ammonia, potentially promoting *Atg1* levels to support autophagy. As cells escape from dormancy, increased glutaminolysis promotes tumor recurrence through the diversion of glutamine's carbon into TCA cycle intermediates to support tumor growth.

Serine biosynthesis pathway: a potential therapeutic target for cancer recurrence

Recently, the serine biosynthesis pathway has emerged as a novel key pathway in cancer metabolism[289, 290]. Particularly, phosphoglycerate dehydrogenase (Phgdh), the enzyme responsible for the conversion of 3-phosphoglycerate into 3-phosphohydroxypyruvate, was found to play an important role in tumorigenesis. Particularly, Phgdh was shown to be required for primary tumor growth in mammary tumors in mice[289, 290]. The association between increased serine biosynthesis, *Phgdh* levels and cancer recurrence warrants further investigation.

In our model, D-[1,2-^{13}C-]-glucose infusion revealed a more active serine biosynthesis pathway in recurrent tumors compared to primary tumors. ^{13}C-MRS studies show marked labeled glycine production from glucose in recurrent tumors relative to primary tumors (Figures 2A and 2B). In the serine biosynthesis pathway, serine is

converted into glycine before glycine is broken down to contribute to nucleotide synthesis. In our model, we assessed the levels of *Phgdh* expression. Indeed, recurrent tumors exhibit increased expression levels of *Phgdh* compared to primary tumors (Figure 2C).

Together, these results provide evidence for increased serine biosynthesis pathway activity in recurrent tumors. The functional implication of these observations on tumor recurrence should be further interrogated.

Myc: the master metabolic regulator of tumor recurrence

In this work, we presented evidence that *Myc* overexpression could be responsible for the increase in glutaminolysis observed in recurrent tumors. Similarly, figure 1A suggests that Myc also regulates expression of the NAD-dependent mitochondrial deacetylase, Sirt3. Sirt3, in turn, modulates Ldhb levels and lactate accumulation in recurrent tumors. While very little evidence is available connecting the serine biosynthesis to Myc, available microarray data through the *Myc* oncogene database (http://www.myc-cancer-gene.org/) suggests that Phgdh might be a Myc target.

Combined, these results lead us to speculate that Myc might act as a master regulator of the metabolic reprogramming that accompanies tumor recurrence (Figure 3). While primary tumors, in which HER2/*neu* is activated, are thought to be mainly dependent on glycolysis for their energy needs, it is possible that *Myc* upregulation in a subset of primary tumor cells might allow those to escape HER2/*neu* downregulation. The metabolic pathways that are activated with Myc overexpression might confer a

survival advantage to the transformed tumor cells and allows= them to undergo dormancy and later recur.

Other potential regulators of metabolic reprogramming in recurrence: Does Akt play a role?

While tumor recurrence in our model is HER2/*neu*-independent, unpublished data from our lab suggests activation of the Akt pathway in recurrent tumors, as evidenced by the detection of high p-Akt levels. With Akt known to play a role in metabolism, it remains to be investigated how the activity of this pathway affects the metabolic reprogramming observed in recurrent tumors. Previous studies have suggested that Akt activity is associated with decreased GSK-3 activity[291]. This, in turn, is known to lead to reduced Myc phosphorylation and reduced Myc degradation[291]. Is it possible that Akt, acting upstream of Myc, might be the ultimate metabolic regulator in tumor recurrence?

In an effort to address this question, we inhibited AKT in a human breast cancer cell line, MCF-7, that we show to be glutamine addicted (Figure 4A and 4B). Within the context of glutamine-addiction, AKT inhibition using 2 different siRNA constructs led to a reduction in *MYC* levels as well as a decrease in both *SLC1A5* and *GLS1* levels (Figure 4C). These data provide preliminary evidence that AKT might act upstream of MYC and regulate glutaminolysis and potentially other metabolic pathways through its effect on MYC. The direct effect of Akt inhibition on the metabolism of recurrent tumor cells in our mouse model remains to be further assessed. We speculate, however, that Akt might be the ultimate regulator of metabolism in tumor recurrence (Figure 4D).

Of note, Akt has been shown to have no effect on glutamine metabolism within the context of Myc overexpression[97]. Our data suggest, however, a potential role of Akt in glutamine metabolism, suggesting that this effect might be context-dependent. Further human association analysis also shows that AKT activity is positively correlated with *SLC1A5* expression in human breast cancer samples, providing further evidence of a potential link between AKT and glutamine metabolism (Table 1). The exact mechanism underlying this observation and the role of AKT in tumor recurrence is not well understood.

Glutamate dehydrogenase: an alternative glutaminolytic target in breast cancer recurrence

Glutamate dehydrogenase (Glud1), in addition to Got1 and Gpt1, is an enzyme responsible for the conversion of glutamate into alpha-ketoglutarate. This enzyme catalyzes a critical step of glutaminolysis with this reaction being the entry point of the glutamine carbon into the TCA cycle to support anaplerosis. Assessment of alpha-ketoglutarate levels in recurrent tumors revealed higher levels of this metabolite relative to primary tumors (Figure 5A). These results were further confirmed with ^{13}C-labeling experiments where we detected higher alpha-ketoglutarate enrichment in recurrent tumors relative to primary tumors, following the infusion of [3-^{13}C]- glutamine (Figure 5B). Genetic profiling of primary and recurrent tumors in our model have shown similar levels of *Gpt1* and *Got1* but higher levels of *Glud1* at both the mRNA and protein level (Figure 5C and 5D). Glud1 has been shown to be an especially promising therapeutic target in cancer. An in vivo study reported cytostatic effects resulting from Glud1 inhibition in tumors, without the nonspecific toxicity usually observed with generalized inhibition of

glutamine metabolism[92]. Another study reported decreased tumor growth in vivo upon inhibition with aminooxyacetate (AOA), an agent that blocks the conversion of glutamate to alpha-ketoglutarate[292]. In light of this evidence and the known upregulation of glutaminolysis in tumor recurrence, investigating the effect of Glud1 inhibition in tumor recurrence is warranted.

Accordingly, we assessed the effect of *Glud1* downregulation on tumor growth using 1 shRNA targeted against this gene. Indeed, downregulation of *Glud1* did lead to a reduction in mean tumor growth rate of recurrent tumors relative to controls (Figure 5E). This provides preliminary evidence of the potential of Glud1 as a therapeutic target of tumor recurrence.

Previous studies have suggested that Glud1 is regulated by Sirt4 in pancreatic beta cells[293]. In our model, we have evidence that Sirt4 levels are higher in recurrent tumors compared to primary tumors (Figure 5F). It remains to be investigated whether *Sirt4* level changes are behind the observed *Glud1* expression level changes in tumor recurrence.

Here, we show preliminary results for a role of Glud1 in tumor recurrence. Further investigation is warranted to better understand the role of Glud1 and to further characterize the mechanism responsible for the changes in its levels.

Hyperpolarized magnetic resonance: potential in breast cancer prognostication

NMR of hyperpolarized precursors has recently emerged as the technique of choice for monitoring dynamic real-time changes in metabolism in vivo, with substantially high resolution and sensitivity[294-307]. By creating an artificial non-equilibrium distribution of the

spins, hyperpolarized imaging allows direct molecular imaging of the molecules containing the hyperpolarized nucleus with a signal-to-noise ratio (SNR) up to 100,000 times greater than typical magnetic resonance techniques[294-296]. This new technique offers many new possibilities for imaging tissue function in vivo[308-313].

For the past few decades, the conventional magnetic resonance (MR) technique used to monitor total metabolite concentrations in vivo has consisted of Nuclear Magnetic Resonance (NMR) spectroscopy, a technique that exploits the magnetic properties of NMR active nuclei[119, 120]. However, this approach can only measure steady-state metabolite levels and is of limited utility in vivo, especially in the case of lactate. Lactate and lipid peaks usually overlap on ^{1}H NMR spectra, such that monitoring modulations in lactate can be difficult even when methods of lipid suppression are used. This is especially a problem in the case of in vivo breast MRS wherein a large percentage of the total composition of the tissue is fat. Similarly, the glutamine and glutamate peaks typically overlap on 1D proton spectra, thereby complicating the accurate quantification of the individual concentration of each of the two metabolites in vivo. ^{13}C-MRS is another conventional MR technique to assess metabolite levels but the low natural abundance of ^{13}C makes its use for *in vivo* studies quite challenging due to SNR limitations.

Here, we propose using hyperpolarized [1-^{13}C]-pyruvate and [5-^{13}C]-glutamine for the in vivo study of cellular metabolism. We plan to investigate the role of their conversion into lactate and glutamate, respectively, as potential biomarkers for cancer progression. Being able to reliably identify metabolic changes in tumor tissue and showing that those changes could reflect *Ldhb* and *Slc1a5* expression levels, might provide evidence for a potential role of this technique in prognosis predication in cancer.

Here, we conducted preliminary experiments in vivo where we injected primary and recurrent tumor-bearing mice with [1-^{13}C]-pyruvate and observed its conversion into lactate in real time. ^{13}C-spectra were collected at 1s intervals and a representative stack of those is presented for one mouse in Figure 6A. The area under each peak at each time point was computed and normalized to the total carbon in the spectra. Normalized peak amplitudes for both lactate and pyruvate were plotted with respect to time for each of the mice assessed in this study (Figure 6B and 6C). Preliminary results show potential differences in dynamic lactate levels between primary and recurrent tumors. Those differences were further quantified by fitting the lactate and pyruvate curves to a modified Bloch equation model for two-site chemical exchange as previously described by Day et al.[310]:

$$L \underset{k_P}{\overset{k_L}{\rightleftharpoons}} P$$

$$dL_z/dt = -\rho_L(L_z - L_\infty) + k_P P_z - k_L L_z$$

$$dP_z/dt = -\rho_P(P_z - P_\infty) + k_L L_z - k_P P_z$$

L and P denote lactate and pyruvate respectively. L_z and P_z are the z-magnetizations of the ^{13}C nucleus in lactate and pyruvate. ρ_L and ρ_P are the spin-lattice relaxation rates, L and P at infinity are the equilibrium magnetizations which are equivalent to their steady state concentrations. The data generated in our experiment were fit to this model using the 5-parameter solution proposed by Ziehurt et al.[314]. The fits obtained from the generated model are presented in Figures 6D and 6E. Representative reaction rates yielded by this model are presented in Table 2 for one primary and one recurrent tumor.

Combined, these results show preliminary evidence that in vivo hyperpolarized magnetic resonance spectroscopy is a viable technique for the assessment of in vivo cancer metabolism. It remains to be investigated how reproducible the detected changes are and whether the observed differences correlate with gene expression changes. If validated, this technique might have potential to play a role in breast cancer prognostication,

Metabolic gene expression signature: how does it measure to current clinical prognostic variables?

In Chapter 3, we presented a metabolic gene expression signature able to predict 5-year recurrence status in a cohort of breast cancer patients diagnosed with HER2-positive breast cancer. Current clinical practice assesses the recurrence risk of breast cancer patients based on a number of clinicoprognostic variables, the most established of which include tumor size, tumor grade, receptor status (ER and PR), and HER2 status. In order to address the potential clinical contribution of our proposed metabolic gene expression signature, we sought to assess whether this signature is an independent predictor of recurrence and whether it adds to the information provided by the traditionally used clinical prognostic variables. Accordingly, we performed logistic regression modeling with recurrence status as the response variable. Clinical variables were only available for a small patient dataset consisting of 31 patients. The first implemented model included the currently used clinical variables that were available for this dataset: tumor size, tumor grade and ER status (Table 3). Independent contribution

of each partial regression coefficient was assessed using the Wald test. Tumor size was an independent predictor of recurrence status.

Following the addition of the metabolic gene expression signature, both tumor size and the metabolic gene expression score were independent contributors to the prediction of recurrence status (Table 3). These results indicate that the metabolic gene expression signature that we propose further adds to the currently used clinical variables when it comes to patient prognosis assessment. These results were further validated by receiver operator curve (ROC) analysis. The ROC curve of the clinical variables alone had an AUC of 0.82. Addition of the metabolic gene expression score significantly added to the performance of the model where the AUC of the new model was 0.91.

These results represent a proof-of-principle analysis and remain to be validated in a larger dataset, with more clinical variables and potentially compared to clinically-used recurrence assays such as Oncotype DX. If validated, the proposed metabolic gene expression signature has significant potential to aid in prognosis prediction in cancer patients.

7.3 Conclusions

In this work, we introduce magnetic resonance-based integrative metabolomics, a process-based systems approach, to understand the metabolic and genetic regulation of breast cancer recurrence. Using this approach, we 1) identified a number of potentially dysregulated metabolic pathways using magnetic resonance spectroscopy in a disease model system, 2) characterized the key affected steps using ^{13}C-labeling experiments, 3) identified the underlying molecular determinants of the observed metabolic changes, 4)

investigated the functional effect of those changes on tumor recurrence, and 5) assessed the translational potential of our findings. This approach was validated in two metabolic pathways, glutaminolysis and lactate metabolism, which were shown to exhibit differences between primary and recurrent tumors in our mouse model. Recurrent tumors exhibit increased glutamine uptake and metabolism. Those Myc-driven changes are caused by increased expression of *Gls1* and *Slc1a5*, two genes that seem to play a role in recurrent tumor growth. Slc1a5 was also associated with human breast cancer prognosis. Similarly, recurrent tumors exhibit increased lactate levels. Sirt3-mediated downregulation of *Ldhb* is responsible for those changes. Downregulation of *Ldhb* seems to promote recurrence in mice and to be associated with decreased recurrence-free survival in human breast cancer patients.

The success of our proposed process-based system in elucidating some of the metabolic regulation of breast cancer recurrence leads us to propose wider adoption of this approach for the investigation of metabolism in tumorigenesis. This system provides a top-down framework that allows multi-level assessment of the clinical and functional relevance of a specific metabolic observation. By combining molecular biology, biochemistry, computational biology, imaging, statistical modeling, clinical science and engineering principles, this interdisciplinary approach allows for rigorous assessment of the diagnostic, prognostic and predictive potential of a given metabolic change. This system might provide for better avenues for clinical translation of metabolic findings and facilitate the adoption of basic science discoveries to aid in the management of cancer patients.

In the era of personalized medicine, identifying tumors with specific metabolic changes using imaging techniques shown to act as biomarkers for established functional

genetic alterations (i.e. affecting tumor growth or progression), might serve as a successful strategy to tailor treatments and prognosis assessment to individual patients. Furthermore, with metabolic changes often occurring prior to morphologic changes in cancer, such technique also has the potential to allow for early detection of tumors and for the early and non-invasive assessment of the patients' response to tailored therapies. Lactate and glutamine imaging might be two such techniques and might aid in the early detection of recurrent tumors and improve the management of breast cancer patients.

7.4 Tables

Table 1. Correlation between AKT pathway activity and *SLC1A5* expression in 12 human breast cancer datasets. Correlation was assessed using Pearson correlation analysis.

Study	Pearson Correlation	P-value
Pawitan	0.386	5.06E-07
Chang	0.334	4.19E-09
Miller	0.321	2.00E-07
Hess	0.282	0.00101
Saal	0.256	0.00831
Chin	0.222	0.0156
VantVeer	0.219	0.0309
Bild	0.188	0.018
Oh	0.127	0.109
Sorlie	0.123	0.357
Wang	0.0926	0.118
Chanrion	-0.126	0.119

Table 2. Representative reaction rate constants computed from hyperpolarized MRS data from one primary and one recurrent tumors using a 5-parameter fit solution to modified Bloch equation model for 2-site chemical exchange. Mice were injected with hyperpolarized [1-13C]-pyruvate.

	Primary Tumor	**Recurrent Tumor**
$K_{pyr \rightarrow lac}$ (s^{-1})	0.037	0.093
$K_{pyr \rightarrow ala}$ (s^{-1})	0.011	0.0016

Table 3. Logistic Regression Analysis to assess independent contribution of metabolic gene expression signature in predicting recurrence risk after adjusting for a number of clinicoprognostic variables in breast cancer patients. (p-value is result of Wald test; Reg. Coef: regression coefficient; p-val: p-value).

Logistic Regression Model of Clinicoprognostic Variables

	Reg. Coef.	**p-val.**
Model Constant	-3.18	0.371
ER Status	-0.29	0.780
Tumor Size	-1.78	0.046
Tumor Grade	1.69	0.1771

Logistic Regression Model of Clinicoprognostic Variables + Metabolic Signature

	Reg. Coef.	**p-val.**
Model Constant	-6.80	0.227
ER Status	-0.80	0.562
Tumor Size	-3.69	0.041
Tumor Grade	3.71	0.081
Metabolic Signature	11.12	**0.043**

7.5 Figure Legends

Figure 1. Model of increased lactate promoting breast cancer recurrence. (A) Downregulation of *Myc* is accompanied by upregulation of *Sirt3* expression. *Myc* downregulation was achieved using 2 different siRNA constructs targeted against this gene. Expression levels were assessed by qRT-PCR and normalized to TBP. (B) Proposed model of how Myc Upregulation contributed to lactate level modulation through its action on Sirt3. Increased lactate is thought to increase Sirt1 levels and acitivty. This affects p53 deacetylation and resulting in pro-survival signaling and apoptosis resistance.

Figure 2. Recurrent tumors exhibit increased serine biosynthesis pathway activity. (A,B) Infusion of D-[1,2-^{13}C]-glucose in 3 primary and 3 recurrent tumor-bearing mice results in markedly higher labeled glycine production in recurrent tumors when compared to primary tumors. Shown are representative ^{13}C-MRS spectra from one primary (A) and one recurrent mouse (B). Area where the glycine peak resides is highlighted in red. Results were reproduced in all 3 primary and 3 recurrent tumors considered. Glycine is produced from serine in the serine biosynthesis pathway. (C) Recurrent tumors exhibit higher PHGDH levels when compared to primary tumors. Expression levels were assessed using qRT-PCR and normalized to TBP. PHGDH is a key enzyme in the serine biosynthesis pathway.

Figure 3. Model of metabolic reprogramming in breast cancer recurrence. In primary tumors, *neu* activation activates the PI3k/AKT pathway, a known key regulator of glycolysis. With doxycycline withdrawal, *neu* and AKT activity are downregulated. Recurring tumors exhibit marked metabolic reprogramming driven by Myc overexpression. Recurrent tumors upregulate lactate metabolism, glutamine metabolism and serine biosynthesis, all shown to be affected by Myc.

Figure 4. AKT might be another regulator of glutamine metabolism. (A) MCF-7 cells are glutamine- addicted and this effect is rescued by alpha-ketoglutarate. Cells were cultured for 96 hours in 1) regular media, 2) glutamine-deprived media and 3) glutamine-deprived media supplemented with alpha-ketoglutarate. (B) Quantification of cell death in each well by trypan blue 96 hours post-incubation. Glutamine withdrawal leads to death of a large proportion of the MCF-7 cells. Viability is restored by the addition of alpha-ketoglutarate. Samples were run in triplicates. (C) AKT inhibition leads to downregulation of *MYC, SLC1A5* and *GLS1* levels in MCF-7 cells. *AKT* inhibition was achieved using 2 different siRNAs targeted against this gene. Expression levels were assessed by qRT-PCR and normalized to TBP. (D) Proposed Model of AKT regulating glutamine metabolism by acting through MYC.

Figure 5. Glud1 as an additional glutaminolytic target in breast cancer recurrence. (A) Recurrent tumors exhibit higher alpha-ketoglutarate levels relative to primary tumors. Results are from 4 primary and 4 recurrent tumors. (B) Recurrent tumors exhibit higher alpha-ketoglutarate enrichment when compared to primary tumors following [3-^{13}C]-

glutamine infusion. Enrichment was assessed using mass spectrometry. Results are presented as mole percent excess (MPE). (C,D) Recurrent tumors exhibit higher levels of Glud1 at both the mRNA and protein levels. mRNA levels were assessed using qRT-PCR and normalized to TBP. In the western blot, tubulin was used as a loading control. (E) *Glud1* downregulation leads to reduced mean growth rate of recurrent tumors. *Glud1* downregulation was achieved by using an shRNA targeted again the gene. (F) Sirt4 exhibits higher expression levels in recurrent tumors when compared to primary tumors as assessed by qRT-PCR. Expression levels were normalized to TBP. Sirt4 has been previously shown to modulate *Glud1* levels.

Figure 6. Hyperpolarized magnetic resonance spectroscopy in primary and recurrent tumor-bearing mice. (A) Representative stacked spectra following the injection of hyperpolarized 13C-pyruvate into the tail vein of a primary tumor-bearing mouse. Spectra were collected at 1 second intervals. (B) Dynamic curves of pyruvate level changes in the primary and recurrent tumors assessed in this study. Each point corresponds to the area under the pyruvate curve at one time point. Data were normalized to total carbon. Muscle was used as a control. (C) Dynamic curves of lactate level changes in the tumors considered. Each point corresponds to the area under the curve at one time point. Data were also normalized to total carbon. Muscle was used as a control. (D) Representative fit of a pyruvate curve from a primary tumor using 5-parameter solution to the 2-site exchange chemical model. (E) Representative fit of a lactate curve from a primary tumor using 5-parameter solution to the 2-site chemical exchange model. The fits were used to estimate the LDH reaction rate.

Figure 7. Performance of metabolic gene expression signature in predicting tumor recurrence in breast cancer patients. Receiver Operator Curve (ROC) analysis was performed on the results from 1) the logistic regression model that incorporates the clinical prognostic variables and 2) the model that incorporates the metabolice gene expression signature in addition to those variables. Area under the curve (AUC) computation revealed an improvement in the performance of the model when the signature is added (AUC=0.91) compared to the model that incorporates the clinical variables only (AUC=0.82).

7.6 Figures

Figure 1

A

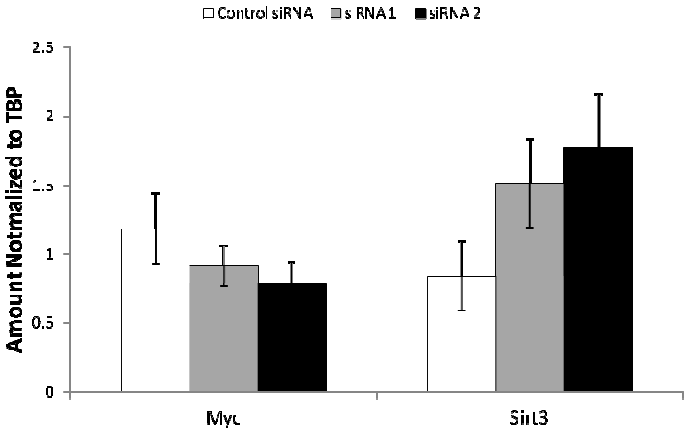

B

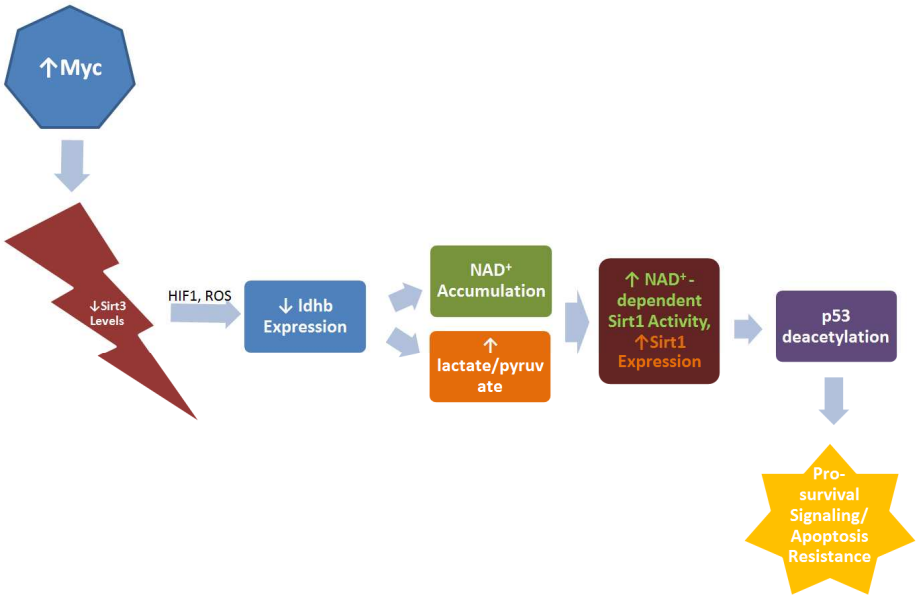

Figure 2

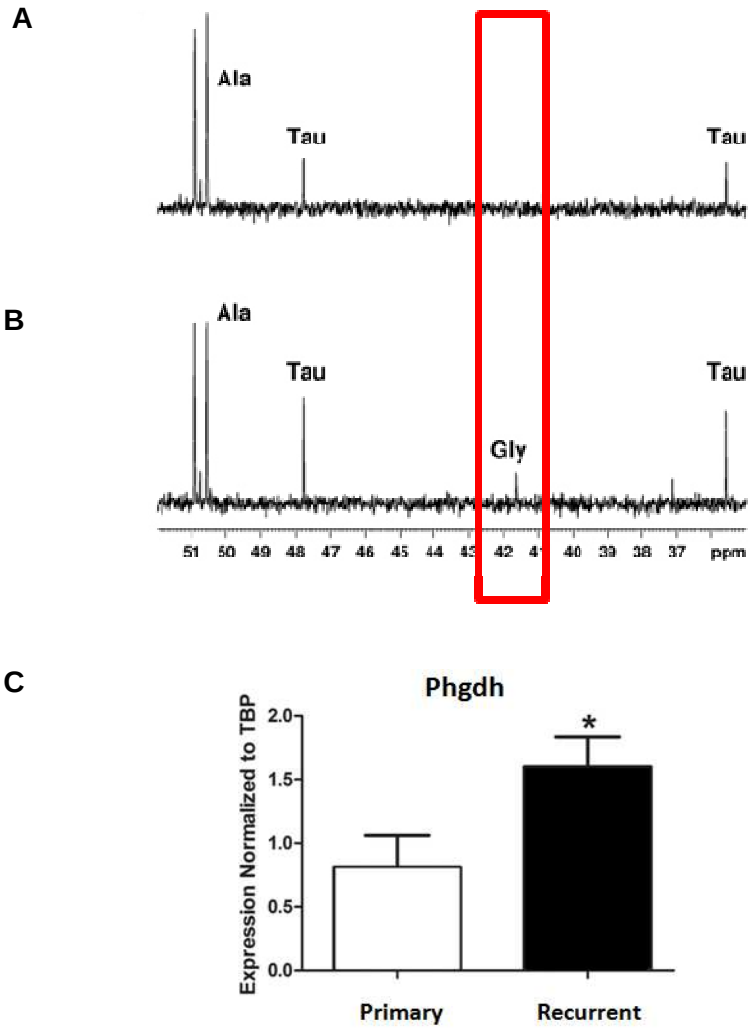
A
Ala
Tau
Tau
B
Ala
Tau
Tau
Gly
51 50 49 48 47 46 45 44 43 42 41 40 39 38 37 ppm
C
Phgdh
Expression Normalized to TBP
2.0
1.5
1.0
0.5
0.0
*
Primary
Recurrent

Figure 3

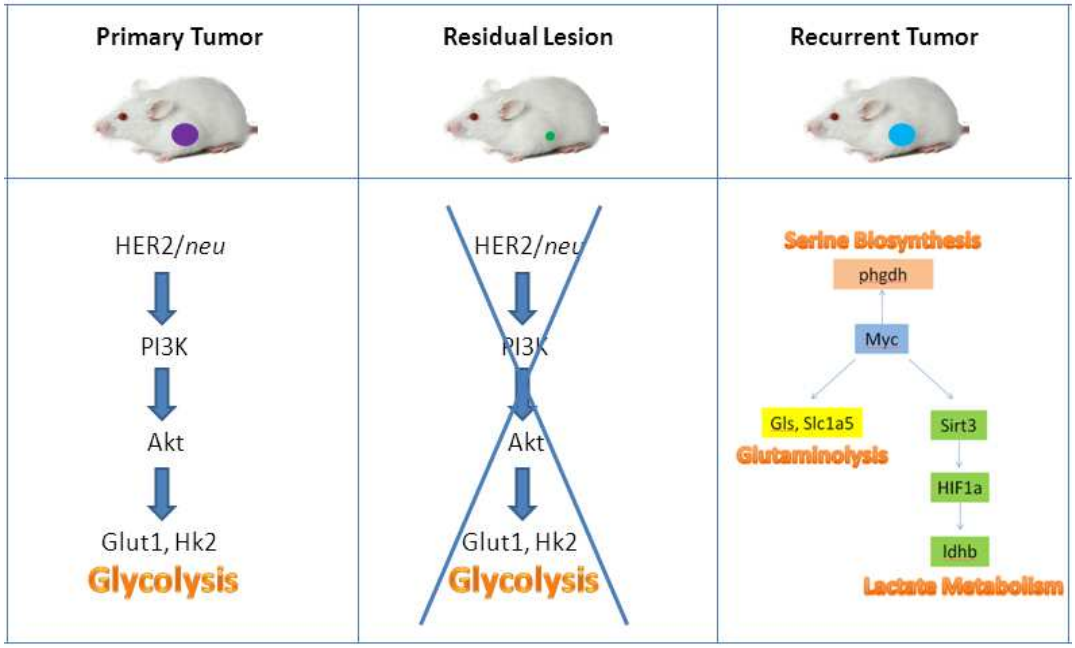
Primary Tumor
Residual Lesion
Recurrent Tumor
HER2/neu
PI3K
Akt
Glut1, Hk2
Glycolysis
HER2/neu
PI3K
Akt
Glut1, Hk2
Glycolysis
Serine Biosynthesis
phgdh
Myc
Gls, Slc1a5
Glutaminolysis
Sirt3
HIF1a
Idhb
Lactate Metabolism

Figure 4

A

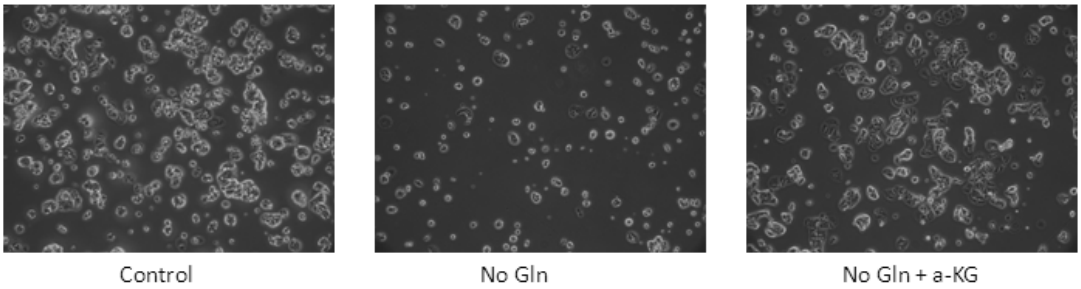

B

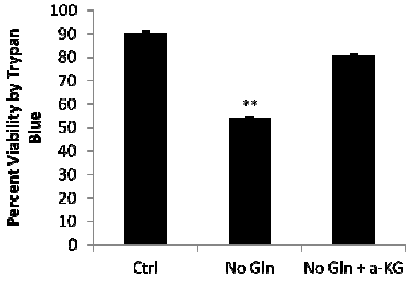

C

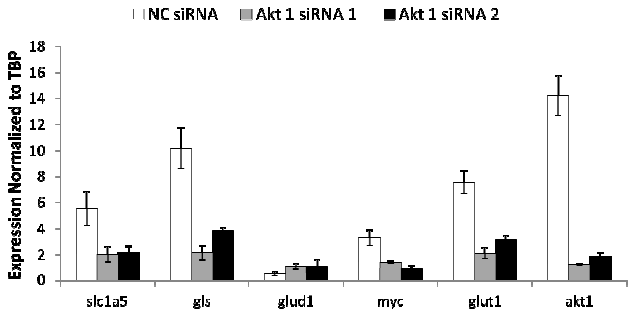

D

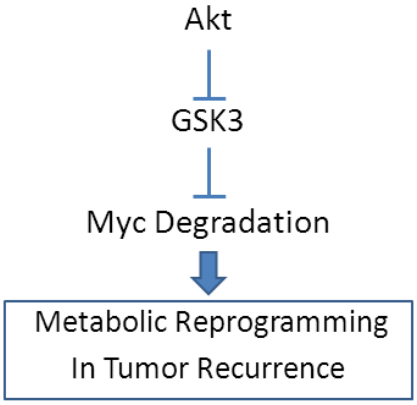

Figure 5

A

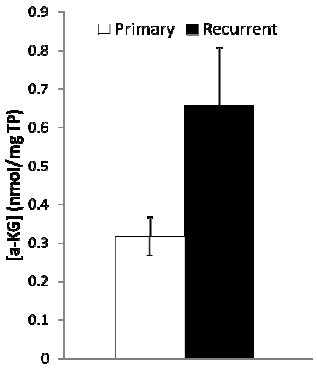

B

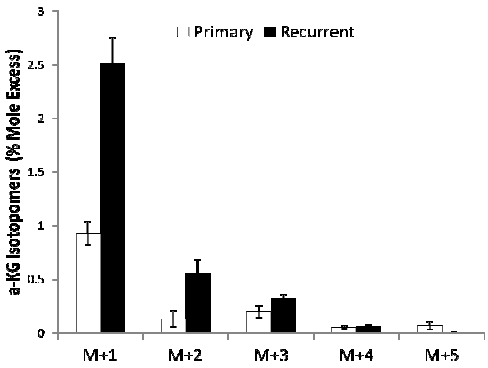

C

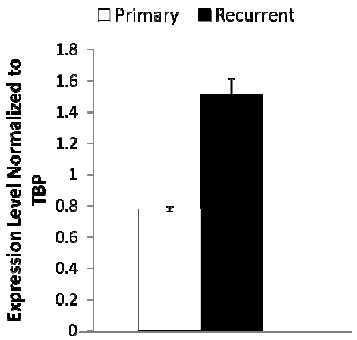

D

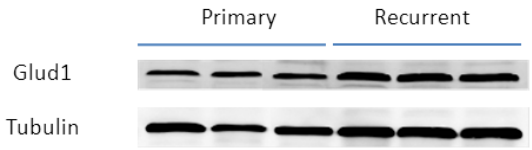

E

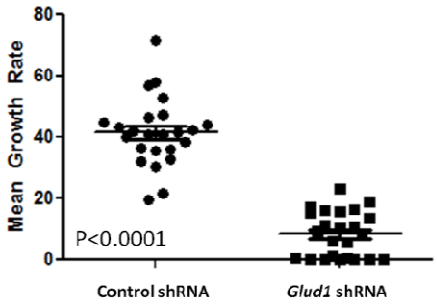

F

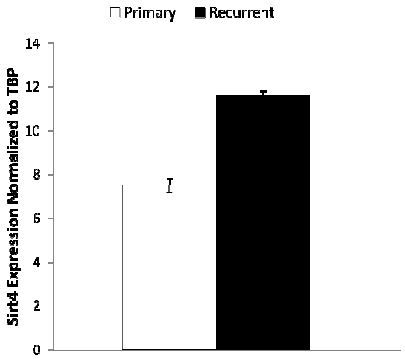

Figure 6

A

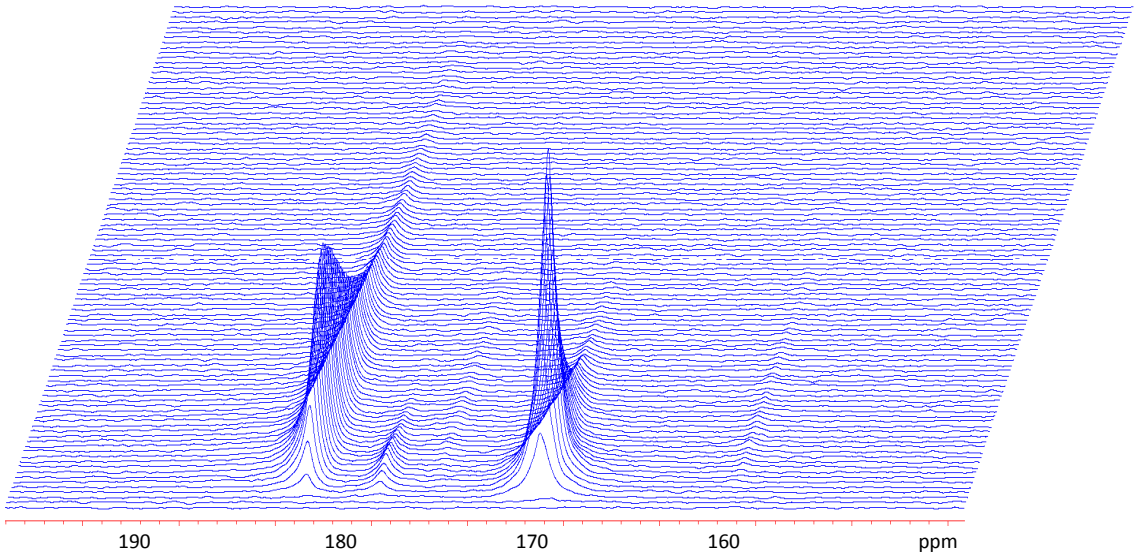

B

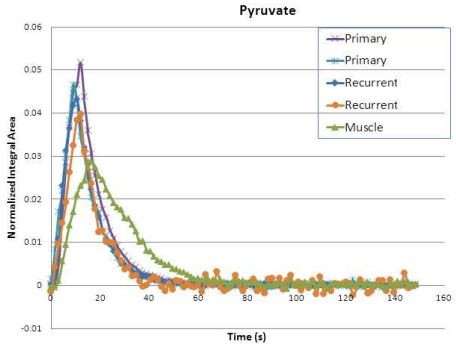

C

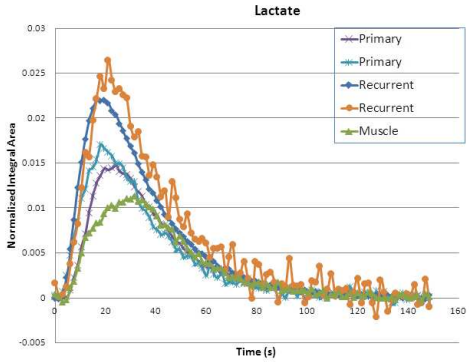

D

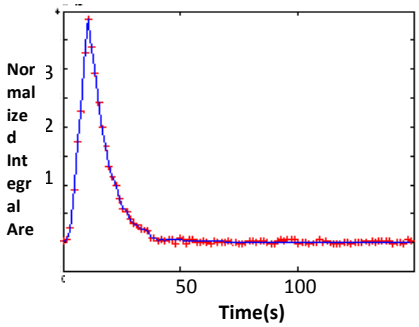

E

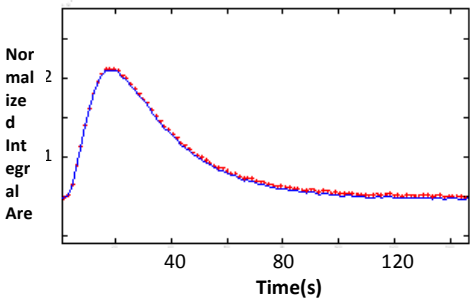

Figure 7

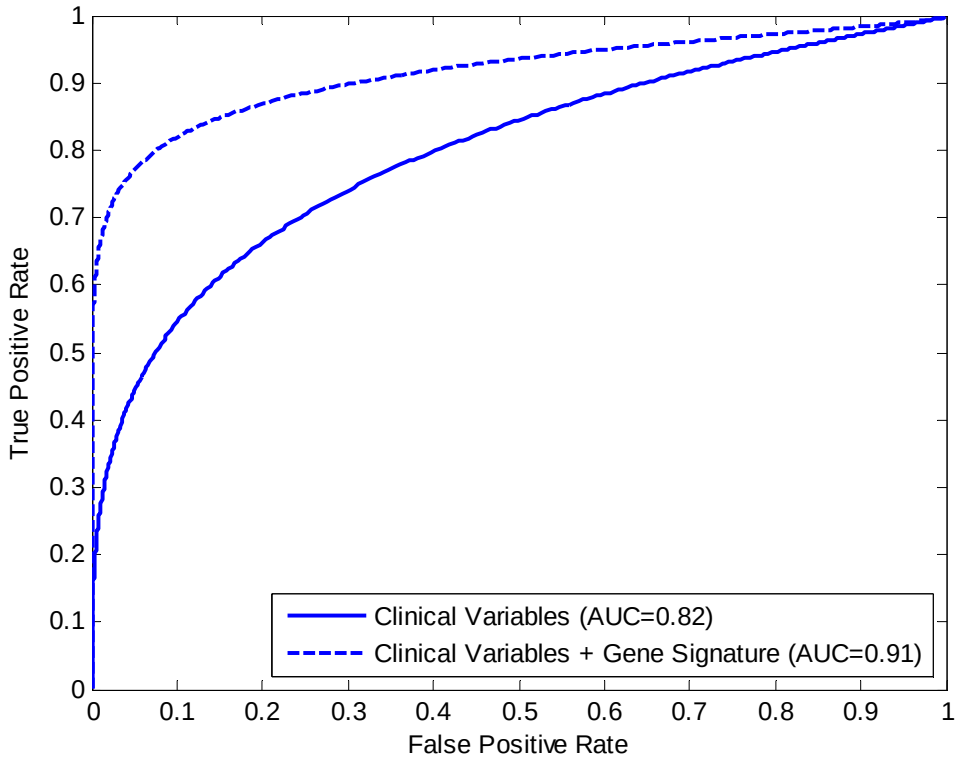
True Positive Rate
False Positive Rate
0
0.1
0.2
0.3
0.4
0.5
0.6
0.7
0.8
0.9
1
Clinical Variables (AUC=0.82)
Clinical Variables + Gene Signature (AUC=0.91)

BIBLIOGRAPHY

1. Jemal A, Bray F, Center MM, Ferlay J, Ward E, Forman D. Global cancer statistics. *CA: a cancer journal for clinicians.* Mar-Apr;61(2):69-90.

2. Siegel R, Naishadham D, Jemal A. Cancer statistics, 2012. *CA: a cancer journal for clinicians.* Jan-Feb;62(1):10-29.

3. Siegel R, Desantis C, Virgo K, et al. Cancer treatment and survivorship statistics, 2012. *CA: a cancer journal for clinicians.* Jul;62(4):220-241.

4. Kohler BA, Ward E, McCarthy BJ, et al. Annual report to the nation on the status of cancer, 1975-2007, featuring tumors of the brain and other nervous system. *Journal of the National Cancer Institute.* May 4;103(9):714-736.

5. Jemal A, Siegel R, Xu J, Ward E. Cancer statistics, 2010. *CA: a cancer journal for clinicians.* Sep-Oct;60(5):277-300.

6. Society AC. Breast Cancer Facts and Figures. *American Cancer Society, Inc, Atlanta* 2009-2020.

7. Colditz GA, Rosner B. Cumulative risk of breast cancer to age 70 years according to risk factor status: data from the Nurses' Health Study. *American journal of epidemiology.* Nov 15 2000;152(10):950-964.

8. Kelsey JL, Gammon MD, John EM. Reproductive factors and breast cancer. *Epidemiologic reviews.* 1993;15(1):36-47.

9. Baselga J, Tripathy D, Mendelsohn J, et al. Phase II study of weekly intravenous recombinant humanized anti-p185HER2 monoclonal antibody in patients with

HER2/neu-overexpressing metastatic breast cancer. *J Clin Oncol.* Mar 1996;14(3):737-744.

10. van den Brandt PA, Spiegelman D, Yaun SS, et al. Pooled analysis of prospective cohort studies on height, weight, and breast cancer risk. *American journal of epidemiology.* Sep 15 2000;152(6):514-527.

11. Maruti SS, Willett WC, Feskanich D, Rosner B, Colditz GA. A prospective study of age-specific physical activity and premenopausal breast cancer. *Journal of the National Cancer Institute.* May 21 2008;100(10):728-737.

12. Hamajima N, Hirose K, Tajima K, et al. Alcohol, tobacco and breast cancer--collaborative reanalysis of individual data from 53 epidemiological studies, including 58,515 women with breast cancer and 95,067 women without the disease. *British journal of cancer.* Nov 18 2002;87(11):1234-1245.

13. Boyd NF, Stone J, Vogt KN, Connelly BS, Martin LJ, Minkin S. Dietary fat and breast cancer risk revisited: a meta-analysis of the published literature. *British journal of cancer.* Nov 3 2003;89(9):1672-1685.

14. Peto J, Mack TM. High constant incidence in twins and other relatives of women with breast cancer. *Nature genetics.* Dec 2000;26(4):411-414.

15. Fisher B, Dignam J, Wolmark N, et al. Tamoxifen in treatment of intraductal breast cancer: National Surgical Adjuvant Breast and Bowel Project B-24 randomised controlled trial. *Lancet.* Jun 12 1999;353(9169):1993-2000.

16. Berry DA, Cronin KA, Plevritis SK, et al. Effect of screening and adjuvant therapy on mortality from breast cancer. *The New England journal of medicine.* Oct 27 2005;353(17):1784-1792.

17. Jatoi I, Tsimelzon A, Weiss H, Clark GM, Hilsenbeck SG. Hazard rates of recurrence following diagnosis of primary breast cancer. *Breast cancer research and treatment.* Jan 2005;89(2):173-178.

18. Davies C, Godwin J, Gray R, et al. Relevance of breast cancer hormone receptors and other factors to the efficacy of adjuvant tamoxifen: patient-level meta-analysis of randomised trials. *Lancet.* Aug 27;378(9793):771-784.

19. Emens LA, Davidson NE. The follow-up of breast cancer. *Seminars in oncology.* Jun 2003;30(3):338-348.

20. Benson JR. Tamoxifen in early breast cancer. *Lancet.* Aug 1 1998;352(9125):404-405.

21. Fisher B, Anderson S, Bryant J, et al. Twenty-year follow-up of a randomized trial comparing total mastectomy, lumpectomy, and lumpectomy plus irradiation for the treatment of invasive breast cancer. *The New England journal of medicine.* Oct 17 2002;347(16):1233-1241.

22. Jacobson JA, Danforth DN, Cowan KH, et al. Ten-year results of a comparison of conservation with mastectomy in the treatment of stage I and II breast cancer. *The New England journal of medicine.* Apr 6 1995;332(14):907-911.

23. Wapnir IL, Anderson SJ, Mamounas EP, et al. Prognosis after ipsilateral breast tumor recurrence and locoregional recurrences in five National Surgical Adjuvant Breast and Bowel Project node-positive adjuvant breast cancer trials. *J Clin Oncol.* May 1 2006;24(13):2028-2037.

24. Fisher B, Bryant J, Dignam JJ, et al. Tamoxifen, radiation therapy, or both for prevention of ipsilateral breast tumor recurrence after lumpectomy in women with invasive breast cancers of one centimeter or less. *J Clin Oncol.* Oct 15 2002;20(20):4141-4149.

25. van Tienhoven G, Voogd AC, Peterse JL, et al. Prognosis after treatment for loco-regional recurrence after mastectomy or breast conserving therapy in two randomised trials (EORTC 10801 and DBCG-82TM). EORTC Breast Cancer Cooperative Group and the Danish Breast Cancer Cooperative Group. *Eur J Cancer.* Jan 1999;35(1):32-38.

26. Voogd AC, van Oost FJ, Rutgers EJ, et al. Long-term prognosis of patients with local recurrence after conservative surgery and radiotherapy for early breast cancer. *Eur J Cancer.* Nov 2005;41(17):2637-2644.

27. Francis M, Cakir B, Ung O, Gebski V, Boyages J. Prognosis after breast recurrence following conservative surgery and radiotherapy in patients with node-negative breast cancer. *The British journal of surgery.* Dec 1999;86(12):1556-1562.

28. Willner J, Kiricuta IC, Kolbl O. Locoregional recurrence of breast cancer following mastectomy: always a fatal event? Results of univariate and multivariate analysis. *International journal of radiation oncology, biology, physics.* Mar 1 1997;37(4):853-863.

29. American Cancer Society A. http://www.cancer.org/Cancer/BreastCancer/DetailedGuide/breast-cancer-survival-by-stage. 2012; http://www.cancer.org/Cancer/BreastCancer/DetailedGuide/breast-cancer-survival-by-stage.

30. Page DL. Prognosis and breast cancer. Recognition of lethal and favorable prognostic types. *The American journal of surgical pathology.* Apr 1991;15(4):334-349.

31. Yarbro JW, Page DL, Fielding LP, Partridge EE, Murphy GP. American Joint Committee on Cancer prognostic factors consensus conference. *Cancer.* Dec 1 1999;86(11):2436-2446.

32. Smitt MC, Nowels KW, Zdeblick MJ, et al. The importance of the lumpectomy surgical margin status in long-term results of breast conservation. *Cancer.* Jul 15 1995;76(2):259-267.

33. Liu S, Edgerton SM, Moore DH, 2nd, Thor AD. Measures of cell turnover (proliferation and apoptosis) and their association with survival in breast cancer. *Clin Cancer Res.* Jun 2001;7(6):1716-1723.

34. Ross JS, Fletcher JA, Linette GP, et al. The Her-2/neu gene and protein in breast cancer 2003: biomarker and target of therapy. *The oncologist.* 2003;8(4):307-325.

35. Goldhirsch A, Glick JH, Gelber RD, Coates AS, Thurlimann B, Senn HJ. Meeting highlights: international expert consensus on the primary therapy of early breast cancer 2005. *Ann Oncol.* Oct 2005;16(10):1569-1583.

36. Paik S, Shak S, Tang G, et al. A multigene assay to predict recurrence of tamoxifen-treated, node-negative breast cancer. *The New England journal of medicine.* Dec 30 2004;351(27):2817-2826.

37. Rojas MP, Telaro E, Russo A, Fossati R, Confalonieri C, Liberati A. Follow-up strategies for women treated for early breast cancer. *Cochrane database of systematic reviews (Online).* 2000(4):CD001768.

38. Montgomery DA, Krupa K, Jack WJ, et al. Changing pattern of the detection of locoregional relapse in breast cancer: the Edinburgh experience. *British journal of cancer.* Jun 18 2007;96(12):1802-1807.

39. Dershaw DD, McCormick B, Osborne MP. Detection of local recurrence after conservative therapy for breast carcinoma. *Cancer.* Jul 15 1992;70(2):493-496.

40. Mumtaz H, Davidson T, Hall-Craggs MA, et al. Comparison of magnetic resonance imaging and conventional triple assessment in locally recurrent breast cancer. *The British journal of surgery.* Aug 1997;84(8):1147-1151.

41. Belli P, Costantini M, Romani M, Marano P, Pastore G. Magnetic resonance imaging in breast cancer recurrence. *Breast cancer research and treatment.* Jun 2002;73(3):223-235.

42. Berg WA, Blume JD, Cormack JB, et al. Combined screening with ultrasound and mammography vs mammography alone in women at elevated risk of breast cancer. *Jama.* May 14 2008;299(18):2151-2163.

43. Kamel EM, Wyss MT, Fehr MK, von Schulthess GK, Goerres GW. [18F]-Fluorodeoxyglucose positron emission tomography in patients with suspected recurrence of breast cancer. *Journal of cancer research and clinical oncology.* Mar 2003;129(3):147-153.

44. Isasi CR, Moadel RM, Blaufox MD. A meta-analysis of FDG-PET for the evaluation of breast cancer recurrence and metastases. *Breast cancer research and treatment.* Mar 2005;90(2):105-112.

45. Cajucom CC, Tsangaris TN, Nemoto T, Driscoll D, Penetrante RB, Holyoke ED. Results of salvage mastectomy for local recurrence after breast-conserving surgery without radiation therapy. *Cancer.* Mar 1 1993;71(5):1774-1779.

46. Haylock BJ, Coppin CM, Jackson J, Basco VE, Wilson KS. Locoregional first recurrence after mastectomy: prospective cohort studies with and without immediate chemotherapy. *International journal of radiation oncology, biology, physics.* Jan 15 2000;46(2):355-362.

47. Andry G, Suciu S, Vico P, et al. Locoregional recurrences after 649 modified radical mastectomies: incidence and significance. *Eur J Surg Oncol.* Dec 1989;15(6):476-485.

48. Flook D, Webster DJ, Hughes LE, Mansel RW. Salvage surgery for advanced local recurrence of breast cancer. *The British journal of surgery.* May 1989;76(5):512-514.

49. Salvadori B, Rovini D, Squicciarini P, Conti R, Cusumano F, Grassi M. Surgery for local recurrences following deficient radical mastectomy for breast cancer: a selected series of 39 cases. *Eur J Surg Oncol.* Oct 1992;18(5):438-441.

50. Yaziji H, Goldstein LC, Barry TS, et al. HER-2 testing in breast cancer using parallel tissue-based methods. *Jama.* Apr 28 2004;291(16):1972-1977.

51. Slamon DJ, Clark GM, Wong SG, Levin WJ, Ullrich A, McGuire WL. Human breast cancer: correlation of relapse and survival with amplification of the HER-2/neu oncogene. *Science.* Jan 9 1987;235(4785):177-182.

52. King CR, Kraus MH, Aaronson SA. Amplification of a novel v-erbB-related gene in a human mammary carcinoma. *Science (New York, N.Y.* Sep 6 1985;229(4717):974-976.

53. Klapper LN, Glathe S, Vaisman N, et al. The ErbB-2/HER2 oncoprotein of human carcinomas may function solely as a shared coreceptor for multiple stroma-derived growth factors. *Proceedings of the National Academy of Sciences of the United States of America.* Apr 27 1999;96(9):4995-5000.

54. Lipton A, Leitzel K, Ali SM, et al. Serum HER-2/neu conversion to positive at the time of disease progression in patients with breast carcinoma on hormone therapy. *Cancer.* Jul 15 2005;104(2):257-263.

55. Paik S, Bryant J, Tan-Chiu E, et al. HER2 and choice of adjuvant chemotherapy for invasive breast cancer: National Surgical Adjuvant Breast and Bowel Project Protocol B-15. *Journal of the National Cancer Institute.* Dec 20 2000;92(24):1991-1998.

56. Gilcrease MZ, Woodward WA, Nicolas MM, et al. Even low-level HER2 expression may be associated with worse outcome in node-positive breast cancer. *The American journal of surgical pathology.* May 2009;33(5):759-767.

57. Kroger N, Milde-Langosch K, Riethdorf S, et al. Prognostic and predictive effects of immunohistochemical factors in high-risk primary breast cancer patients. *Clin Cancer Res.* Jan 1 2006;12(1):159-168.

58. Ritter CA, Perez-Torres M, Rinehart C, et al. Human breast cancer cells selected for resistance to trastuzumab in vivo overexpress epidermal growth factor receptor and ErbB ligands and remain dependent on the ErbB receptor network. *Clin Cancer Res.* Aug 15 2007;13(16):4909-4919.

59. Lu Y, Zi X, Zhao Y, Mascarenhas D, Pollak M. Insulin-like growth factor-I receptor signaling and resistance to trastuzumab (Herceptin). *J Natl Cancer Inst.* Dec 19 2001;93(24):1852-1857.

60. Shattuck DL, Miller JK, Carraway KL, 3rd, Sweeney C. Met receptor contributes to trastuzumab resistance of Her2-overexpressing breast cancer cells. *Cancer Res.* Mar 1 2008;68(5):1471-1477.

61. Molina MA, Saez R, Ramsey EE, et al. NH(2)-terminal truncated HER-2 protein but not full-length receptor is associated with nodal metastasis in human breast cancer. *Clin Cancer Res.* Feb 2002;8(2):347-353.

62. D'Cruz CM, Gunther EJ, Boxer RB, et al. c-MYC induces mammary tumorigenesis by means of a preferred pathway involving spontaneous Kras2 mutations. *Nat Med.* Feb 2001;7(2):235-239.

63. Moody SE, Sarkisian CJ, Hahn KT, et al. Conditional activation of Neu in the mammary epithelium of transgenic mice results in reversible pulmonary metastasis. *Cancer Cell.* Dec 2002;2(6):451-461.

64. Gunther EJ, Moody SE, Belka GK, et al. Impact of p53 loss on reversal and recurrence of conditional Wnt-induced tumorigenesis. *Genes Dev.* Feb 15 2003;17(4):488-501.

65. Boxer RB, Jang JW, Sintasath L, Chodosh LA. Lack of sustained regression of c-MYC-induced mammary adenocarcinomas following brief or prolonged MYC inactivation. *Cancer Cell.* Dec 2004;6(6):577-586.

66. Moody SE, Perez D, Pan TC, et al. The transcriptional repressor Snail promotes mammary tumor recurrence. *Cancer Cell.* Sep 2005;8(3):197-209.

67. Hynes NE, Lane HA. ERBB receptors and cancer: the complexity of targeted inhibitors. *Nat Rev Cancer.* May 2005;5(5):341-354.

68. Stal O, Perez-Tenorio G, Akerberg L, et al. Akt kinases in breast cancer and the results of adjuvant therapy. *Breast Cancer Res.* 2003;5(2):R37-44.

69. Clark AS, West K, Streicher S, Dennis PA. Constitutive and inducible Akt activity promotes resistance to chemotherapy, trastuzumab, or tamoxifen in breast cancer cells. *Mol Cancer Ther.* Jul 2002;1(9):707-717.

70. Smith MJ, Culhane AC, Killeen S, et al. Mechanisms driving local breast cancer recurrence in a model of breast-conserving surgery. *Ann Surg Oncol.* Oct 2008;15(10):2954-2964.

71. Engelman JA, Luo J, Cantley LC. The evolution of phosphatidylinositol 3-kinases as regulators of growth and metabolism. *Nat Rev Genet.* Aug 2006;7(8):606-619.

72. Vander Heiden MG, Cantley LC, Thompson CB. Understanding the Warburg effect: the metabolic requirements of cell proliferation. *Science.* May 22 2009;324(5930):1029-1033.

73. DeBerardinis RJ. Is cancer a disease of abnormal cellular metabolism? New angles on an old idea. *Genet Med.* Nov 2008;10(11):767-777.

74. DeBerardinis RJ, Lum JJ, Hatzivassiliou G, Thompson CB. The biology of cancer: metabolic reprogramming fuels cell growth and proliferation. *Cell Metab.* Jan 2008;7(1):11-20.

75. Deberardinis RJ, Sayed N, Ditsworth D, Thompson CB. Brick by brick: metabolism and tumor cell growth. *Curr Opin Genet Dev.* Feb 2008;18(1):54-61.

76. Warburg O. [Origin of cancer cells.]. *Oncologia.* 1956;9(2):75-83.

77. Elstrom RL, Bauer DE, Buzzai M, et al. Akt stimulates aerobic glycolysis in cancer cells. *Cancer Res.* Jun 1 2004;64(11):3892-3899.

78. Rathmell JC, Fox CJ, Plas DR, Hammerman PS, Cinalli RM, Thompson CB. Akt-directed glucose metabolism can prevent Bax conformation change and promote growth factor-independent survival. *Mol Cell Biol.* Oct 2003;23(20):7315-7328.

79. Plas DR, Talapatra S, Edinger AL, Rathmell JC, Thompson CB. Akt and Bcl-xL promote growth factor-independent survival through distinct effects on mitochondrial physiology. *J Biol Chem.* Apr 13 2001;276(15):12041-12048.

80. Kroemer G, Pouyssegur J. Tumor cell metabolism: cancer's Achilles' heel. *Cancer cell.* Jun 2008;13(6):472-482.

81. Holroyde CP, Axelrod RS, Skutches CL, Haff AC, Paul P, Reichard GA. Lactate metabolism in patients with metastatic colorectal cancer. *Cancer research.* Dec 1979;39(12):4900-4904.

82. Swietach P, Vaughan-Jones RD, Harris AL. Regulation of tumor pH and the role of carbonic anhydrase 9. *Cancer metastasis reviews.* Jun 2007;26(2):299-310.

83. Christofk HR, Vander Heiden MG, Wu N, Asara JM, Cantley LC. Pyruvate kinase M2 is a phosphotyrosine-binding protein. *Nature.* Mar 13 2008;452(7184):181-186.

84. Miller P. Forest Flora and Fauna. *Library Sparks.* 2011;8(8):52-55.

85. Markert CL, Shaklee JB, Whitt GS. Evolution of a gene. Multiple genes for LDH isozymes provide a model of the evolution of gene structure, function and regulation. *Science.* Jul 11 1975;189(4197):102-114.

86. Koukourakis MI, Giatromanolaki A, Sivridis E, et al. Prognostic and predictive role of lactate dehydrogenase 5 expression in colorectal cancer patients treated with PTK787/ZK 222584 (vatalanib) antiangiogenic therapy. *Clin Cancer Res.* Jul 15;17(14):4892-4900.

87. Leiblich A, Cross SS, Catto JW, et al. Lactate dehydrogenase-B is silenced by promoter hypermethylation in human prostate cancer. *Oncogene.* May 11 2006;25(20):2953-2960.

88. Eagle H. The specific amino acid requirements of a human carcinoma cell (Stain HeLa) in tissue culture. *J Exp Med.* Jul 1 1955;102(1):37-48.

89. Kvamme E, Svenneby G. Effect of anaerobiosis and addition of keto acids on glutamine utilization by Ehrlich ascites-tumor cells. *Biochim Biophys Acta.* Jul 29 1960;42:187-188.

90. DeBerardinis RJ, Cheng T. Q's next: the diverse functions of glutamine in metabolism, cell biology and cancer. *Oncogene.* Jan 21;29(3):313-324.

91. DeBerardinis RJ, Mancuso A, Daikhin E, et al. Beyond aerobic glycolysis: transformed cells can engage in glutamine metabolism that exceeds the requirement for protein and nucleotide synthesis. *Proc Natl Acad Sci U S A.* Dec 4 2007;104(49):19345-19350.

92. Wise DR, Thompson CB. Glutamine addiction: a new therapeutic target in cancer. *Trends Biochem Sci.* Aug;35(8):427-433.

93. Yang C, Sudderth J, Dang T, Bachoo RM, McDonald JG, DeBerardinis RJ. Glioblastoma cells require glutamate dehydrogenase to survive impairments of glucose metabolism or Akt signaling. *Cancer Res.* Oct 15 2009;69(20):7986-7993.

94. Eng CH, Yu K, Lucas J, White E, Abraham RT. Ammonia derived from glutaminolysis is a diffusible regulator of autophagy. *Science signaling.*3(119):ra31.

95. Marino G, Kroemer G. Ammonia: a diffusible factor released by proliferating cells that induces autophagy. *Science signaling.*3(124):pe19.

96. Dang CV, Le A, Gao P. MYC-induced cancer cell energy metabolism and therapeutic opportunities. *Clin Cancer Res.* Nov 1 2009;15(21):6479-6483.

97. Wise DR, DeBerardinis RJ, Mancuso A, et al. Myc regulates a transcriptional program that stimulates mitochondrial glutaminolysis and leads to glutamine addiction. *Proc Natl Acad Sci U S A.* Dec 2 2008;105(48):18782-18787.

98. Gao P, Tchernyshyov I, Chang TC, et al. c-Myc suppression of miR-23a/b enhances mitochondrial glutaminase expression and glutamine metabolism. *Nature.* Apr 9 2009;458(7239):762-765.

99. Dang CV, Hamaker M, Sun P, Le A, Gao P. Therapeutic targeting of cancer cell metabolism. *J Mol Med.* Feb 8.

100. Wang JB, Erickson JW, Fuji R, et al. Targeting mitochondrial glutaminase activity inhibits oncogenic transformation. *Cancer Cell.* Sep 14;18(3):207-219.

101. Erickson JW, Cerione RA. Glutaminase: A hot spot for regulation of cancer cell metabolism? *Oncotarget.* Dec;1(8):734-740.

102. Lonn U, Lonn S, Nilsson B, Stenkvist B. Prognostic value of erb-B2 and myc amplification in breast cancer imprints. *Cancer.* Jun 1 1995;75(11):2681-2687.

103. Berns EM, Klijn JG, van Putten WL, van Staveren IL, Portengen H, Foekens JA. c-myc amplification is a better prognostic factor than HER2/neu amplification in primary breast cancer. *Cancer Res.* Mar 1 1992;52(5):1107-1113.

104. Berns EM, Klijn JG, van Staveren IL, Portengen H, Noordegraaf E, Foekens JA. Prevalence of amplification of the oncogenes c-myc, HER2/neu, and int-2 in one thousand human breast tumours: correlation with steroid receptors. *Eur J Cancer.* 1992;28(2-3):697-700.

105. Berns EM, Foekens JA, van Putten WL, et al. Prognostic factors in human primary breast cancer: comparison of c-myc and HER2/neu amplification. *J Steroid Biochem Mol Biol.* Sep 1992;43(1-3):13-19.

106. Borg A, Baldetorp B, Ferno M, Olsson H, Sigurdsson H. c-myc amplification is an independent prognostic factor in postmenopausal breast cancer. *Int J Cancer.* Jul 9 1992;51(5):687-691.

107. Guerin M, Barrois M, Terrier MJ, Spielmann M, Riou G. Overexpression of either c-myc or c-erbB-2/neu proto-oncogenes in human breast carcinomas: correlation with poor prognosis. *Oncogene Res.* 1988;3(1):21-31.

108. Varley JM, Swallow JE, Brammar WJ, Whittaker JL, Walker RA. Alterations to either c-erbB-2(neu) or c-myc proto-oncogenes in breast carcinomas correlate with poor short-term prognosis. *Oncogene.* 1987;1(4):423-430.

109. Naidu R, Wahab NA, Yadav M, Kutty MK. Protein expression and molecular analysis of c-myc gene in primary breast carcinomas using immunohistochemistry and differential polymerase chain reaction. *Int J Mol Med.* Feb 2002;9(2):189-196.

110. Schlotter CM, Vogt U, Bosse U, Mersch B, Wassmann K. C-myc, not HER-2/neu, can predict recurrence and mortality of patients with node-negative breast cancer. *Breast Cancer Res.* 2003;5(2):R30-36.

111. Deming SL, Nass SJ, Dickson RB, Trock BJ. C-myc amplification in breast cancer: a meta-analysis of its occurrence and prognostic relevance. *Br J Cancer.* Dec 2000;83(12):1688-1695.

112. Coleman PS. Membrane cholesterol and tumor bioenergetics. *Annals of the New York Academy of Sciences.* 1986;488:451-467.

113. Metallo CM, Gameiro PA, Bell EL, et al. Reductive glutamine metabolism by IDH1 mediates lipogenesis under hypoxia. *Nature.* Jan 19;481(7381):380-384.

114. Krycer JR, Sharpe LJ, Luu W, Brown AJ. The Akt-SREBP nexus: cell signaling meets lipid metabolism. *Trends in endocrinology and metabolism: TEM.* May;21(5):268-276.

115. Yang YA, Han WF, Morin PJ, Chrest FJ, Pizer ES. Activation of fatty acid synthesis during neoplastic transformation: role of mitogen-activated protein kinase and phosphatidylinositol 3-kinase. *Experimental cell research.* Sep 10 2002;279(1):80-90.

116. Bauer DE, Hatzivassiliou G, Zhao F, Andreadis C, Thompson CB. ATP citrate lyase is an important component of cell growth and transformation. *Oncogene.* Sep 15 2005;24(41):6314-6322.

117. Hatzivassiliou G, Zhao F, Bauer DE, et al. ATP citrate lyase inhibition can suppress tumor cell growth. *Cancer cell.* Oct 2005;8(4):311-321.

118. Swinnen JV, Brusselmans K, Verhoeven G. Increased lipogenesis in cancer cells: new players, novel targets. *Current opinion in clinical nutrition and metabolic care.* Jul 2006;9(4):358-365.

119. Bhujwalla ZM, Glickson JD. Detection of tumor response to radiation therapy by in vivo proton MR spectroscopy. *Int J Radiat Oncol Biol Phys.* Oct 1 1996;36(3):635-639.

120. Nelson SJ. Multivoxel magnetic resonance spectroscopy of brain tumors. *Mol Cancer Ther.* May 2003;2(5):497-507.

121. Group USCSW. United States Cancer Statistics: 1999–2006 Incidence and Mortality Web-based Report. *Department of Health and Human Services, Centers for Disease Control and Prevention, and National Cancer Institute.* 2010.

122. Brewster AM, Hortobagyi GN, Broglio KR, et al. Residual risk of breast cancer recurrence 5 years after adjuvant therapy. *J Natl Cancer Inst.* Aug 20 2008;100(16):1179-1183.

123. Berger MS, Locher GW, Saurer S, et al. Correlation of c-erbB-2 gene amplification and protein expression in human breast carcinoma with nodal status and nuclear grading. *Cancer Res.* Mar 1 1988;48(5):1238-1243.

124. DeBerardinis RJ, Cheng T. Q's next: the diverse functions of glutamine in metabolism, cell biology and cancer. *Oncogene.* Jan 21 2010;29(3):313-324.

125. Scheenen TW, Futterer J, Weiland E, et al. Discriminating cancer from noncancer tissue in the prostate by 3-dimensional proton magnetic resonance spectroscopic imaging: a prospective multicenter validation study. *Invest Radiol.* Jan 2011;46(1):25-33.

126. Castillo M, Smith JK, Kwock L. Correlation of myo-inositol levels and grading of cerebral astrocytomas. *AJNR Am J Neuroradiol.* Oct 2000;21(9):1645-1649.

127. McKnight TR, Lamborn KR, Love TD, et al. Correlation of magnetic resonance spectroscopic and growth characteristics within Grades II and III gliomas. *J Neurosurg.* Apr 2007;106(4):660-666.

128. Lehnhardt FG, Bock C, Rohn G, Ernestus RI, Hoehn M. Metabolic differences between primary and recurrent human brain tumors: a 1H NMR spectroscopic investigation. *NMR Biomed.* Oct 2005;18(6):371-382.

129. Lehnhardt FG, Rohn G, Ernestus RI, Grune M, Hoehn M. 1H- and (31)P-MR spectroscopy of primary and recurrent human brain tumors in vitro: malignancy-characteristic profiles of water soluble and lipophilic spectral components. *NMR Biomed.* Aug 2001;14(5):307-317.

130. Asiago VM, Alvarado LZ, Shanaiah N, et al. Early detection of recurrent breast cancer using metabolite profiling. *Cancer Res.* Nov 1;70(21):8309-8318.

131. Bertini I, Cacciatore S, Jensen BV, et al. Metabolomic NMR fingerprinting to identify and predict survival of patients with metastatic colorectal cancer. *Cancer Res.* Jan 1 2012;72(1):356-364.

132. Gunther EJ, Belka GK, Wertheim GB, et al. A novel doxycycline-inducible system for the transgenic analysis of mammary gland biology. *Faseb J.* Mar 2002;16(3):283-292.

133. Sitter B, Sonnewald U, Spraul M, Fjosne HE, Gribbestad IS. High-resolution magic angle spinning MRS of breast cancer tissue. *NMR Biomed.* Aug 2002;15(5):327-337.

134. Wertheim GB, Yang TW, Pan TC, et al. The Snf1-related kinase, Hunk, is essential for mammary tumor metastasis. *Proc Natl Acad Sci U S A.* Sep 15 2009;106(37):15855-15860.

135. Desmedt C, Piette F, Loi S, et al. Strong time dependence of the 76-gene prognostic signature for node-negative breast cancer patients in the TRANSBIG multicenter independent validation series. *Clin Cancer Res.* Jun 1 2007;13(11):3207-3214.

136. Ivshina AV, George J, Senko O, et al. Genetic reclassification of histologic grade delineates new clinical subtypes of breast cancer. *Cancer research.* Nov 1 2006;66(21):10292-10301.

137. Schmidt M, Bohm D, von Torne C, et al. The humoral immune system has a key prognostic impact in node-negative breast cancer. *Cancer research.* Jul 1 2008;68(13):5405-5413.

138. Sotiriou C, Wirapati P, Loi S, et al. Gene expression profiling in breast cancer: understanding the molecular basis of histologic grade to improve prognosis. *Journal of the National Cancer Institute.* Feb 15 2006;98(4):262-272.

139. Wang Y, Klijn JG, Zhang Y, et al. Gene-expression profiles to predict distant metastasis of lymph-node-negative primary breast cancer. *Lancet.* Feb 19-25 2005;365(9460):671-679.

140. Contal CaOQ, J. An application of changepoint methods in studying the effect of age on survival in breast cancer. *Computational Statistics and Data Analysis.* 1999;30:253-270.

141. Team RDC. A language and environment for statistical computing. *R Foundation for Statistical Computing, Vienna, Austria.* 2011.

142. Bathen TF, Jensen LR, Sitter B, et al. MR-determined metabolic phenotype of breast cancer in prediction of lymphatic spread, grade, and hormone status. *Breast cancer research and treatment.* Aug 2007;104(2):181-189.

143. Sitter B, Lundgren S, Bathen TF, Halgunset J, Fjosne HE, Gribbestad IS. Comparison of HR MAS MR spectroscopic profiles of breast cancer tissue with clinical parameters. *NMR Biomed.* Feb 2006;19(1):30-40.

144. Cheng LL, Chang IW, Smith BL, Gonzalez RG. Evaluating human breast ductal carcinomas with high-resolution magic-angle spinning proton magnetic resonance spectroscopy. *J Magn Reson.* Nov 1998;135(1):194-202.

145. Walenta S, Wetterling M, Lehrke M, et al. High lactate levels predict likelihood of metastases, tumor recurrence, and restricted patient survival in human cervical cancers. *Cancer research.* Feb 15 2000;60(4):916-921.

146. Mountford CE, Somorjai RL, Malycha P, et al. Diagnosis and prognosis of breast cancer by magnetic resonance spectroscopy of fine-needle aspirates analysed using a statistical classification strategy. *The British journal of surgery.* Sep 2001;88(9):1234-1240.

147. Hirschhaeuser F, Sattler UG, Mueller-Klieser W. Lactate: a metabolic key player in cancer. *Cancer Res.* Nov 15 2011;71(22):6921-6925.

148. Le A, Cooper CR, Gouw AM, et al. Inhibition of lactate dehydrogenase A induces oxidative stress and inhibits tumor progression. *Proc Natl Acad Sci U S A.* Feb 2 2010;107(5):2037-2042.

149. Ding SJ, Li Y, Shao XX, et al. Proteome analysis of hepatocellular carcinoma cell strains, MHCC97-H and MHCC97-L, with different metastasis potentials. *Proteomics.* Apr 2004;4(4):982-994.

150. Locasale JW, Grassian AR, Melman T, et al. Phosphoglycerate dehydrogenase diverts glycolytic flux and contributes to oncogenesis. *Nat Genet.* Sep 2011;43(9):869-874.

151. Possemato R, Marks KM, Shaul YD, et al. Functional genomics reveal that the serine synthesis pathway is essential in breast cancer. *Nature.* Aug 18 2011;476(7360):346-350.

152. Zhang WC, Shyh-Chang N, Yang H, et al. Glycine decarboxylase activity drives non-small cell lung cancer tumor-initiating cells and tumorigenesis. *Cell.* Jan 20 2012;148(1-2):259-272.

153. Lobo C, Ruiz-Bellido MA, Aledo JC, Marquez J, Nunez De Castro I, Alonso FJ. Inhibition of glutaminase expression by antisense mRNA decreases growth and tumourigenicity of tumour cells. *The Biochemical journal.* Jun 1 2000;348 Pt 2:257-261.

154. Seltzer MJ, Bennett BD, Joshi AD, et al. Inhibition of glutaminase preferentially slows growth of glioma cells with mutant IDH1. *Cancer Res.* Nov 15;70(22):8981-8987.

155. Glunde K, Bhujwalla ZM, Ronen SM. Choline metabolism in malignant transformation. *Nat Rev Cancer.* 2011;11(12):835-848.

156. Cuadrado A, Carnero A, Dolfi F, Jimenez B, Lacal JC. Phosphorylcholine: a novel second messenger essential for mitogenic activity of growth factors. *Oncogene.* Nov 1993;8(11):2959-2968.

157. Katz-Brull R, Seger D, Rivenson-Segal D, Rushkin E, Degani H. Metabolic markers of breast cancer: enhanced choline metabolism and reduced choline-ether-phospholipid synthesis. *Cancer Res.* Apr 1 2002;62(7):1966-1970.

158. Ramirez de Molina A, Gutierrez R, Ramos MA, et al. Increased choline kinase activity in human breast carcinomas: clinical evidence for a potential novel antitumor strategy. *Oncogene.* Jun 20 2002;21(27):4317-4322.

159. Ramirez de Molina A, Rodriguez-Gonzalez A, Gutierrez R, et al. Overexpression of choline kinase is a frequent feature in human tumor-derived cell lines and in lung, prostate, and colorectal human cancers. *Biochem Biophys Res Commun.* Aug 23 2002;296(3):580-583.

160. Gallego-Ortega D, Ramirez de Molina A, Ramos MA, et al. Differential role of human choline kinase alpha and beta enzymes in lipid metabolism: implications in cancer onset and treatment. *PLoS One.* 2009;4(11):e7819.

161. Ruiz-Cabello J, Berghmans K, Kaplan O, Lippman ME, Clarke R, Cohen JS. Hormone dependence of breast cancer cells and the effects of tamoxifen and estrogen: 31P NMR studies. *Breast cancer research and treatment.* Mar 1995;33(3):209-217.

162. Ramirez de Molina A, Penalva V, Lucas L, Lacal JC. Regulation of choline kinase activity by Ras proteins involves Ral-GDS and PI3K. *Oncogene.* Jan 31 2002;21(6):937-946.

163. Al-Saffar NM, Jackson LE, Raynaud FI, et al. The phosphoinositide 3-kinase inhibitor PI-103 downregulates choline kinase alpha leading to phosphocholine and total choline decrease detected by magnetic resonance spectroscopy. *Cancer Res.* Jul 1 2010;70(13):5507-5517.

164. Ramirez de Molina A, Sarmentero-Estrada J, Belda-Iniesta C, et al. Expression of choline kinase alpha to predict outcome in patients with early-stage non-small-cell lung cancer: a retrospective study. *Lancet Oncol.* Oct 2007;8(10):889-897.

165. King A, Selak MA, Gottlieb E. Succinate dehydrogenase and fumarate hydratase: linking mitochondrial dysfunction and cancer. *Oncogene.* Aug 7 2006;25(34):4675-4682.

166. Benn DE, Croxson MS, Tucker K, et al. Novel succinate dehydrogenase subunit B (SDHB) mutations in familial phaeochromocytomas and paragangliomas, but an absence of somatic SDHB mutations in sporadic phaeochromocytomas. *Oncogene.* Mar 6 2003;22(9):1358-1364.

167. Beckonert O, Monnerjahn J, Bonk U, Leibfritz D. Visualizing metabolic changes in breast-cancer tissue using 1H-NMR spectroscopy and self-organizing maps. *NMR Biomed.* Feb 2003;16(1):1-11.

168. Brand A, Richter-Landsberg C, Leibfritz D. Multinuclear NMR studies on the energy metabolism of glial and neuronal cells. *Dev Neurosci.* 1993;15(3-5):289-298.

169. Ross BD. Biochemical considerations in 1H spectroscopy. Glutamate and glutamine; myo-inositol and related metabolites. *NMR Biomed.* Apr 1991;4(2):59-63.

170. Fuchs BC, Bode BP. Stressing out over survival: glutamine as an apoptotic modulator. *The Journal of surgical research.* Mar 2006;131(1):26-40.

171. Kovacevic Z, Morris HP. The role of glutamine in the oxidative metabolism of malignant cells. *Cancer Res.* Feb 1972;32(2):326-333.

172. Yuneva M, Zamboni N, Oefner P, Sachidanandam R, Lazebnik Y. Deficiency in glutamine but not glucose induces MYC-dependent apoptosis in human cells. *The Journal of cell biology.* Jul 2 2007;178(1):93-105.

173. Sabine JR, Kopelovich L, Abraham S, Morris HP. Control of lipid metabolism in hepatomas: conversion of glutamate carbon to fatty acid carbon via citrate in several transplantable hepatomas. *Biochim Biophys Acta.* Mar 8 1973;296(3):493-498.

174. Le A, Lane AN, Hamaker M, et al. Glucose-Independent Glutamine Metabolism via TCA Cycling for Proliferation and Survival in B Cells. *Cell Metab.* Jan 4 2012;15(1):110-121.

175. Wellen KE, Lu C, Mancuso A, et al. The hexosamine biosynthetic pathway couples growth factor-induced glutamine uptake to glucose metabolism. *Genes Dev.* Dec 15;24(24):2784-2799.

176. Yoo H, Antoniewicz MR, Stephanopoulos G, Kelleher JK. Quantifying reductive carboxylation flux of glutamine to lipid in a brown adipocyte cell line. *The Journal of biological chemistry.* Jul 25 2008;283(30):20621-20627.

177. Wise DR, Ward PS, Shay JE, et al. Hypoxia promotes isocitrate dehydrogenase-dependent carboxylation of alpha-ketoglutarate to citrate to support cell growth and viability. *Proc Natl Acad Sci U S A.* Dec 6 2011;108(49):19611-19616.

178. Metallo CM, Gameiro PA, Bell EL, et al. Reductive glutamine metabolism by IDH1 mediates lipogenesis under hypoxia. *Nature.* Nov 20 2011.

179. Scott DA, Richardson AD, Filipp FV, et al. Comparative metabolic flux profiling of melanoma cell lines: beyond the Warburg effect. *The Journal of biological chemistry.* Dec 9 2011;286(49):42626-42634.

180. Holleran AL, Briscoe DA, Fiskum G, Kelleher JK. Glutamine metabolism in AS-30D hepatoma cells. Evidence for its conversion into lipids via reductive carboxylation. *Molecular and cellular biochemistry.* Nov 22 1995;152(2):95-101.

181. Mullen AR, Wheaton WW, Jin ES, et al. Reductive carboxylation supports growth in tumour cells with defective mitochondria. *Nature.* Nov 20 2011.

182. Meng M, Chen S, Lao T, Liang D, Sang N. Nitrogen anabolism underlies the importance of glutaminolysis in proliferating cells. *Cell cycle (Georgetown, Tex.* Oct 1;9(19):3921-3932.

183. Gaglio D, Soldati C, Vanoni M, Alberghina L, Chiaradonna F. Glutamine deprivation induces abortive s-phase rescued by deoxyribonucleotides in k-ras transformed fibroblasts. *PloS one.* 2009;4(3):e4715.

184. Colombo SL, Palacios-Callender M, Frakich N, et al. Molecular basis for the differential use of glucose and glutamine in cell proliferation as revealed by synchronized HeLa cells. *Proc Natl Acad Sci U S A.* Dec 27 2011;108(52):21069-21074.

185. Fuchs BC, Bode BP. Amino acid transporters ASCT2 and LAT1 in cancer: partners in crime? *Seminars in cancer biology.* Aug 2005;15(4):254-266.

186. Nicklin P, Bergman P, Zhang B, et al. Bidirectional transport of amino acids regulates mTOR and autophagy. *Cell.* Feb 6 2009;136(3):521-534.

187. Fuchs BC, Finger RE, Onan MC, Bode BP. ASCT2 silencing regulates mammalian target-of-rapamycin growth and survival signaling in human hepatoma cells. *American journal of physiology.* Jul 2007;293(1):C55-63.

188. Hamanaka RB, Chandel NS. Mitochondrial reactive oxygen species regulate cellular signaling and dictate biological outcomes. *Trends Biochem Sci.* Sep 2010;35(9):505-513.

189. Sattler M, Winkler T, Verma S, et al. Hematopoietic growth factors signal through the formation of reactive oxygen species. *Blood.* May 1 1999;93(9):2928-2935.

190. Iiyama M, Kakihana K, Kurosu T, Miura O. Reactive oxygen species generated by hematopoietic cytokines play roles in activation of receptor-mediated signaling and in cell cycle progression. *Cellular signalling.* Feb 2006;18(2):174-182.

191. Weinberg F, Hamanaka R, Wheaton WW, et al. Mitochondrial metabolism and ROS generation are essential for Kras-mediated tumorigenicity. *Proc Natl Acad Sci U S A.* May 11 2010;107(19):8788-8793.

192. Hu W, Zhang C, Wu R, Sun Y, Levine A, Feng Z. Glutaminase 2, a novel p53 target gene regulating energy metabolism and antioxidant function. *Proc Natl Acad Sci U S A.* Apr 20;107(16):7455-7460.

193. Suzuki S, Tanaka T, Poyurovsky MV, et al. Phosphate-activated glutaminase (GLS2), a p53-inducible regulator of glutamine metabolism and reactive oxygen species. *Proceedings of the National Academy of Sciences of the United States of America.* Apr 20 2010;107(16):7461-7466.

194. Roth E, Oehler R, Manhart N, et al. Regulative potential of glutamine--relation to glutathione metabolism. *Nutrition (Burbank, Los Angeles County, Calif.* Mar 2002;18(3):217-221.

195. Wu G, Fang YZ, Yang S, Lupton JR, Turner ND. Glutathione metabolism and its implications for health. *The Journal of nutrition.* Mar 2004;134(3):489-492.

196. Sato H, Tamba M, Ishii T, Bannai S. Cloning and expression of a plasma membrane cystine/glutamate exchange transporter composed of two distinct proteins. *The Journal of biological chemistry.* Apr 23 1999;274(17):11455-11458.

197. Knox WE, Horowitz ML, Friedell GH. The proportionality of glutaminase content to growth rate and morphology of rat neoplasms. *Cancer Res.* Mar 1969;29(3):669-680.

198. Linder-Horowitz M, Knox WE, Morris HP. Glutaminase activities and growth rates of rat hepatomas. *Cancer Res.* Jun 1969;29(6):1195-1199.

199. Weinberg F, Hamanaka R, Wheaton WW, et al. Mitochondrial metabolism and ROS generation are essential for Kras-mediated tumorigenicity. *Proc Natl Acad Sci U S A.* May 11;107(19):8788-8793.

200. Dang CV. Rethinking the Warburg effect with Myc micromanaging glutamine metabolism. *Cancer Res.* Feb 1;70(3):859-862.

201. Gaglio D, Metallo CM, Gameiro PA, et al. Oncogenic K-Ras decouples glucose and glutamine metabolism to support cancer cell growth. *Mol Syst Biol.* 2011;7:523.

202. Wellen KE, Thompson CB. Cellular metabolic stress: considering how cells respond to nutrient excess. *Molecular cell.* Oct 22;40(2):323-332.

203. Curthoys NP, Watford M. Regulation of glutaminase activity and glutamine metabolism. *Annu Rev Nutr.* 1995;15:133-159.

204. Olalla L, Gutierrez A, Jimenez AJ, et al. Expression of the scaffolding PDZ protein glutaminase-interacting protein in mammalian brain. *J Neurosci Res.* Feb 1 2008;86(2):281-292.

205. Szeliga M, Obara-Michlewska M, Matyja E, et al. Transfection with liver-type glutaminase cDNA alters gene expression and reduces survival, migration and proliferation of T98G glioma cells. *Glia.* Jul 2009;57(9):1014-1023.

206. Amary MF, Bacsi K, Maggiani F, et al. IDH1 and IDH2 mutations are frequent events in central chondrosarcoma and central and periosteal chondromas but not in other mesenchymal tumours. *J Pathol.* Jul 2011;224(3):334-343.

207. Parsons DW, Jones S, Zhang X, et al. An integrated genomic analysis of human glioblastoma multiforme. *Science (New York, N.Y.* Sep 26 2008;321(5897):1807-1812.

208. Yan H, Parsons DW, Jin G, et al. IDH1 and IDH2 mutations in gliomas. *The New England journal of medicine.* Feb 19 2009;360(8):765-773.

209. Mardis ER, Ding L, Dooling DJ, et al. Recurring mutations found by sequencing an acute myeloid leukemia genome. *The New England journal of medicine.* Sep 10 2009;361(11):1058-1066.

210. Ward PS, Cross JR, Lu C, et al. Identification of additional IDH mutations associated with oncometabolite R(-)-2-hydroxyglutarate production. *Oncogene.* Sep 26 2011.

211. Cairns RA, Iqbal J, Lemonnier F, et al. IDH2 mutations are frequent in angioimmunoblastic T-cell lymphoma. *Blood.* Jan 3 2012.

212. Pansuriya TC, van Eijk R, d'Adamo P, et al. Somatic mosaic IDH1 and IDH2 mutations are associated with enchondroma and spindle cell hemangioma in Ollier disease and Maffucci syndrome. *Nat Genet.* Dec 2011;43(12):1256-1261.

213. Dang L, White DW, Gross S, et al. Cancer-associated IDH1 mutations produce 2-hydroxyglutarate. *Nature.* Dec 10 2009;462(7274):739-744.

214. Ward PS, Patel J, Wise DR, et al. The common feature of leukemia-associated IDH1 and IDH2 mutations is a neomorphic enzyme activity converting alpha-ketoglutarate to 2-hydroxyglutarate. *Cancer cell.* Mar 16 2010;17(3):225-234.

215. Ito S, Shen L, Dai Q, et al. Tet proteins can convert 5-methylcytosine to 5-formylcytosine and 5-carboxylcytosine. *Science (New York, N.Y.* Sep 2 2011;333(6047):1300-1303.

216. Chowdhury R, Yeoh KK, Tian YM, et al. The oncometabolite 2-hydroxyglutarate inhibits histone lysine demethylases. *EMBO reports.* May 1;12(5):463-469.

217. He YF, Li BZ, Li Z, et al. Tet-mediated formation of 5-carboxylcytosine and its excision by TDG in mammalian DNA. *Science (New York, N.Y.* Sep 2 2011;333(6047):1303-1307.

218. Xu W, Yang H, Liu Y, et al. Oncometabolite 2-hydroxyglutarate is a competitive inhibitor of alpha-ketoglutarate-dependent dioxygenases. *Cancer cell.* Jan 18;19(1):17-30.

219. Figueroa ME, Abdel-Wahab O, Lu C, et al. Leukemic IDH1 and IDH2 mutations result in a hypermethylation phenotype, disrupt TET2 function, and impair hematopoietic differentiation. *Cancer cell.* Dec 14 2010;18(6):553-567.

220. Reitman ZJ, Jin G, Karoly ED, et al. Profiling the effects of isocitrate dehydrogenase 1 and 2 mutations on the cellular metabolome. *Proc Natl Acad Sci U S A.* Feb 22;108(8):3270-3275.

221. Gottlieb E, Tomlinson IP. Mitochondrial tumour suppressors: a genetic and biochemical update. *Nature reviews.* Nov 2005;5(11):857-866.

222. Eng C, Kiuru M, Fernandez MJ, Aaltonen LA. A role for mitochondrial enzymes in inherited neoplasia and beyond. *Nature reviews.* Mar 2003;3(3):193-202.

223. Isaacs JS, Jung YJ, Mole DR, et al. HIF overexpression correlates with biallelic loss of fumarate hydratase in renal cancer: novel role of fumarate in regulation of HIF stability. *Cancer cell.* Aug 2005;8(2):143-153.

224. Selak MA, Armour SM, MacKenzie ED, et al. Succinate links TCA cycle dysfunction to oncogenesis by inhibiting HIF-alpha prolyl hydroxylase. *Cancer cell.* Jan 2005;7(1):77-85.

225. MacKenzie ED, Selak MA, Tennant DA, et al. Cell-permeating alpha-ketoglutarate derivatives alleviate pseudohypoxia in succinate dehydrogenase-deficient cells. *Molecular and cellular biology.* May 2007;27(9):3282-3289.

226. Frezza C, Zheng L, Folger O, et al. Haem oxygenase is synthetically lethal with the tumour suppressor fumarate hydratase. *Nature.* Sep 8 2011;477(7363):225-228.

227. Kaadige MR, Elgort MG, Ayer DE. Coordination of glucose and glutamine utilization by an expanded Myc network. *Transcription.* Jul;1(1):36-40.

228. Sloan EJ, Ayer DE. Myc, Mondo, and Metabolism. *Genes & cancer.* Jun 1;1(6):587-596.

229. Love DC, Hanover JA. The hexosamine signaling pathway: deciphering the "O-GlcNAc code". *Sci STKE.* Nov 29 2005;2005(312):re13.

230. Dennis JW, Nabi IR, Demetriou M. Metabolism, cell surface organization, and disease. *Cell.* Dec 24 2009;139(7):1229-1241.

231. Billin AN, Eilers AL, Coulter KL, Logan JS, Ayer DE. MondoA, a novel basic helix-loop-helix-leucine zipper transcriptional activator that constitutes a positive branch of a max-like network. *Molecular and cellular biology.* Dec 2000;20(23):8845-8854.

232. Stoltzman CA, Peterson CW, Breen KT, Muoio DM, Billin AN, Ayer DE. Glucose sensing by MondoA:Mlx complexes: a role for hexokinases and direct regulation of thioredoxin-interacting protein expression. *Proc Natl Acad Sci U S A.* May 13 2008;105(19):6912-6917.

233. Kaadige MR, Looper RE, Kamalanaadhan S, Ayer DE. Glutamine-dependent anapleurosis dictates glucose uptake and cell growth by regulating MondoA transcriptional activity. *Proc Natl Acad Sci U S A.* Sep 1 2009;106(35):14878-14883.

234. Cheng T, Sudderth J, Yang C, et al. Pyruvate carboxylase is required for glutamine-independent growth of tumor cells. *Proc Natl Acad Sci U S A.* May 24;108(21):8674-8679.

235. Lora J, Alonso FJ, Segura JA, Lobo C, Marquez J, Mates JM. Antisense glutaminase inhibition decreases glutathione antioxidant capacity and increases apoptosis in Ehrlich

ascitic tumour cells. *European journal of biochemistry / FEBS.* Nov 2004;271(21):4298-4306.

236. Vander Heiden MG. Targeting cancer metabolism: a therapeutic window opens. *Nat Rev Drug Discov.* Sep 2011;10(9):671-684.

237. Rajagopalan KN, Deberardinis RJ. Role of glutamine in cancer: therapeutic and imaging implications. *J Nucl Med.* Jul;52(7):1005-1008.

238. Qu W, Zha Z, Ploessl K, et al. Synthesis of optically pure 4-fluoro-glutamines as potential metabolic imaging agents for tumors. *Journal of the American Chemical Society.* Feb 2;133(4):1122-1133.

239. Lieberman BP, Ploessl K, Wang L, et al. PET imaging of glutaminolysis in tumors by 18F-(2S,4R)4-fluoroglutamine. *Journal of nuclear medicine : official publication, Society of Nuclear Medicine.* Dec 2011;52(12):1947-1955.

240. Qu W, Oya S, Lieberman BP, et al. Preparation and Characterization of L-[5-11C]-Glutamine for Metabolic Imaging of Tumors. *Journal of nuclear medicine : official publication, Society of Nuclear Medicine.* Jan 2012;53(1):98-105.

241. Rothman DL, Hanstock CC, Petroff OA, Novotny EJ, Prichard JW, Shulman RG. Localized 1H NMR spectra of glutamate in the human brain. *Magn Reson Med.* May 1992;25(1):94-106.

242. Sibson NR, Dhankhar A, Mason GF, Behar KL, Rothman DL, Shulman RG. In vivo 13C NMR measurements of cerebral glutamine synthesis as evidence for glutamate-glutamine cycling. *Proc Natl Acad Sci U S A.* Mar 18 1997;94(6):2699-2704.

243. Rothman DL, Novotny EJ, Shulman GI, et al. 1H-[13C] NMR measurements of [4-13C]glutamate turnover in human brain. *Proc Natl Acad Sci U S A.* Oct 15 1992;89(20):9603-9606.

244. Gallagher FA, Kettunen MI, Day SE, et al. Detection of tumor glutamate metabolism in vivo using (13)C magnetic resonance spectroscopy and hyperpolarized [1-(13)C]glutamate. *Magn Reson Med.* Jul 2011;66(1):18-23.

245. Gallagher FA, Kettunen MI, Day SE, Lerche M, Brindle KM. 13C MR spectroscopy measurements of glutaminase activity in human hepatocellular carcinoma cells using hyperpolarized 13C-labeled glutamine. *Magn Reson Med.* Aug 2008;60(2):253-257.

246. Qu W, Zha Z, Lieberman BP, et al. Facile Synthesis [5-(13)C-4-(2)H(2)]-L-Glutamine for Hyperpolarized MRS Imaging of Cancer Cell Metabolism. *Academic radiology.* Aug;18(8):932-939.

247. Parkin DM, Bray F, Ferlay J, Pisani P. Global cancer statistics, 2002. *CA Cancer J Clin.* Mar-Apr 2005;55(2):74-108.

248. Joensuu H, Kellokumpu-Lehtinen PL, Bono P, et al. Adjuvant docetaxel or vinorelbine with or without trastuzumab for breast cancer. *The New England journal of medicine.* Feb 23 2006;354(8):809-820.

249. Pegram MD, Konecny G, Slamon DJ. The molecular and cellular biology of HER2/neu gene amplification/overexpression and the clinical development of herceptin (trastuzumab) therapy for breast cancer. *Cancer treatment and research.* 2000;103:57-75.

250. Stebbing J, Copson E, O'Reilly S. Herceptin (trastuzamab) in advanced breast cancer. *Cancer treatment reviews.* Aug 2000;26(4):287-290.

251. Romond EH, Perez EA, Bryant J, et al. Trastuzumab plus adjuvant chemotherapy for operable HER2-positive breast cancer. *The New England journal of medicine.* Oct 20 2005;353(16):1673-1684.

252. Kohl NE, Omer CA, Conner MW, et al. Inhibition of farnesyltransferase induces regression of mammary and salivary carcinomas in ras transgenic mice. *Nat Med.* Aug 1995;1(8):792-797.

253. Yeh ES, Yang TW, Jung JJ, Gardner HP, Cardiff RD, Chodosh LA. Hunk is required for HER2/neu-induced mammary tumorigenesis. *J Clin Invest.* Mar;121(3):866-879.

254. Banerjee MR, Wood BG, Kinder DL. Whole mammary gland organ culture: selection of appropriate gland. *In Vitro.* Sep-Oct 1973;9(2):129-133.

255. Qu W, Oya S, Lieberman BP, et al. Preparation and characterization of L-[5-11C]-glutamine for metabolic imaging of tumors. *J Nucl Med.* Jan 2012;53(1):98-105.

256. Loening AM, Gambhir SS. AMIDE: a free software tool for multimodality medical image analysis. *Molecular imaging.* Jul 2003;2(3):131-137.

257. Nissim I, Horyn O, Daikhin Y, Wehrli SL, Yudkoff M, Matschinsky FM. Effects of a Glucokinase Activator on Hepatic Intermediary Metabolism: Study With 13C Isotopomer-Based Metabolomics. *The Biochemical journal.* Mar 26 2012.

258. Chang HY, Nuyten DS, Sneddon JB, et al. Robustness, scalability, and integration of a wound-response gene expression signature in predicting breast cancer survival. *Proc Natl Acad Sci U S A.* Mar 8 2005;102(10):3738-3743.

259. Chin K, DeVries S, Fridlyand J, et al. Genomic and transcriptional aberrations linked to breast cancer pathophysiologies. *Cancer Cell.* Dec 2006;10(6):529-541.

260. Hess KR, Anderson K, Symmans WF, et al. Pharmacogenomic predictor of sensitivity to preoperative chemotherapy with paclitaxel and fluorouracil, doxorubicin, and cyclophosphamide in breast cancer. *J Clin Oncol.* Sep 10 2006;24(26):4236-4244.

261. Oh DS, Troester MA, Usary J, et al. Estrogen-regulated genes predict survival in hormone receptor-positive breast cancers. *J Clin Oncol.* Apr 10 2006;24(11):1656-1664.

262. Szondy Z, Newsholme EA. The effect of time of addition of glutamine or nucleosides on proliferation of rat cervical lymph-node T-lymphocytes after stimulation by concanavalin A. *Biochem J.* Sep 1 1991;278 (Pt 2):471-474.

263. McCauley RD, Heel KA, Hall JC. Enteral branched-chain amino acids increase the specific activity of jejunal glutaminase and reduce jejunal atrophy. *J Gastroenterol Hepatol.* Jun 1997;12(6):429-433.

264. Dang CV. MYC, microRNAs and glutamine addiction in cancers. *Cell cycle (Georgetown, Tex.* Oct 15 2009;8(20):3243-3245.

265. Witte D, Ali N, Carlson N, Younes M. Overexpression of the neutral amino acid transporter ASCT2 in human colorectal adenocarcinoma. *Anticancer research.* Sep-Oct 2002;22(5):2555-2557.

266. Li R, Younes M, Frolov A, et al. Expression of neutral amino acid transporter ASCT2 in human prostate. *Anticancer research.* Jul-Aug 2003;23(4):3413-3418.

267. Brizel DM, Schroeder T, Scher RL, et al. Elevated tumor lactate concentrations predict for an increased risk of metastases in head-and-neck cancer. *International journal of radiation oncology, biology, physics.* Oct 1 2001;51(2):349-353.

268. Schwickert G, Walenta S, Sundfor K, Rofstad EK, Mueller-Klieser W. Correlation of high lactate levels in human cervical cancer with incidence of metastasis. *Cancer research.* Nov 1 1995;55(21):4757-4759.

269. Walenta S, Salameh A, Lyng H, et al. Correlation of high lactate levels in head and neck tumors with incidence of metastasis. *The American journal of pathology.* Feb 1997;150(2):409-415.

270. Yokota H, Guo J, Matoba M, Higashi K, Tonami H, Nagao Y. Lactate, choline, and creatine levels measured by vitro 1H-MRS as prognostic parameters in patients with non-small-cell lung cancer. *J Magn Reson Imaging.* May 2007;25(5):992-999.

271. Thorn CC, Freeman TC, Scott N, Guillou PJ, Jayne DG. Laser microdissection expression profiling of marginal edges of colorectal tumours reveals evidence of increased lactate metabolism in the aggressive phenotype. *Gut.* Mar 2009;58(3):404-412.

272. Shim H, Dolde C, Lewis BC, et al. c-Myc transactivation of LDH-A: implications for tumor metabolism and growth. *Proceedings of the National Academy of Sciences of the United States of America.* Jun 24 1997;94(13):6658-6663.

273. Christofk HR, Vander Heiden MG, Harris MH, et al. The M2 splice isoform of pyruvate kinase is important for cancer metabolism and tumour growth. *Nature.* Mar 13 2008;452(7184):230-233.

274. Fantin VR, St-Pierre J, Leder P. Attenuation of LDH-A expression uncovers a link between glycolysis, mitochondrial physiology, and tumor maintenance. *Cancer cell.* Jun 2006;9(6):425-434.

275. Finley LW, Carracedo A, Lee J, et al. SIRT3 opposes reprogramming of cancer cell metabolism through HIF1alpha destabilization. *Cancer cell.* Mar 8;19(3):416-428.

276. Fischer K, Hoffmann P, Voelkl S, et al. Inhibitory effect of tumor cell-derived lactic acid on human T cells. *Blood.* May 1 2007;109(9):3812-3819.

277. Stern R, Shuster S, Neudecker BA, Formby B. Lactate stimulates fibroblast expression of hyaluronan and CD44: the Warburg effect revisited. *Experimental cell research.* May 15 2002;276(1):24-31.

278. Bouzier AK, Voisin P, Goodwin R, Canioni P, Merle M. Glucose and lactate metabolism in C6 glioma cells: evidence for the preferential utilization of lactate for cell oxidative metabolism. *Developmental neuroscience.* 1998;20(4-5):331-338.

279. Bouzier-Sore AK, Canioni P, Merle M. Effect of exogenous lactate on rat glioma metabolism. *Journal of neuroscience research.* Sep 15 2001;65(6):543-548.

280. Sonveaux P, Vegran F, Schroeder T, et al. Targeting lactate-fueled respiration selectively kills hypoxic tumor cells in mice. *The Journal of clinical investigation.* Dec 2008;118(12):3930-3942.

281. Rattigan YI, Patel BB, Ackerstaff E, et al. Lactate is a mediator of metabolic cooperation between stromal carcinoma associated fibroblasts and glycolytic tumor cells in the tumor microenvironment. *Experimental cell research.* Feb 15;318(4):326-335.

282. Semenza GL. Tumor metabolism: cancer cells give and take lactate. *The Journal of clinical investigation.* Dec 2008;118(12):3835-3837.

283. Maekawa M, Taniguchi T, Ishikawa J, Sugimura H, Sugano K, Kanno T. Promoter hypermethylation in cancer silences LDHB, eliminating lactate dehydrogenase isoenzymes 1-4. *Clinical chemistry.* Sep 2003;49(9):1518-1520.

284. Kennedy KaD, MW. Cellullar Responses to Lactate in Breast Cancer. Paper presented at: American Society of Clinical Oncology 2012 Annual Meeting2012; Chicago, Illinois.

285. Majmundar AJ, Wong WJ, Simon MC. Hypoxia-inducible factors and the response to hypoxic stress. *Molecular cell.* Oct 22;40(2):294-309.

286. Fulco M, Schiltz RL, Iezzi S, et al. Sir2 regulates skeletal muscle differentiation as a potential sensor of the redox state. *Mol Cell.* Jul 2003;12(1):51-62.

287. Solomon JM, Pasupuleti R, Xu L, et al. Inhibition of SIRT1 catalytic activity increases p53 acetylation but does not alter cell survival following DNA damage. *Mol Cell Biol.* Jan 2006;26(1):28-38.

288. Cheong H, Lindsten T, Thompson CB. Autophagy and ammonia. *Autophagy.* Jan;8(1):122-123.

289. Locasale JW, Grassian AR, Melman T, et al. Phosphoglycerate dehydrogenase diverts glycolytic flux and contributes to oncogenesis. *Nature genetics.* Sep;43(9):869-874.

290. Possemato R, Marks KM, Shaul YD, et al. Functional genomics reveal that the serine synthesis pathway is essential in breast cancer. *Nature.* Aug 18;476(7360):346-350.

291. Huang S, Ren X, Wang L, Zhang L, Wu X. Lung-cancer chemoprevention by induction of synthetic lethality in mutant KRAS premalignant cells in vitro and in vivo. *Cancer prevention research (Philadelphia, Pa.* May;4(5):666-673.

292. Thornburg JM, Nelson KK, Clem BF, et al. Targeting aspartate aminotransferase in breast cancer. *Breast Cancer Res.* 2008;10(5):R84.

293. Haigis MC, Mostoslavsky R, Haigis KM, et al. SIRT4 inhibits glutamate dehydrogenase and opposes the effects of calorie restriction in pancreatic beta cells. *Cell.* Sep 8 2006;126(5):941-954.

294. Golman K, Olsson LE, Axelsson O, Mansson S, Karlsson M, Petersson JS. Molecular imaging using hyperpolarized 13C. *Br J Radiol.* 2003;76 Spec No 2:S118-127.

295. Golman K, Petersson JS. Metabolic imaging and other applications of hyperpolarized 13C1. *Acad Radiol.* Aug 2006;13(8):932-942.

296. Golman K, Zandt RI, Lerche M, Pehrson R, Ardenkjaer-Larsen JH. Metabolic imaging by hyperpolarized 13C magnetic resonance imaging for in vivo tumor diagnosis. *Cancer Res.* Nov 15 2006;66(22):10855-10860.

297. Hoffman EA, van Beek E. Hyperpolarized media MR imaging--expanding the boundaries? *Acad Radiol.* Aug 2006;13(8):929-931.

298. Keshari KR, Kurhanewicz J, Jeffries RE, et al. Hyperpolarized (13)C spectroscopy and an NMR-compatible bioreactor system for the investigation of real-time cellular metabolism. *Magn Reson Med.* Feb;63(2):322-329.

299. Kohler SJ, Yen Y, Wolber J, et al. In vivo 13 carbon metabolic imaging at 3T with hyperpolarized 13C-1-pyruvate. *Magn Reson Med.* Jul 2007;58(1):65-69.

300. Merritt ME, Harrison C, Storey C, Jeffrey FM, Sherry AD, Malloy CR. Hyperpolarized 13C allows a direct measure of flux through a single enzyme-catalyzed step by NMR. *Proc Natl Acad Sci U S A.* Dec 11 2007;104(50):19773-19777.

301. Nelson SJ, Vigneron D, Kurhanewicz J, Chen A, Bok R, Hurd R. DNP-Hyperpolarized C Magnetic Resonance Metabolic Imaging for Cancer Applications. *Appl Magn Reson.* 2008;34(3-4):533-544.

302. Rowland IJ, Peterson ET, Gordon JW, Fain SB. Hyperpolarized (13)Carbon MR. *Curr Pharm Biotechnol.* May 24.

303. Schroder L, Lowery TJ, Hilty C, Wemmer DE, Pines A. Molecular imaging using a targeted magnetic resonance hyperpolarized biosensor. *Science.* Oct 20 2006;314(5798):446-449.

304. Svensson J. Contrast-enhanced magnetic resonance angiography: development and optimization of techniques for paramagnetic and hyperpolarized contrast media. *Acta Radiol Suppl.* Jul 2003;429:1-30.

305. Viale A, Aime S. Current concepts on hyperpolarized molecules in MRI. *Curr Opin Chem Biol.* Feb;14(1):90-96.

306. Viale A, Reineri F, Santelia D, et al. Hyperpolarized agents for advanced MRI investigations. *Q J Nucl Med Mol Imaging.* Dec 2009;53(6):604-617.

307. Yen YF, Kohler SJ, Chen AP, et al. Imaging considerations for in vivo 13C metabolic mapping using hyperpolarized 13C-pyruvate. *Magn Reson Med.* Jul 2009;62(1):1-10.

308. Albers MJ, Bok R, Chen AP, et al. Hyperpolarized 13C lactate, pyruvate, and alanine: noninvasive biomarkers for prostate cancer detection and grading. *Cancer Res.* Oct 15 2008;68(20):8607-8615.

309. Chen AP, Albers MJ, Cunningham CH, et al. Hyperpolarized C-13 spectroscopic imaging of the TRAMP mouse at 3T-initial experience. *Magn Reson Med.* Dec 2007;58(6):1099-1106.

310. Day SE, Kettunen MI, Gallagher FA, et al. Detecting tumor response to treatment using hyperpolarized 13C magnetic resonance imaging and spectroscopy. *Nat Med.* Nov 2007;13(11):1382-1387.

311. Harris T, Eliyahu G, Frydman L, Degani H. Kinetics of hyperpolarized 13C1-pyruvate transport and metabolism in living human breast cancer cells. *Proc Natl Acad Sci U S A.* Oct 27 2009;106(43):18131-18136.

312. Ward CS, Venkatesh HS, Chaumeil MM, et al. Noninvasive detection of target modulation following phosphatidylinositol 3-kinase inhibition using hyperpolarized 13C magnetic resonance spectroscopy. *Cancer Res.* Feb 15;70(4):1296-1305.

313. Witney TH, Kettunen MI, Day SE, et al. A comparison between radiolabeled fluorodeoxyglucose uptake and hyperpolarized (13)C-labeled pyruvate utilization as methods for detecting tumor response to treatment. *Neoplasia.* Jun 2009;11(6):574-582, 571 p following 582.

314. Zierhut ML, Yen YF, Chen AP, et al. Kinetic modeling of hyperpolarized 13C1-pyruvate metabolism in normal rats and TRAMP mice. *J Magn Reson.* Jan;202(1):85-92.